

IFAC

INTERNATIONAL FEDERATION
OF AUTOMATIC CONTROL



WARSZAWA 1969

Power Systems Boiler and Steam Controls

Fourth Congress of the International
Federation of Automatic Control
Warszawa 16–21 June 1969

TECHNICAL
SESSION

54



Organized by
Naczelna Organizacja Techniczna w Polsce

INTERNATIONAL FEDERATION OF AUTOMATIC CONTROL

Power Systems

Boiler and Steam Controls

TECHNICAL SESSION No 54

**FOURTH CONGRESS OF THE INTERNATIONAL
FEDERATION OF AUTOMATIC CONTROL
WARSZAWA 16 – 21 JUNE 1969**



**Organized by
Naczelna Organizacja Techniczna w Polsce**



K-1322

Biblioteka
Politechniki Białostockiej



1181071

Contents

Paper No		Page
54.1	Pl - M.Duda, M.Plucińska-Klawe, J.Rakowski, S.Waglowski - Analysis and Design of 200 MW Boiler - Turbine Unit Control Systems Through Analog and Digital Simulation...	3
54.2	F - H.Apter, J.F.Le Corre, R.Mezencev, Y.Tho- mas - Optimum Control of a Steam Boiler.	24
54.3	J - K.Itch, M.Fujii, H.Ohno, K.Sagara - Com- parison of Dynamics Between Natural Cir- culation Boiler and Forced Circulation Boiler.....	51
54.4	D - H.Unbehauen, P.Necker - On the Optimal /GFR/ Temperature Control of the Multivariable Control System "Once-Through Boiler" Un- der Fast Load Changes.....	66
54.5	PL - K.Taramina - Optimum Control Algorithm by Means of Surplus Air in Fireboxes of Stea- dy Fuel Fired Steam Boilers 	81
54.6	CS - B.Hanuš - Investigation of the Direct Di- gital Control of an One-Through-Boiler..	94
54.7	USA - T.Giras, R.Uram - Digital Control Tech- niques for Power Plant Applications.....	102

Wydawnictwa Czasopism Technicznych NOT - Polska

Zakład Poligraficzny WCT NOT. Zam. 71/89.

ANALYSIS AND DESIGN OF 200 MW BOILER - TURBINE UNIT CONTROL SYSTEMS THROUGH ANALOG AND DIGITAL SIMULATION

DUDA M.

PLUCINSKA-KIAWE M.

RAKOWSKI J.

WAGLOWSKI S.

Institute of Power - Warszawa

The paper describes the simulation approach which has been applied in the design of steam and temperature control systems of a power boiler. This approach is illustrated on the example of a coal fired boiler of natural circulation /type OP-650K/ designed for block operation with a 200 MW single-shaft turbine. However the results presented herein may be extended to other boilers of similar type. The OP-650 k boiler is rated at 650 t/h; 138 at; 540/540°C.

The superheater /comprising five stages/ and the reheater /comprising two stages/ are divided into two parallel ducts. In order to confine the volume of this paper considerations on the adapted simulation technique of the boiler - turbine units is skipped. This problem in conjunction with the discussion of adopted simplifying assumptions was the subject of earlier publications of the same authors^{2,6}. The same refers to the simulation method of a complex heat exchanger as this is the case with the boiler type OP-650-k in which the flue gases in the convection ducts sweep simultaneously two or even three of the heated surfaces making part of different sections of the superheater, having various parameters of the heated medium.

The steam temperature change at one of those surfaces affects the temperature distribution of flue gases and, thereby, the heat flux transmitted to other surfaces. The transfer functions of such a complex heat exchanger are given in a previous paper⁵.

1. Investigation of steam pressure control systems

The diagram of the considered steam pressure control systems is presented in fig.1. The study of those systems was carried out on a linearized analog model /fig,2/.

The following mathematical representation of the particular elements of the boiler-turbine unit was adopted:

Coal mill

The mill was simulated together with the primary air control system /fig,3/. The primary air controller is set in such a way that the change of pulverized fuel flow - caused by a step change of the quantity of raw fuel - may be approximated by the response of a single inertial element of the I-st order. Hence, it was adopted that:

$$G_{ML}/s/ = \frac{\Delta B_{PL}}{\Delta B_{RW}} /s/ \cong \frac{k_{ML}}{1 + T_{ML}s} \quad /1/$$

Combustion chamber

In the case of suspension firing combustion proceeds much quicker than the process of steam pressure change⁷. Therefore, it was assumed that the changes of heat quantity transferred to the steam generator follow immediately the changes of pulverized fuel flow:

$$G_{FN}/s/ = \frac{\Delta Q_{SG}}{\Delta B_{PL}} /s/ = k_{FN} \quad /2a/$$

The above relations are only valid when the combustion chamber is not slagged. When slagging is taken into account the transfer function is expressed by¹:

$$G_{FN}/s/ = \frac{\Delta Q_{SG}}{\Delta B_{PL}} /s/ = e^{-T_{FN}s} \frac{k_{FN}}{1 + T_{FN}s} \quad /2b/$$

where:

$$T_{FN} = 0,077 \frac{\delta^2}{a} ; \quad T_{FN} = 1,08 \frac{\delta^2}{a} \quad [\text{sek}]$$

and

δ - average thickness of slag deposit in mm
 a - temperature equalization factor in mm^2/s

Steam generator

The transfer function of the steam generator was determined the equations given in the paper of Shumskaya⁸.

$$G_{SG1}/s/ = \frac{\Delta p_{DR}}{\Delta Q_{SG}} /s/ = \frac{k_{SG1}}{s}$$

$$G_{SG2}/s/ = \frac{\Delta p_{DR}}{\Delta M_{FW}} /s/ = \frac{k_{SG2}}{s} \quad /3/$$

$$G_{SG3}/s/ = \frac{\Delta p_{DR}}{\Delta M_{DR}} /s/ = \frac{k_{SG3}}{s}$$

Steam superheater with connecting pipes

The transfer function of the superheater together with the pipes connecting the boiler outlet with the turbine was calculated treating the superheater as a single capacity element C_{SH} and a hydraulic resistance R_{SH} proportional to the square of steam flow:

$$G_{SH1}/s/ = \frac{\Delta M_{DR}}{\Delta /p_{DR} - p_{TU}} /s/ = k_{SH1}$$

/4/

$$G_{SH2}/s/ = \frac{\Delta p_{TU}}{\Delta /M_{DR} - M_{TU}} /s/ = \frac{k_{SH2}}{s}$$

Where:

$$k_{SH1} = \frac{1}{R_{SH}} = \left[\frac{M_{TU}}{2/p_{DR} - p_{TU}} \right] 100\%; k_{SH2} = \frac{1}{C_{SH}} = \left[\frac{1}{v_{SH} \frac{\partial \rho}{\partial p} /SH} \right] 100\%$$

Turbine

According to Rushchensky⁷ it was assumed that the turbine time constants are very short in relation to those of the steam generator. Therefore the turbine transfer functions may be expressed as follows:

$$G_{TU1}/s/ = \frac{\Delta M_{TU}}{\Delta p_{TU}} /s/ = k_{TU1} \quad /5/$$

$$G_{TU2}/s/ = \frac{\Delta M_{TU}}{\Delta \dot{M}_{TU}} /s/ = k_{TU2}$$

For the case of the boiler type OP-650-k with a mill type MKM-33 and turbine type TK-200 the values of model factors are:

$$\begin{aligned} k_{ML} &= 1 & k_{SG3} &= 5,34 \cdot 10^{-2} \frac{\text{at/min}}{\text{t/h}} \\ k_{FN} &= 1,44 \cdot 10^3 \text{ Mcal/t} & k_{SH1} &= 24,3 \frac{\text{t/h}}{\text{at}} \\ k_{SG1} &= 1,87 \cdot 10^{-4} \frac{\text{at/min}}{\text{Mcal/h}} & k_{SH2} &= 15,6 \frac{\text{at/min}}{\text{t/h}} \\ k_{SG2} &= 0,43 \cdot 10^{-2} \frac{\text{at/min}}{\text{t/h}} & T_{ML} &= 2 \text{ min} \end{aligned}$$

Test results

The model intended for the study of steam pressure control was designed assuming that the combustion chamber is lagged. The minimum regulation time at a damping coefficient of 0,85 was adopted as criterion of regulation. Following control systems according to fig.1 were used:

$$a/ \text{PI} / z_1 = z_2 = z_3 = 0 /$$

$$b/ \text{PID} / z_1 = z_2 = z_3 = 0 /$$

$$c/ \text{PI} + \text{D}/\mu_{\text{DR}} / z_1=1, z_2=z_3=0,$$

$$d/ \text{PID} + \text{D}/\mu_{\text{TU}} / z_2=1, z_1=z_3=0/$$

$$e/ \text{PID} + \text{D}/\mu_{\text{TU}} / z_3=1, z_1=z_2=0/$$

$$f/ \text{PID} + \text{D}/\mu_{\text{DR}} + \text{D}/\mu_{\text{TU}} / z_1=z_3=1, z_2=0/$$

The characteristics plotted in figs. 4, 5, 6, 7 show that in the case of internal /fuel flow/ disturbances ^{the system PID is better than} the system PID without auxiliary signals. However in practice it is difficult to obtain the drum pressure derivative signal because of the pulsation of this pressure. Therefore the system provided only with the PID controller should be considered sufficient.

In the case of external disturbances the smallest fluctuation amplitudes are obtained when using the PID + D/ μ_{TU} / system, but it can be seen that at frequencies below 3×10^{-3} Hz this system is equivalent with the PID system without auxiliary signals. Hence, it results that at low disturbance frequencies the PID controller without auxiliary signals is fully sufficient.

2. Investigation of steam temperature control systems

The interaction of the pressure control system on the steam temperature variation was stated. Therefore a simplified pressure control system model was connected with that of the temperature control system, to study this interaction effects.

The task of the temperature control system consists in maintaining the steam temperatures beyond the particular stages of the superheater in compliance with fig. 8.

It should be stressed that the temperature beyond stage III should change with the boiler load.

According to a previous paper⁶ the particular stages of the superheater were treated as separate heat exchangers each of which may be characterized by following transfer functions:

$$G_1/s/ = \frac{\Delta \mathcal{V}_{D0}}{\Delta \mathcal{V}_{D1}} = I_1 \exp / - \frac{T_R s}{1 + T_R s} \quad \chi_D / \quad /6/$$

$$\text{where } I_1 = 1; \quad T_R = \frac{m_R c_R}{F_D \alpha_D}; \quad D = \frac{F_D \alpha_D}{M_D c_D}$$

$$G_2/s/ = \frac{\Delta v_0}{\Delta M_{TU}} = I_2 \frac{1}{1 + T_D s} \quad /7/$$

$$\text{where } I_2 = \frac{v_1 - v_0}{M_{TU}}; \quad T_D = \alpha_D T_R$$

$$G_3/s/ = \frac{\Delta v_0}{\Delta B} = k_B \frac{1}{1 + T_D s} \quad /8/$$

$$G_4/s/ = \frac{\Delta v_0}{\Delta \alpha} = k_\alpha \frac{1}{1 + T_D s} \quad /9/$$

For the simulation of the transfer-functions $G_1/s/$ the B.Hanus' approximation method³ was adopted. The remaining transfer-functions were simulated in a direct manner.

Thermocouples were considered to be single inertial elements

$$G_T/s/ = \frac{1}{1 + T s} \quad /10/$$

Injector desuperheaters were during the first stage of the study considered as non-inertial elements having an amplification factor:

$$k_{DS} = \frac{\partial v_1 / \partial H}{\partial H} = k_1 \cdot k_2 \quad /11/$$

where

$$k_1 = \frac{i_D - i_{spr}}{M_D c_D}; \quad k_2 = \frac{\partial M_{spr} / \partial H}{\partial H}$$

The connecting pipelines /unheated sections/ were simulated in compliance with:

Table 1

Numerical coefficients occurring in expressions for the
transfer-functions $G_1/s/ - G_4/s/$

No	Coefficient	Dimension	I	II	III	IV	V	I"	II"
1	T_D	sek	52	27	39	40	62	150	90
2	T_R	sek	4,7	4,1	4,1	6,8	13	23	21
3	$\%_D$	-	11	6,7	9,5	5,8	4,8	6,5	4,3
4	I_2	$\frac{^{\circ}C}{t/h}$	-0,03	-0,04	-0,135	-0,059	-0,062	-0,21	-0,165
5	k_B	$\frac{^{\circ}C}{t/h}$	0,25	0,335	0,735	0,465	0,6	1,1	0,81
6	k	$\frac{^{\circ}C}{\%}$	-	-	-	+0,36	-	-0,75	-0,29
7	k_{DS}	$\frac{^{\circ}C}{\%}$	0,063	0,105	0,17	0,278	-	0,045	-

$$G / s / = \frac{T_R s}{T_R + T_2 + T_3} / s + 1 \quad /12/$$

where

$$T_R = - \frac{m_R}{F_D} \frac{c_R}{\alpha_D} ; \quad T_2 = \frac{m_D}{M_D} ; \quad T_3 = \frac{m_R}{M_D} \frac{c_R}{c_D}$$

Fig.9 shows the diagram of steam temperatures system and fig.10 presents the block diagrams of:

- a/ the model of all the superheater stages together with the simplified model of the pressure control system,
- b/ the studied variants of control system.

The IIInd stage of the superheater is fully radiated. This means that the steam temperature rise, produced by it, decreases with the increase of the boiler load. Therefore, the control of the inlet steam temperature to this stage was adopted. This solution facilitates the obtention of a decreasing static steam temperature characteristic beyond the IIIrd stage /in compliance with the requirements presented in fig.8/. Moreover, in order to reach this aim a signal representing the boiler load was introduced to the main controller. During the study it was analysed whether it should be the steam flow or the main turbine valve position signal. The results obtained /fig.11/ indicate that the latter solution is more advantageous.

A cascade control system was foreseen for the Vth superheater stage. It was similar to that applied for the IIIrd stage but with a constant desired value preset on the main controller. Finally the effect of the introduction to auxiliary controllers /beyond the IIIrd and Vth superheater stages/ wither of the signal from the derivative $\frac{dM_{TU}}{dt}$ or of the combination of signals M_{TU} and B was investigated. It was stated that the optimum values were for the first case $T_{DI} = 373$ s and $T_2 = 0$ and for the second case $M_{TU}/B_{RW} = 3$ /fig.11 c+d/. The study was carried out taking into account two types of disturbances:

- a/ 10% change of fuel flow,
- b/ 10% change of turbine valve position in compliance with the VDI/VDE Richtlinien 3507/.

It was stated that the disturbances "a" /caused by change of fuel flow/ cause much smaller fluctuations of controlled temperatures than disturbances "b" /due to steam flow/.

Therefore, in fig.12 temperature variations during steam flow disturbances are only presented. They were obtained on a model in compliance with fig.10 when using the signal dM_{TU}/dt as well as when using the signals B_{RW} and M_{TU} .

Fig.14 presents the maximum error of the regulated quantity plotted against the frequency of steam flow disturbances /of amplitude 2.5%/.

The results presented above were obtained for the assumption that static characteristic $M_{spr} = f/H/$ is linear over the whole range /without limitation/. However the actual characteristic of spray valves injection desuperheater system is generally non-linear. Typical Δu_2 and Δu_3 curves assuming a characteristic $M_{spr} = f/H/$ in compliance with fig. 15 are presented in fig.13.

The temperature control of reheated steam is carried out by controlling both the dampers in the flue gas path and the spray valves. This system foresees a PI controller controlling the spray valves and an auxiliary controller controlling the flue gases dampers in such a manner as to assure in steady state that the spray water flow corresponds with a desired value independently of the boiler load and the configuration of the operating mills. In this way small temperature fluctuations shall be eliminated by means of injection control, and the greater ones exceeding the relatively narrow range of the injection desuperheater by means of flue gas dampers. Hence, the dampers which are used for coarse regulation /and the position of which when changed brings about a disturbance in the primary steam temperature and in the combustion chamber vacuum/, shall only act in the case of greater disturbances.

It was analysed whether the auxiliary controller should be an integrating element /variant I in which $Z_9 = 1$ $Z_{10} = 0/$ or a non-linear element of relief type having an insensibility zone covering the regulation range of the injection desuper-

heater /variant II in which $Z_9=0$ $Z_{10}=1/$.

Fig.16 gives the comparison of the control process in both variants following a sudden turbine valve closing by 10%, and fig.17 - the comparison of frequency responses of those variants.

3. Assesments of temperature control on base of frequency responses characteristics

The selection of the structure of control systems may only be made when the spectrum of disturbances affecting the boiler-turbine unit is known. As in the considered case the set is not yet installed the disturbance spectrum is not known. The test results allowed only to prepare the data indispensable for the selection of the optimum structure. The decision may be taken when the disturbance spectrum $Z /j\omega/$ for the investigated unit shall be determined. It is only then that the actual spectra $A /j\omega/$ of controlled parametres may be calculated:

$$\left| G /j\omega / \cdot Z /j\omega / \right| = \left| A /j\omega / \right| \quad /13/$$

where $G /j\omega/$ - system response to "white" noise,

The characteristic $A /j\omega/$ shall serve as a base for comparing the considered variants. This comparison may be carried out basing on the regulation criterion:

$$K_t = \int_0^{\infty} \left(\mathcal{Y} + a \cdot \frac{d\mathcal{Y}}{dt} \right)^2 dt \quad /14/$$

to which corresponds:

$$K_{\omega} = \int_0^{\infty} \left(1 + a^2 \omega^2 \right) \left| A /j\omega / \right|^2 d\omega \quad /15/$$

the coefficient "a" being adopted independently for each control system. The control structure for which the calculated value of the criterion K_{ω} reaches minimum, should be selected, as being the best one.

Conclusions

A method that enables the choice of optimal pressure and temperature control systems configuration has been illustrated using as an example the OP-650 k type power boiler. This modeling techniques can be applied to investigate the control systems of other boiler-turbine units, prior to their actual operation.

NOTATIONS

C - specific heat	$\frac{\text{kcal}}{\text{kg}^{\circ}\text{C}}$
F - heating surface	m^2
G/s - transfer-function	-
M - flow of steam or flue gases	$\frac{t}{h}; \frac{\text{m}^3}{h}$
m - mass	kg
B - fuel flow	t/h
H - position of injection valve	%
p - pressure	atm
q - per unit heat flux	$\frac{\text{kcal}}{\text{h m}^2}$
s - Laplace operator	$\frac{1}{s}$
t - time	s; h
T - time constant	s; min
τ - time lag	s
α - position of flue gas damper or heat exchange coefficient	% $\frac{\text{kcal}}{\text{h}^{\circ}\text{C m}^2}$
ϑ - temperature	$^{\circ}\text{C}$
μ - position of turbine regulating valve	%

$$\mathcal{K} = \frac{F\alpha}{Mc}$$

INDICES

R - pipe
D - steam
spr - injection water
i - input
o - output
1, 2, 3, 4, 5 - steam temperature beyond the respective
stage of the superheater
TU - turbine
FW - feed water
RW - raw fuel
PL - pulverized fuel
ML - coal mill
FN - furnace
SG - steam generator
SH - superheater
PR - primary air
DR - drum

BIBLIOGRAPHY

1. Duda M.: Effect of slagging on boiler dynamics /in Polish/ - Energetyka 1967 No 11 - Biul.ImEn. No 11/12
2. Duda M., Plucińska-Klawe M., Rakowski J., Waglowski S.- Analysis and Design of 200 MW Boiler Turbine Unit Control Systems /in Polish/, Report of the Institute of Power 1967, No 6229.
3. Hanuš B.: Vereinfachte Nachbildung des Regelverhaltens eines Dampfüberhitzers am Analogrechner - Regelungstechnik, Heft 1, 1965.
4. Profos P.: Die Regelung von Dampfanlagen - Springer Verlag 1962.
5. Rakowski J., Duda M., Waglowski S.: Das Mathematische Modell eines zusammengesetzten Wärmeaustauschers - Neue Technik A 2/1968 p.95-102 /Zürich/
6. Rakowski J., Waglowski S., Duda M.: Dynamic representation of a boiler - Press Academiques Européennes: International Seminar Automatic Control in Production and Distribution of Electrical Power - Brussels 1966.
7. Rushchinsky W.M.: Analytical method of determining dynamic characteristics of boiler-turbine units /in Russian/ - CNIKA 1966, Moscow.
8. Shumskaya L.S.: Main control parametres of natural circulation boilers under transient conditions /in Russian/ - Gosenergoizdat 1961.



C A P T I O N S

Fig.1. Diagram of investigated steam pressure control systems.

Fig.2. Structural diagram of the model of the boiler type OP-650 k as an object of steam pressure control.

Fig.3. Structural diagram of the model of mill system.

Fig.4. Steam pressure transients following a 8% step fuel flow disturbance.

Notations: 1 - without control; 2 - PI; 3 - PID or PID + D / μ_{TU} /; 4 - PI + D/P_{DR} / or

PI + D/P_{DR} / + D / μ_{TU} /.

Fig.5. Steam pressure transients following a 10% step turbine valve disturbance.

Notations: 1 - without control; 2 - PI; 3 - PID; 4 - PI + D/P_{DR} /; 5 - PID + D/P_{DR} /;

6 - PI + D/P_{DR} / + D / μ_{TU} / .

Fig.6. Frequency response of the investigated steam pressure control systems /fuel flow disturbance/.

Notations: same as in fig.4.

Fig.7. Frequency response of the investigated steam pressure control systems /turbine disturbance/.

Notations: same as in fig.5.

Fig.8. Steam temperatures beyond particular superheater stages /1 to 5/ plotted against the unit of load.

Fig.9. Diagram of investigated temperature control system.

Fig.10. Block diagram of the model of a boiler type OP-650 k treated as an object for temperature control /the investigated control systems included/.

Fig.11a. and b. Investigation of varying the desired value set on the temperature controller in compliance with the signals from:

- 1 - position of the main turbine value
- 2 - steam flow

c. and d. Selection of ΔM_{TU} and ΔB signals combinations for correcting the auxiliary temperature controller action.

$$1/ \frac{\Delta M_{TU}}{\Delta B_{RW}} = 0.3 \quad 2/ \frac{\Delta M_{TU}}{\Delta B_{RW}} = 1.0 \quad 3/ \frac{\Delta M_{TU}}{\Delta B_{RW}} = 3.0$$

a and c - fuel flow change

b and d - turbine valve change

Fig.12. Temperature and spray valve position transients following turbine valve position change.

a and b - with control system of steam temperature at:

$$Z_1 = Z_3 = 1; \quad Z_2 = Z_4 = Z_5 = Z_6 = Z_7 = Z_8 = Z_9 = \\ = Z_{10} = 0$$

c and d - at $Z_3 = Z_r = Z_5 = 1;$

$$Z_1 = Z_2 = Z_6 = Z_7 = Z_8 = Z_9 = Z_{10} = 0 \text{ and } \frac{\Delta M_{TU}}{\Delta B_{RW}} = 3$$

Fig.13. Comparison of temperature transients:

1 - without limitation of injection water,

2 - with non-linear characteristics of spray valves

a and b see fig.12.

c and d

Fig.14. Frequency response of investigated steam temperature control systems during turbine valve disturbance.

1 - see fig.12 a and b

2 - see fig. 12 c and d

Fig.15. Static characteristic of spray water valve.

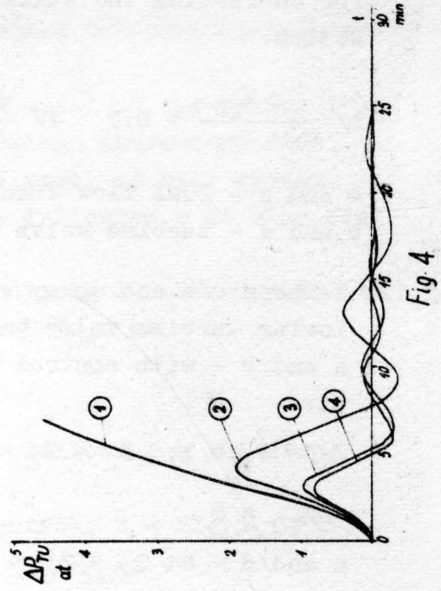
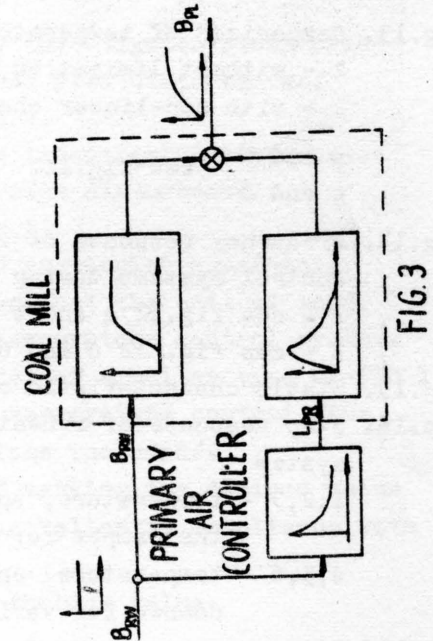
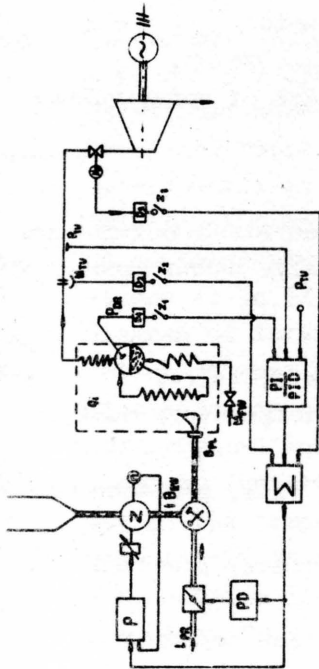
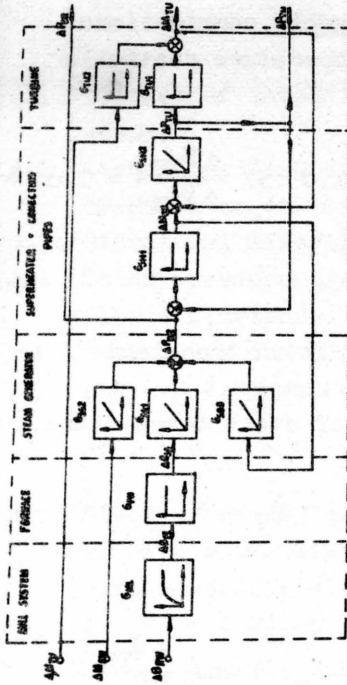
Fig.16. Step response of reheated steam temperature control system

1,2,3 - temperature, spray water flow, position of the damper for variant I

4,5,6 - temperature, spray water flow, position of damper for variant II

Fig.17. Frequency response of reheated steam temperature control system

1 - variant I, 2 - variant II.



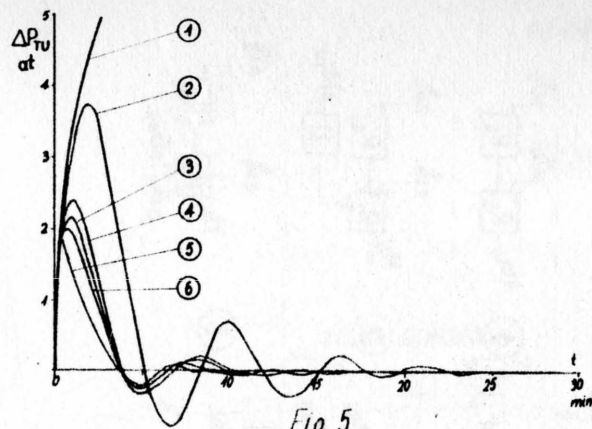


Fig 5.

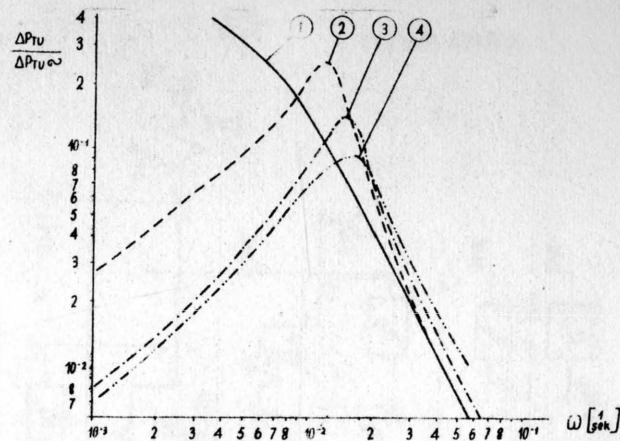


Fig 6

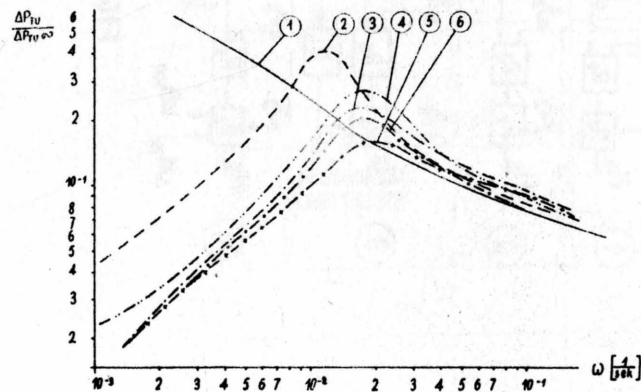


Fig 7.

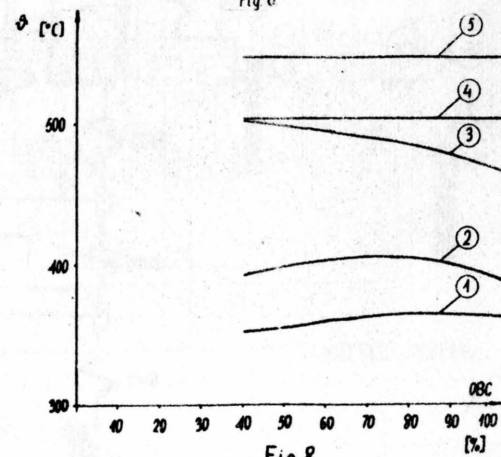


Fig 8

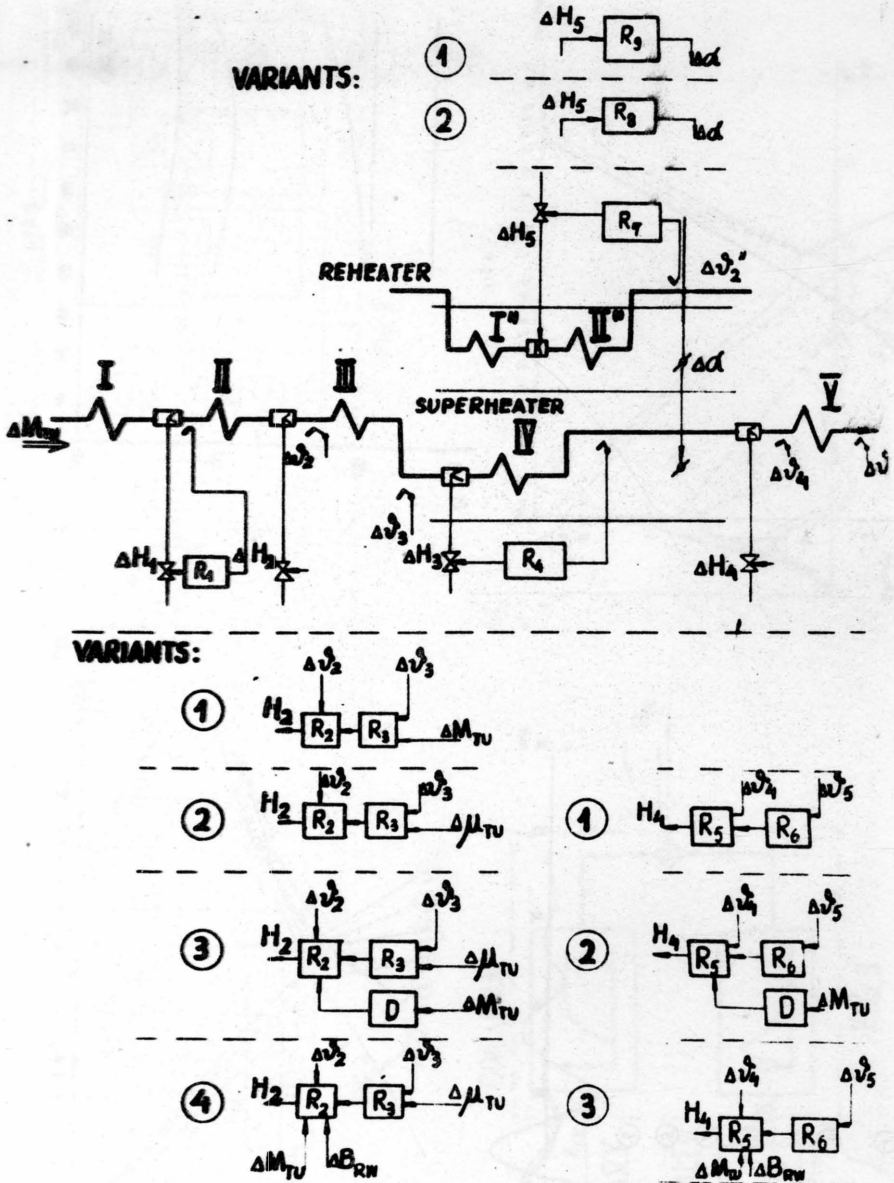


FIG. 9

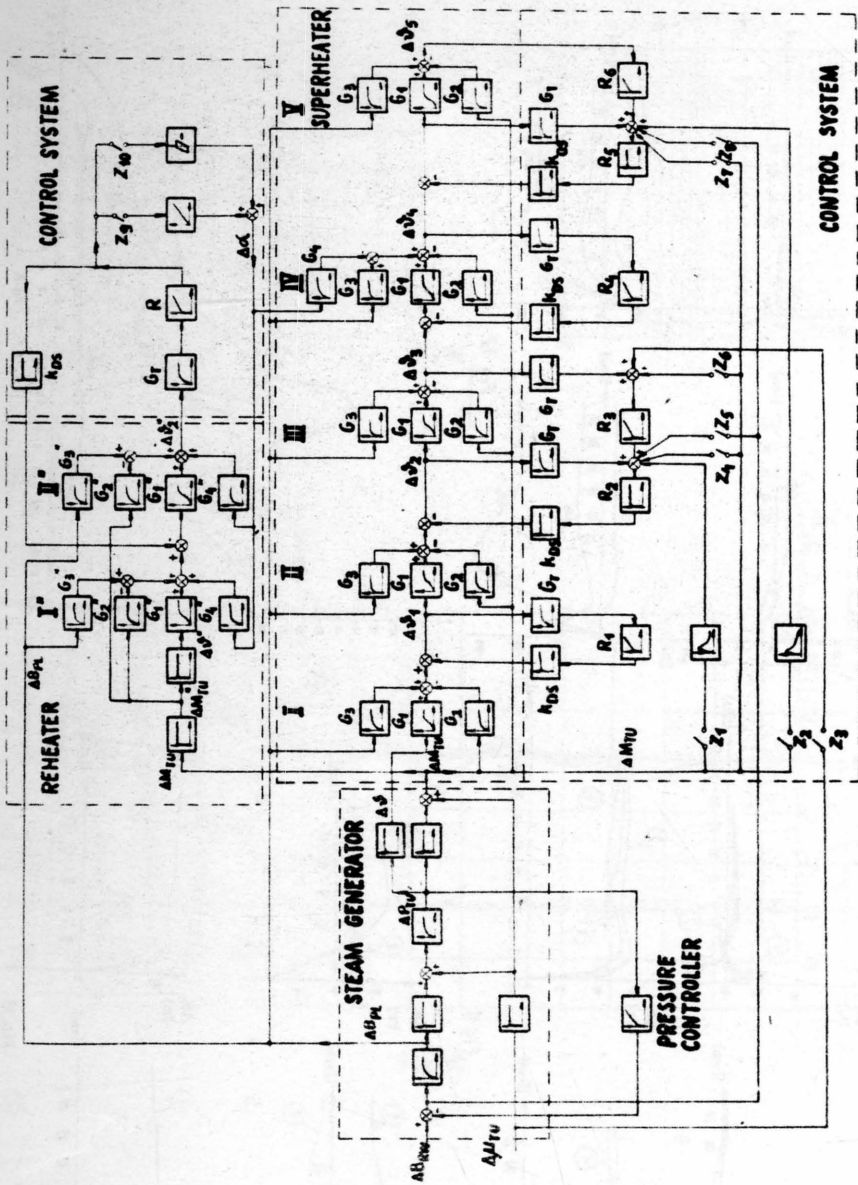


FIG. 10

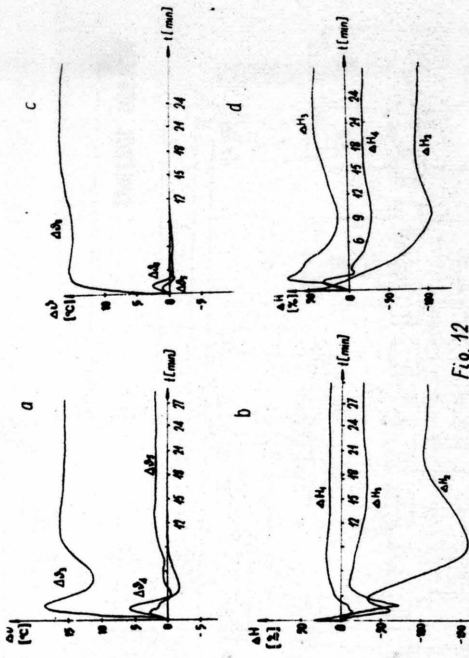


Fig. 12

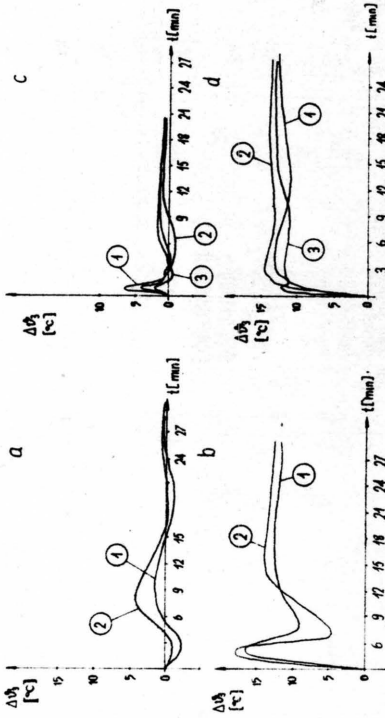


Fig. 11

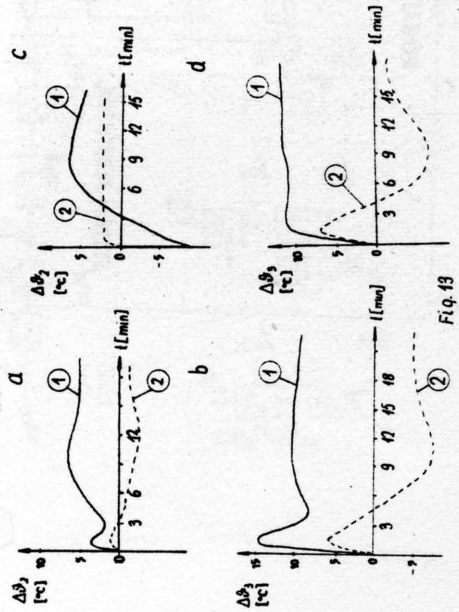


Fig. 13

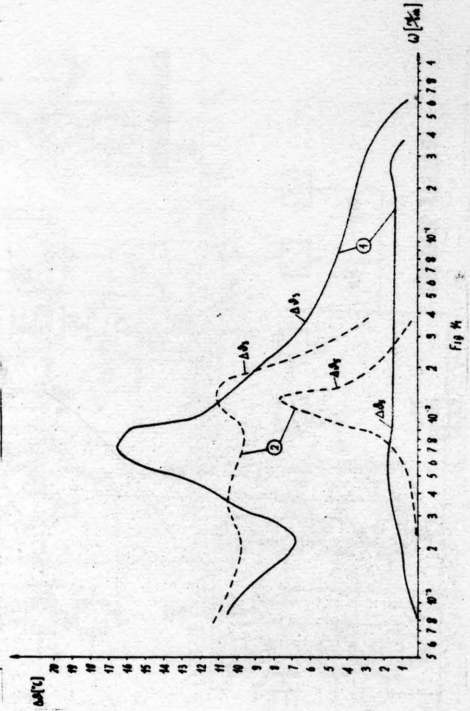


Fig. 14

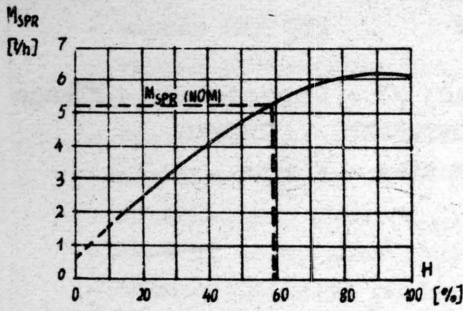


Fig. 15

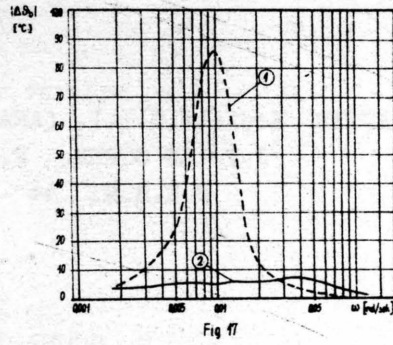


Fig. 17

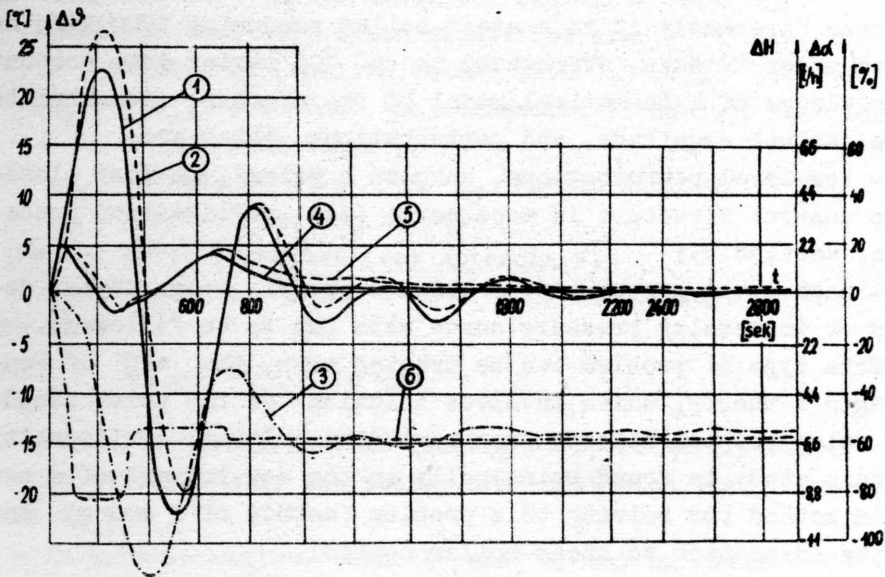


Fig. 46

OPTIMUM CONTROL OF A STEAM BOILER

by

H. APTER Société C.I.I. (ANALAC) 78 - Louveciennes - France
 J.F. LE CORRE, R. MEZENCEV, Y. THOMAS
 E.N.S.M. 44 - Nantes - France

1. SCOPE OF THE STUDY

The aim of this study is to obtain an optimal control of a process (presently it is a steam-boiler producing 1800 kg/h of steam under 22 bars, overheated to 360 °C) taking into account a knowledge of mathematical model of the process, constraints upon control magnitude, and perturbations, which are:

- low-level perturbations, unknown a priori, so that closed loop control structure is necessary (see reinitiation procedure, section 8);
- high-level perturbation, known a priori (e.g. power demand or increasing pressure curve which has to be followed).

This type of problem can be treated with the aid of Pontryagin's theory, which involves solution of two point boundary value problem raising important difficulties. Originality of this study is found principally in the development of a new rapid method for solving this problem (method of f and g) and in its adaptation to steam-boiler control.

We shall first define precisely the process model and performance index applied, then we'll proceed to detailed description of strategy relative to the method mentioned above.

2. PROCESS MODEL (Figure 1)

We recall that the steam-boiler can be described by:

- state variables:

- drum pressure (p_D)
- turbine pressure (p_S)

- superheating temperature (θ_S)
- water level in the drum (N)
- excess air (E)
- vacuum pressure in boiler furnace (D_F)
- control variables:
 - fuel flow (q_C)
 - air flow (q_A)
 - superheating flow (q_{DS})
 - feeding water flow (q_E)
 - chimney register position (R_F)
- main perturbation: load.

From a point of view of optimum design we consider the pressure only and its control variable: fuel flow (Fig. 2).

Conditions that rely other quantities are:

- $N = \text{const} = N_C$ (desired value) with $q_E = q_V$
- $q_A = f(q_C)$ such that the combustion is correct for each load value
- $q_{DS} = \text{const}$, so θ_S and p_S change arbitrarily
- $D_F = \text{const}$ by acting on R_F

We can write therefore (see Appendix 1):

$$\dot{p}_B = a q_C - b q_V \text{ with } a \text{ and } b \text{ both constant}$$

note that

$$q_{C \min} \leq q_C \leq q_{C \max}$$

In fact, for various load values, we could verify that:

- in steady state, the ratio b/a variation is lower or equal to 5 % ,
- in dynamic regime, both b and a may be known within accuracy 15 % (see Appendix 1).

3. PERFORMANCE INDEX

Performance index selection is justified by the following:

- 1) Control performances usually required (small deviations, low-level of control signal - in order to decrease the cost or to limit valve shocks) lead us to select a quadratic performance index with fixed terminal time T which, on the other hand, makes more easy the solution of Pontryagin's problem (in

fact it is known that in this case a complete theory can be established if no constraints are present, see Athans and Falb - Optimal Control, chapter 9).

2) Referring to the model equation (previous section), we consider fuel flow as a control variable. It would also be possible to choose for this purpose dq_c/dt which would allow us to take into account a performance deterioration due to valve shocks, but we would have then a second class process and a constraint upon state variable (q_c), i.e. two difficulties that we preferred to avoid in a first stage of the study.

3) As the high level perturbation known a priori - a pressure desired value is selected. We suppose that it varies in a step manner at a time instant t_p , belonging to interval $(0, T)$.

It is also possible to consider the instantaneous variations of steam flow; this would bring as however, for control variable selected as above, to a performance index inconsistent with essential physical significance. It doesn't represent any restriction to the generality of our study.

In addition we note that since Pontryagin's theory allows to introduce into design procedure the perturbation known a priori, we implement a predictive control.

Given these three principal conditions, we define

$$J(T) = \frac{1}{2} \int_0^T [(P - P_C(t))^2 + \mathcal{L} \dot{P}^2] dt$$

where $\mathcal{L} = \text{const}$ and T fixed.

4. PROBLEM STATEMENT

A recapitulation of the last two sections allows us to restate the problem.

knowing that $\dot{x} = u$

and $u \leq B$ ($B = \text{const}$)² with

$$\begin{cases} x = P - P_{c1} \\ u = aq_c - bq_c \\ q_v = \text{const} \end{cases}$$

determine $u(t)$ that minimizes $J(u) = \frac{1}{2} \int_0^T [(P - P_c)^2 + \alpha^2 u^2] dt$
for $t \in [0, T]$

$$\mathcal{L} = \text{const} \quad T \text{ fixed}$$

$$P_c(t) = P_{c1} + (P_{c2} - P_{c1}) \Gamma(t - t_p)$$

$$\Gamma(t - t_p) = 0 \text{ for } t < t_p$$

$$= 1 \text{ for } t > t_p$$

By application of the Pontryagin's theorem³ we obtain a canonical system as follows:

$$\dot{\Psi} = -x + (P_{c2} - P_{c1}) \Gamma(t - t_p)$$

$$\dot{x} = u$$

with $u = -\frac{\Psi}{\alpha^2}$ or B - the values that minimize the hamiltonian;

$$\begin{aligned} \text{boundary conditions are } \Psi(T) &= 0 \\ \dot{\Psi}(0) &= -x(0) \end{aligned}$$

Control structure is represented in Fig. 3, and the diffi-

² The case where u cannot exceed a maximal value is considered only, due to facts that the desired value step change $P_{c1} - P_{c2}$ arising at t_p is supposed positive and that $P(0) - P_{c1}$ is near zero. From theoretical point of view the problem is no more complex if it is supposed that $B_1 \leq u \leq B_2$.

³ We applied here the minimum principle, which differs from maximum principle by the fact that Ψ_0 is taken equal to +1 (in lieu of -1). Under such conditions, the adjoint variables Ψ written here are of opposite sign with respect to the adjoint variables of maximum principle.

culty of solution remains essentially in the determining of $\Psi(0)$.

5. CONTROL DETERMINING WHEN IT IS BELOW LIMIT B

In this case one has to solve:

$$\ddot{\Psi} - \frac{\Psi}{\alpha^2} = P_c(t) = (P_{c2} - P_{c1}) \delta(t - t_p)^{\equiv} \quad (1)$$

taking into account the boundary conditions $\Psi(T) = 0$ and $\dot{\Psi}(0) = -x(0)$.

Determining of $\Psi(0)$ can be performed with the aid of auxiliary functions f and g defined by

$$\Psi(t) + f(t) \dot{\Psi}(t) = g(t) \quad (2)$$

with $f(T) = g(T) = 0$ which involve therefore $\Psi(T) = 0$ independently of $\dot{\Psi}(T)$.

We differentiate equation (2)

$$\dot{\Psi}(1 + \dot{f}) + f \ddot{\Psi} = \dot{g} \quad (3)$$

Solutions $\Psi, \dot{\Psi}, \ddot{\Psi}$ of a linear system (1), (2), (3), have to be independent of the functions f and g , so they will take the form of $\frac{0}{0}$.

This involves two relationships for f and g

$$\dot{f} = \frac{f^2}{\alpha^2} - 1$$

$$\dot{g} = \dot{f} \left(\frac{g}{\alpha^2} - \dot{\Psi}_c \right)$$

which have to be integrated in backward time direction, since $f(T) = g(T) = 0$.

Having obtained so $f(0)$ and $g(0)$, according to (2) we may write:

\equiv

$\delta(t - t_p)$ - unit impulse.

$$\Psi(0) = g(0) - f(0) \dot{\Psi}(0) = g(0) + f(0) x(0) \quad (= \Psi_{01})^{\#}$$

Remark. In present case all computations may be performed manually and some results are given in the Appendix 2.

6. CONTROL DETERMINING WHEN IT REACHES THE LIMIT B

Assuming that $x(0)$ is near zero ~~we~~ we have a probable control trajectory as in Fig. 4 (t_1 can be zero) ~~we~~.

Referring to the canonical system in section 4, we'll can obtain $u(t)$ for $t \in [0, T]$ with the aid of the analog scheme represented in Fig. 3; however, we have to compute the initial value $\Psi(0)$ before.

We recall that the equations to be solved are:

$$\ddot{\Psi} - \frac{\Psi}{\mathcal{L}^2} = 0 \quad \text{for segments 1 and 3}$$

$$\dot{x} = B$$

$$\dot{\Psi} = -x + (P_{c2} - P_{c1}) \Gamma(t - t_p) \quad \text{for segment 2}$$

We have otherwise the boundary conditions

$$\Psi(T) = 0 \quad \dot{\Psi}(0) = -x(0) \quad \text{and switching conditions}$$

$$\Psi(t_1) = \Psi(t_2) = -\mathcal{L}^2 B, \quad \dot{\Psi}(t_1^-) = \dot{\Psi}(t_1^+)$$

$$\dot{\Psi}(t_2^-) = \dot{\Psi}(t_2^+) \quad (\text{if } t_2 \neq t_p)$$

Principle of determining $\Psi(0)$ is as follows: (Fig. 5):

For segment 3 we have

$$\Psi + f\dot{\Psi} = 0 \quad (2) \quad (g = 0 \quad \text{since } \dot{\Psi}_c = 0, \text{ see section 5}).$$

[#] Notation used in the general flow-diagram.

^{we} The value of $x(0) = P(0) - P_{c2}$ in the case when it doesn't reach the limit B could be specified with the aid of the obtained trajectories.

^{we} Taking into account that $\Psi(T) = 0$, that the desired value step arises at time t_p which is placed naturally between $T/4$ and $3T/4$, and that \mathcal{L} assumes a moderate weighting value.

If, integrating f in the backward time direction from $t = T$, we suppose that at actual time instant t , $\psi(t) = -\mathcal{L}^2 B$, i.e. that $t = \tilde{t}_2$, using (2) we have

$$\tilde{\psi}(\tilde{t}_2) = \frac{\mathcal{L}^2 B}{f(\tilde{t}_2)}.$$

Taking so \tilde{t}_2 , $\tilde{\psi}(\tilde{t}_2) = -\mathcal{L}^2 B$, and $\tilde{\dot{\psi}}(\tilde{t}_2)$, we can immediately obtain $\tilde{\psi}(0)$ and $\tilde{\dot{\psi}}(0)$ by solving algebraic equations (see shape of trajectories in Fig. 6).

When $\tilde{\dot{\psi}}(0) = -x(0)$ we have $t = \tilde{t}_2 = t_2$ and $\tilde{\psi}(0) = \psi(0) (= \psi_{02})$ (the initial condition for ψ integrator on Figure 2.).

In the same manner as in previous section, only one integration in backward time direction supplies the backing initial condition.

When the time instant t_1 is zero, the method in finding $\psi(0)$ (called now ψ_{03}) remains the same. However, the formula for $\dot{\psi}(0)$ is different now, because of the lack of segment 1, which makes necessary to solve a new algebraic equations system, then apply an appropriate logic (see general flow-diagram).

Finally, if in the interval $[t_p, T]$, covered in the backward time direction, the equations $\dot{\psi}(0) = -x(0)$ are never satisfied, the control is not saturated and we have to return to the solution of section 5.

Since the function $g(t)$ is zero in $[t_p, T]$, these three cases presented in sections 5 and 6 meet together and may be summarized in the flow-diagram presented below.

This flow-diagram was implemented on two analog computers, Analac A 10 for computation of $\psi(0)$, and T.R. 48 for computation of fuel flow control with a synchronous logic system DES 30 which took care of the logic control of the overall system.

~~xxx~~ Sign \sim means that the functions $\psi, \dot{\psi}$ and the variable t_2 are not yet necessarily optimal.

~~xxx~~ Notation used in the general flow diagram.

7. REINITIATION PROCEDURE

The computation of $\Psi(0)$ is periodically repeated (period τ) for a new value of state variable $P(\tau) - P_{c1}$ and allows to restore periodically the initial conditions of control integrator (of Ψ).

This type of closed loop control with re-adjusting allows us:

1) To perfect analog performances, which becomes of primary importance when sensibility coefficient $\partial \Psi(T) / \partial \Psi(0)$ is very high

($= \text{ch } \frac{T}{\alpha}$ if the constraint is not present).

In fact, for low values of α , an insufficient accuracy of the computation of $\Psi(0)$ makes the system divergent, which can be avoided by reinitiation.

2) To compensate model inaccuracies.

3) To react against moderate-level perturbations.

8. EXPERIMENTAL RESULTS

We distinguish simulation results and results obtained on the process, mentioning that the simulation was performed with the values identical to real process characteristics.

1) Simulation results

Method of computation of $\Psi(0)$ presented above enable to plot the control and pressure evolutions for various values of the parameters \mathcal{L} , t_p , T , $P_{c2} - P_{c1}$, B and $P(0) - P_{c1}$.

Figures 6 and 6bis represent evolution of x and \dot{x} for various α , with and without magnitude constraint upon x ($= u$) ($P(0) - P_{c1} = 0$, $T = 200$ sec, $t_p = T/2$).

We note that for low values of α , the control conforms to unit impulse $\delta(t - t_p)$ while for high α , u becomes identically zero. This clarifies well the meaning of α .

For low values of α , the computation of $\Psi(0)$ appears to be insufficiently accurate, since the sensibility coefficient $\partial \Psi(T) / \partial \Psi(0)$ assumes high value (equal to $\text{ch } \frac{T}{\alpha}$ if the constraint is not present). This justifies partially the need of

control reinitiation.

Finally we note that the hypothesis on necessary saturation of the saturated control at time t_p is verified.

If now α is fixed at 100 sec (and $P(0) - P_{c1} = 0$) and if t_p varies between 0 and T, curves in Fig. 7 present a predictive nature of this optimization.

Another important point may be outlined: (case with constraint, Fig. 7bis). If t_p is below some value which may be called critical (here 100 when $B = 0.01$), the control becomes independent of t_p . It can be otherwise verified (7 ter) that $\psi(t, t_p)$ is unique for $-(\psi/\alpha^2) \leq B$. This is consistent to the structure of the hamiltonian which has a step arising at t_p (we find by calculation

$$H(t) = [P(T) - P_{c2}]^2 + \eta(t) [(P_{c2} - P_{c1})(P(t_p) - P_{c1}) - \frac{1}{2} (P_{c2} - P_{c1})^2],$$

$$(\eta(t) = 0 \quad \forall t \in]t_p, T] \quad \eta(t) = 1 \quad \forall t \in [0, t_p])$$

(this can be verified in Fig. 11)). Under these circumstances, the curves $\psi(t, t_p)$ in Fig. 7 ter have to be "parallel" for t lower than the lowest value of t_p considered in this figure (here $t_p = 40$ sec).

In Fig. 8 the variations of T when constraint is present are shown (in fact if there is no constraint, x and \dot{x} are functions of t/α , t_p/α and T/α , and the curve system with T variable can be obtained from similar system with variable which is shown in Fig. 6).

Finally in Figures 9 (9bis) and 10, the plots of x and \dot{x} as functions of $P(0) - P_{c1}$ and of B, are shown. This completes a set of curves that permit:

- to verify a good accuracy of the "method of f and g" with respect to the vanishing of $\psi(T)$, and to the behavior of hamiltonian as a step function;
- to select a priori (by a user) the coefficients α and T;
- to provide a quasi-optimum control for which the formula for $\psi(0)$ computed algebraically on-line would be obtained

by regression based on the whole set of above simulation results.

2) Results obtained on the process

First we ascertain that the model selected has an acceptable static and dynamic accuracy as well. In fact, in absence of perturbation, the reinitiation with period $T/4$ doesn't involve any significant impulse of control signal, which proves that even during considerable time interval $T/4$ the system dynamics can be approached by a simple integrator.

On the other hand, if the optimization is performed on the basis of steady state, the fuel flow values at time instants 0 and T are nearly the same, which implies that the accuracy of 5 % (mentioned earlier) for the b/a ratio is preserved in steady state.

Under these circumstances, a reinitiation period of order of $T/10$ would appear satisfactory to make the difference between simulation and process trajectories lower than 1 %.

Finally, in order to obtain a more efficient control in presence of random perturbations, we performed some experiments with reinitiation period $T/20$.

A study undertaken now will enable us undoubtedly to increase the reinitiation period by readjusting model parameters during optimization process, thus decreasing the performance index value.

We show here the records of pressure deviation and fuel flow for following values: $q_{c \max} = 125 \text{ kg/h}$, $\tau = 100 \text{ sec}$, $T = 200 \text{ sec}$, reinitiation period = 10 sec, each record corresponding to another initial value of pressure deviation. So from Fig. 12 to Fig. 15 we proceed from an unsaturated trajectory to a trajectory saturated from the very beginning of the optimization procedure.

9. CONCLUSION

We came to establish a method for determining optimal control for a simple process.

This method is quick and accurate. However it makes necessary the use of a considerable installation, which could be

improved by application of more adapted technical facilities. We mean here a use of a hybrid type II system. It would be advantageous to interconnect a real-time digital computer to an analog computer (type TR 48).

The use of this advanced technology seems to be of capital weight for application of the method of f and g to a more complex process.

The hybrid type II system would have to be implemented after a study on reinitiation, intended to determine the optimal value of reinitiation period under random perturbations and model inaccuracies, is performed. This system could also adapt itself during operation.

Besides, it would be interesting to try to simplify the f and g method. We have in mind to obtain from plots shown previously and from the functions computed in the analog solution presented - the approximate algebraic formulas giving initial conditions for adjoint variables. These formulas could be numerically computed in real time and introduced to an analog set-up representing the adjoint system.

These simplified methods, by their form as well as implementation, would enable to undertake an optimal multivariable control for a line of pressure of superheated steam (pressure and temperature), for which an identification is performed actually.

Note. These researches are performed in the framework of a contract of D.G.R.S.T. (Automation Committee).

REFERENCES

1. Pontryagin et al., The Mathematical Theory of Optimal Processes. J. Wiley 1962.
2. F. Garnier, H. Ghoulahouri, Elements de théorie pour la résolution de certains problèmes d'optimisation avec modèle mathématique. Publication Analac, 1er octobre 1965.
3. P. Naslin, Introduction à la commande optimale. Dunod 1966.
4. M. Athans, P.L. Falb, Optimal Control. Mc Graw Hill 1966.
5. Y. Thomas, J.F. Le Corre, H. Apter, Application du principe du maximum à la détermination sur calculateur analogique d'une commande optimale de chaudière. Congrès AICA 67, Lausanne 28 août, 2 septembre.

Appendix I

DETERMINING OF THE MATHEMATICAL MODEL USED
TO OBTAIN AN OPTIMAL CONTROL

Steam-boiler equations may be classified into two groups:

- equations of thermal equilibrium of flue gases and exchangers,
- equations of steam-generator.

Heat flux into exchangers in steady state

In order to determine a rate of heat flux supplied to fluid circulating in each exchanger (evaporator, superheater, downpipes), a total flux supplied by combustion and furnace temperature is calculated first. Next, energy conservation laws for each exchanger are written.

It can be shown therefore that, in steady state:

$$\phi_{ev} = k_{ev} \phi \quad (1)$$

$$\phi_s = k_s \phi \quad (2)$$

$$\phi_{ec} = k_{ec} \phi \quad (3)$$

$$\phi = k_c \omega_c$$

where

ϕ = total heat flux produced by the combustion

h_c = fuel calorific value

ω_c = fuel flow

ϕ_{ev} = heat flux supplied to the fluid in evaporator tubes

ϕ_s = heat flux supplied to the steam in the superheater

ϕ_{ec} = heat flux supplied to the water in downpipes

k_{ev}, k_s, k_{ec} - coefficients depending in particular on boiler load and on excess air control

$$k_{ev} + k_s + k_{ec} < 1$$

Steam-generator operation in steady state

Steam generator consists of:

- nest of tubes
- drum
- downpipes or economizers

Equations of energy and continuity in evaporator tubes

Let E_{ev} be the energy accumulated in evaporator tubes. We have:

$$\phi_{ev} + \omega^{ec} h_{e1} - \omega_e^{ev} h_e^{ev} - \omega_v^{ev} h_v^{ev} = \dot{E}_{ev} \quad (5)$$

where:

ω^{ec} = circulating water flow at the input of evaporator tubes

h_{e1} = water enthalpy at the input of evaporator tubes

ω_e^{ev} = water flow at the output of evaporator tubes

h_e^{ev} = water enthalpy at the output of evaporator tubes

ω_v^{ev} = steam flow at the output of evaporator tubes

h_v^{ev} = steam enthalpy at the output of evaporator tubes

We shall suppose that:

$h_e^{ev} = H_e(p)$ = water enthalpy at saturation pressure p

$h_v^{ev} = H_v(p)$ = steam enthalpy at saturation pressure p

and that the pressure at each point is equal to the saturation pressure p .

Let M_e^{ev} and M_v^{ev} be the mass of water and steam respectively, in the evaporator tubes; we have

$$\omega^{ec} - (\omega_e^{ev} + \omega_v^{ev}) = \dot{M}_e^{ev} + \dot{M}_v^{ev} \quad (6)$$

Equations of drum operation

We have a mass conservation law

$$\omega_{ea} - \omega^{ec} + \omega_e^{ev} + \omega_v^{ev} - \omega_v^B = \dot{M}_e^B + \dot{M}_v^B \quad (7)$$

where:

ω_{ea} = feeding water flow

v^B = drum inner volume

$M_{e,v}^B$ = mass of water, steam, in the drum.

We shall neglect the phenomenons of condensation or evaporation inside the drum, which supposes that the steam and the water are at the saturation temperature at each point inside the drum.

Next, we shall assume that the feeding water is mixed with circulating water at the input of downpipes and that there is no heat exchange between water and walls in the drum. Neglecting also the phenomenons of vaporisation and recondensation in the drum, we can write:

$$\omega_v^{ev} - \omega_v^B = \dot{M}_v^B \quad (8)$$

We'll write now the energy conservation equation of the drum which is supposed to receive no heat flux.

$$-\omega_v^B H_v + \omega_e^{ev} H_e - \omega_v^{ev} H_v - (\omega^{ec} - \omega_{ea}) H_e = \dot{E}^B \quad (9)$$

where E^B = energy accumulated in the drum.

Equations of downpipes operation

Energy conservation equation is:

$$\omega^{ec} h_{eo} - \omega^{ec} h_{e1} + \phi_{ec} = \dot{E}_{ec} \quad (10)$$

where

$h_{eo,1}$ = water enthalpy at the downpipes input or output

E_{ec} = energy contained in the water of downpipes

On the other hand, the mixing of feeding water with circulating water issued from drum proceeds with energy conservation, thus:

$$\omega_e H_e + \omega_{ea} h_{ea} = \omega^{ec} h_{eo}$$

$$(\omega^{ec} - \omega_{ea}) H_e + \omega_{ea} h_{ea} = \omega^{ec} h_{eo}$$

$$\omega^{ec} H_e - \omega_{ea} (H_e - h_{ea}) = \omega^{ec} h_{eo}$$

$$\omega^{ec}(H_e - h_{eo}) = \omega_{ea}(H_e - h_{ea}) \quad (11)$$

Simplification of equations for steady-state operation

In steady-state, the equations (5) - (9) and (10) become respectively:

$$\phi_{ev} + \omega^{ec}h_{e1} - \omega_e^{ev}H_e(p) - \omega_v^{ev}H_v(p) = 0 \quad (12)$$

$$\omega^{ec} - (\omega_e^{ev} + \omega_v^{ev}) = 0 \quad (13)$$

$$\omega_{ea} - \omega^{ec} + \omega_e^{ev} + \omega_v^{ev} - \omega_v^B = 0 \quad (14)$$

$$\omega_v^{ev} - \omega_v^B = 0 \quad (15)$$

$$-\omega_v^B H_v(p) + \omega_e^{ev} H_e(p) - \omega_v^{ev} H_v(p) (\omega^{ec} - \omega_{ea}) H_e(p) = 0 \quad (16)$$

$$\omega^{ec}h_{eo} - \omega^{ec}h_{e1} + \phi_{ec} = 0 \quad (17)$$

Summing equations (13), (14) and (15) we have:

$$\omega_{ea} - \omega_v^B = 0 \quad (18)$$

Summing equations (12), (16), (17) and (18) we have:

$$\phi_{ev} + \phi_{ec} - \omega_v^B H_v(p) + \omega_{ea} H_e(p) = 0 \quad (19)$$

Using (18) and, on the other hand, (1), (3) and (4), equation (19) becomes:

$$(k_{ev} + k_{ec})h_c \omega_c - H_v(p) - H_e(p) \omega_v^B = 0 \quad (20)$$

We define then the coefficients \mathcal{L} and β such that:

$$\mathcal{L} = (k_{ev} + k_{ec})h_c, \quad \beta = H_v(p) - H_e(p)$$

Equation (20) can be written now:

$$\alpha \omega_c - \beta \omega_v^B = 0$$

This equation is satisfied in steady-state only. However, it is known by experience that for slowly varying regimes one can write:

$$\alpha \omega_c - \beta \omega_v^B = k \dot{p}$$

Or, dividing by k and setting:

$$a = \alpha/k, \quad b = \beta/k \quad \text{we have} \quad \dot{p} = a \omega_c - b \omega_v^B$$

We have determined experimentally the coefficients a and b in the following manner: for steam flow values varying between 45 % and 95 % of its nominal value,

1) fuel flow is varied until $\dot{p} = 0$ (steady state) (for the rest all other quantities are stable), so the ratio b/a is obtained: $b/a = 0.09$ within 5 %;

2) starting from steady-state, we feed the step inputs to ω_c (and next to ω_v^B), and obtain b and a within accuracy of 15 %

$$(a = 1.25 \text{ bar/kg}, \quad b = 0.1125 \text{ bar/kg})$$

Appendix II

SOME RESULTS OF CALCULATION

$$\text{The control is} \quad u = -\frac{\psi}{\alpha^2}$$

$$\begin{aligned} \text{with } \psi \text{ being solution of } \ddot{\psi} - \frac{\psi}{\alpha^2} &= \dot{P}_c(t) = \\ &= (P_{c2} - P_{c1}) \delta(t - t_p) \end{aligned}$$

$$(\psi(T) = 0, \quad \dot{\psi}(0) = -x(0))$$

We obtain

$$\psi(t) = +\psi(0) \operatorname{ch} t/\alpha + \alpha \dot{\psi}(0) \operatorname{sh} t/\alpha +$$

$$+ \alpha(P_{c2} - P_{c1}) \operatorname{sh} \frac{t - t_p}{\alpha} \Gamma(t - t_p) \quad *$$

which gives

$$\Psi(0) = \alpha x(0) \operatorname{th} \frac{T}{\alpha} - \alpha(P_{c2} - P_{c1}) \frac{\operatorname{sh} \frac{T - t_p}{\alpha}}{\operatorname{ch} \frac{T}{\alpha}}$$

Knowing that $u = -\frac{\dot{x}}{\alpha}$ and $\dot{x} = u$ we can calculate also:

$$x(T) = (P_{c2} - P_{c1}) + \frac{x(0) - (P_{c2} - P_{c1}) \operatorname{ch} t_p / \alpha}{\operatorname{ch} T / \alpha}$$

On the other hand, we can represent $H(t)$ by

$$H(t) = H(T) - \int_t^T \frac{\partial H}{\partial t} dt$$

we take

$$H(t) = (P(T) - P_{c2})^2 + \eta(t) \left[(P_{c2} - P_{c1})(P(t_p) - P_{c1}) + \right. \\ \left. - \frac{1}{2} (P_{c2} - P_{c1})^2 \right]$$

$$\eta(t) = 0 \quad \forall t \in]t_p, T] \quad \eta(t) = 1 \quad \forall t \in [0, t_p[$$

We recall that $x = P - P_{c1}$.

* $\Gamma(t - t_p) = \text{unit step.}$

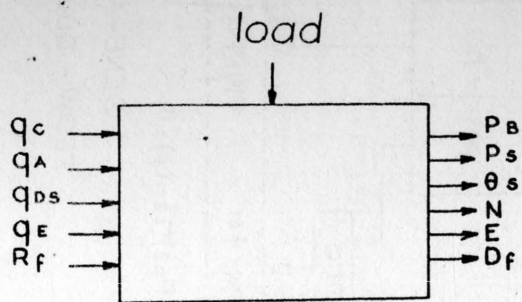


fig. 1

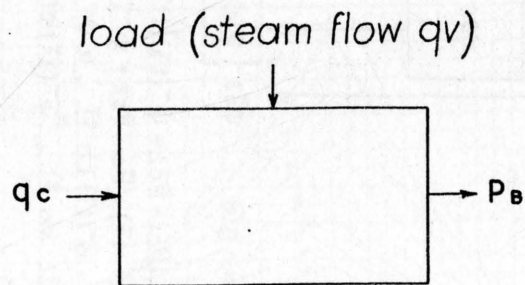


fig. 2

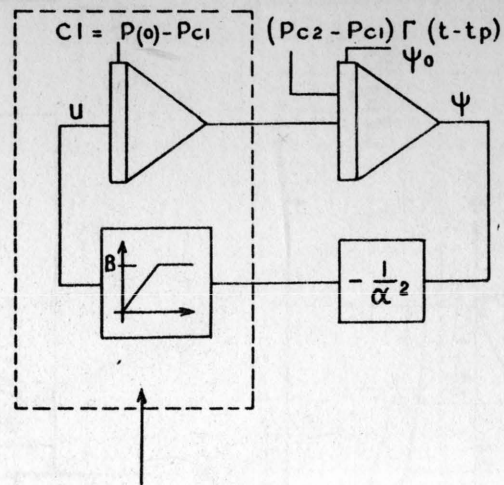


fig. 3

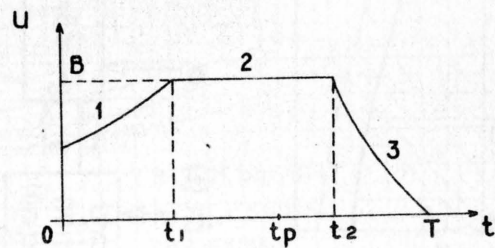


fig. 4

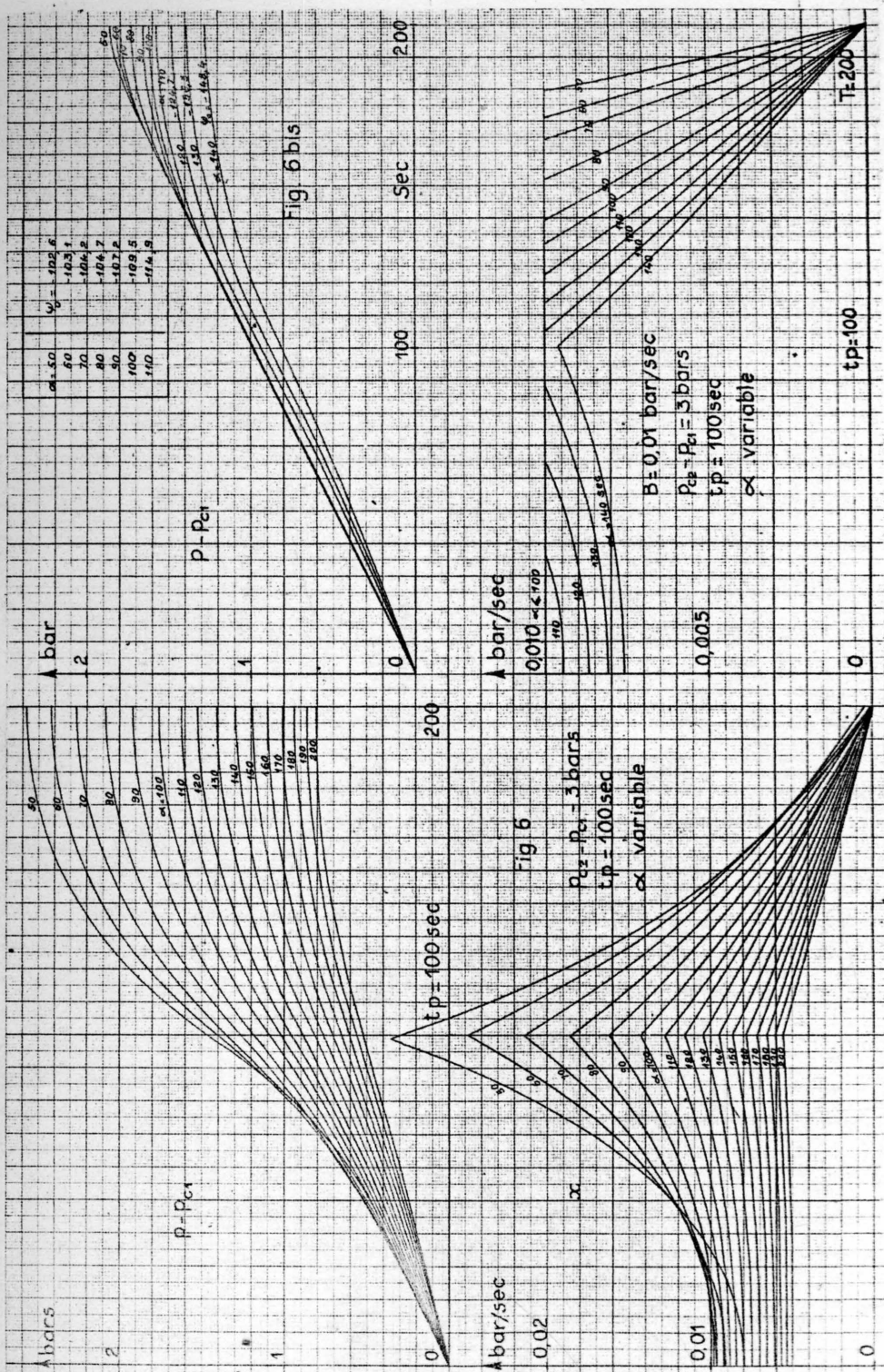
The flowchart illustrates the algorithm for the numerical solution of the problem of the stability of the motion of a system with respect to a parameter. The process begins with inputs α and $\dot{p}_c(t)$ entering a block labeled "backward integration of $f(t)$ and $g(t)$ ". This block outputs f and g . The input α also enters a block labeled $g = -\alpha^2 B + f\dot{\psi}$, which also receives f from the first block. The output of this block is $\dot{\psi}^{\sim}(t^{\sim}z)$. This derivative is then integrated in a block labeled "backward integration" to produce $\psi^{\sim}(t^{\sim}z)$. The initial condition for this integration is given by the equation $\psi^{\sim}(t^{\sim}1) = \psi^{\sim}(t^{\sim}2) = -\alpha^2 B$. The $\psi^{\sim}(t^{\sim}z)$ signal is then fed into two blocks labeled "see system of equations**" and "see system of equations*", which are connected by a bidirectional arrow labeled $t = t^{\sim}z$. The output of the "see system of equations**" block is $\dot{\psi}^{\sim}(0) = -P(0) + P_{c1}$, which enters a decision block with "yes" and "no" outputs. The output of the "see system of equations*" block is $\dot{\psi}^{\sim}(0) = P(0) + P_{c1}$, which enters another decision block with "yes" and "no" outputs. The "yes" outputs of both decision blocks lead to an "and" block. The "no" outputs of both decision blocks lead to a dashed box containing the final results: $\psi(0) = \psi^{\sim}03$, $\psi(0) = \psi^{\sim}01$, $\psi(0) = \psi^{\sim}02$, and $\psi^{\sim}02$. The initial output of the first block also leads to the final result $f(0)(P(0) - P_{c1}) + g(0)$.

$$\begin{aligned} & -\frac{B}{2}(t\bar{z}-t\bar{t})^2 + [P_{C1}-P_{C2}+\psi^{\sim}(t\bar{z})](t\bar{t}-t\bar{z}) + (P_{C1}-P_{C2})(t\bar{z}-t_p) = 0 \\ & \psi(t\bar{t}) = -B(t\bar{t}-t\bar{z}) + P_{C1}-P_{C2} + \psi^{\sim}(t\bar{z}) \\ & \psi_{oz} = \psi^{\sim}(o) = \psi^{\sim}(t\bar{t}) \operatorname{ch} \frac{t\bar{t}}{\alpha} - \alpha \psi^{\sim}(t\bar{t}) \operatorname{sh} \frac{t\bar{t}}{\alpha} \\ & \psi^{\sim}(o) = -\frac{\psi^{\sim}(t\bar{t})}{\alpha} \operatorname{sh} \frac{t\bar{t}}{\alpha} + \frac{\alpha}{\psi^{\sim}(t\bar{t})} \operatorname{ch} \frac{t\bar{t}}{\alpha} \end{aligned}$$

GENERAL
FLOW DIAGRAM

$$\psi^*(t_0) = B \tilde{t}^2 + P_{c1} - P_{c2} + \tilde{\psi}(\tilde{t}^2)$$

$$\gamma(t_0) = -\alpha^2 B - \tilde{\psi}(\tilde{t}^2) \tilde{t}^2 + (P_{c2} - P_{c1}) t_p - \frac{B}{\alpha} \tilde{t}^2$$



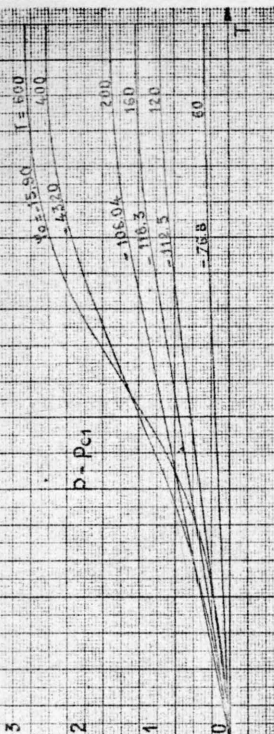


Fig 7 ter

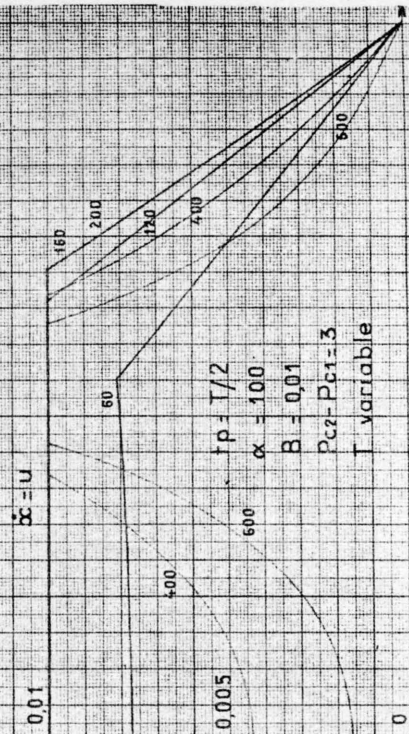


Fig. 8

$$t_p = T/2$$

$x = 100$

B-001

Doc. 101-3

9
8
7
6
5
4
3
2
1

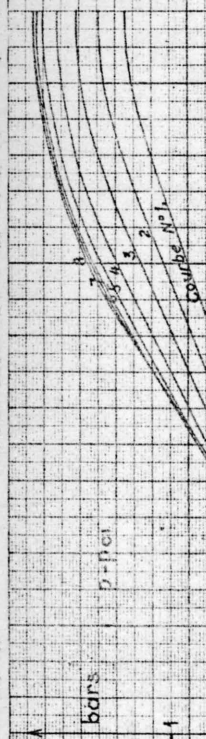


fig 10

Courbes	N°	α	β
1	1	-162.18	0.007
2	2	-143.92	0.008
3	3	-126.39	0.009
4	4	-109.75	0.010
5	5	-96.48	0.012
6	6	-85.04	0.013
7	7	-74.50	0.014
8	8	-64.50	0.016

$\alpha = U$

bar/sec

Courbe N° 1

$\alpha = 100$

$t_p = 100$

$T = 200$

$p_{02} - p_{01} = 3$ bars

B variable

$\Delta \text{ bar}^2$

$p(t) - p_{01} = 2$ bars

$2H(t)$

$\alpha = 100 \text{ sec}$

$p_{02} - p_{01} = 3$ bars

$t_p = 100 \text{ sec}$

Sans Butée

without constraint

$p(t) - p_{01}$

$2H(t)$

$p(t) - p_{01} = 2$ bars

$2H(t)$

Secondes

fig 11

$\Delta p - p_{c1} \text{ (bars)}$

3

2

1

0

0

100

200

$\alpha = 100$
 $T = 200s$
 $t_p = 100s$
 $p_0 - p_{c1} = 1,5 \text{ bar}$

fig. 12

$\Delta q_c \text{ (kg/h)}$

$q_c \text{ max}$

120

100

80

0

100

200

$\alpha = 100$
 $T = 200s$
 $t_p = 100s$
 $p_0 - p_{c1} = 1,5 \text{ bar}$

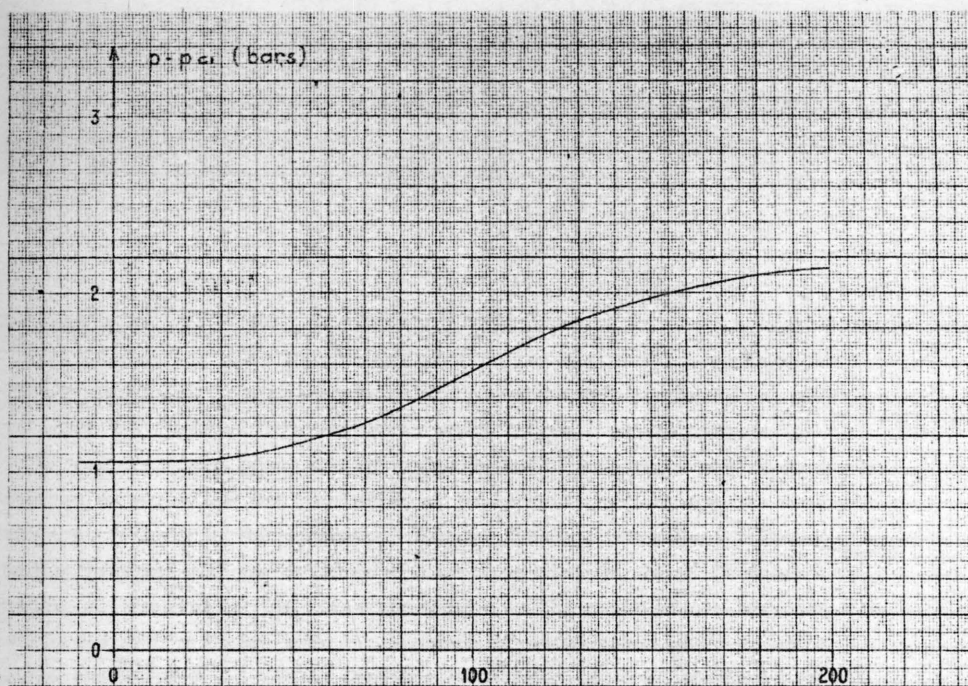
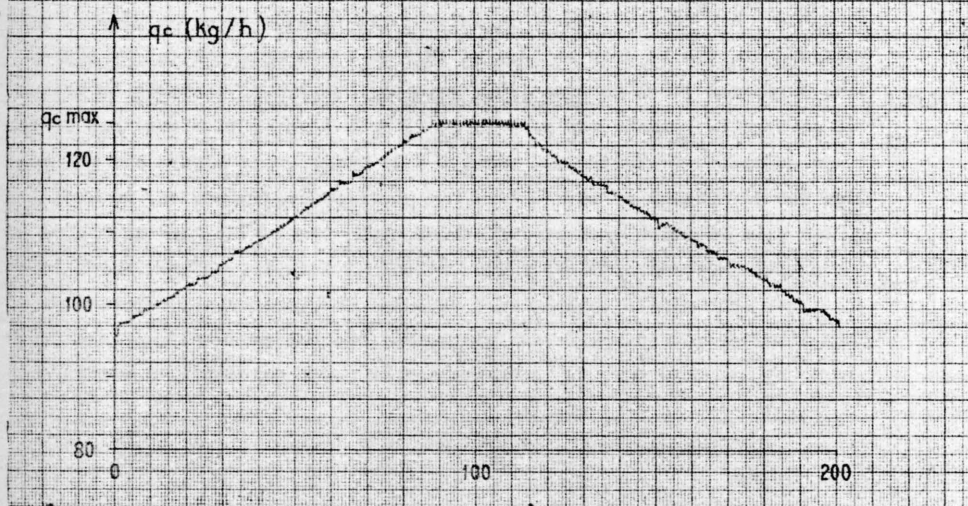


fig. 13



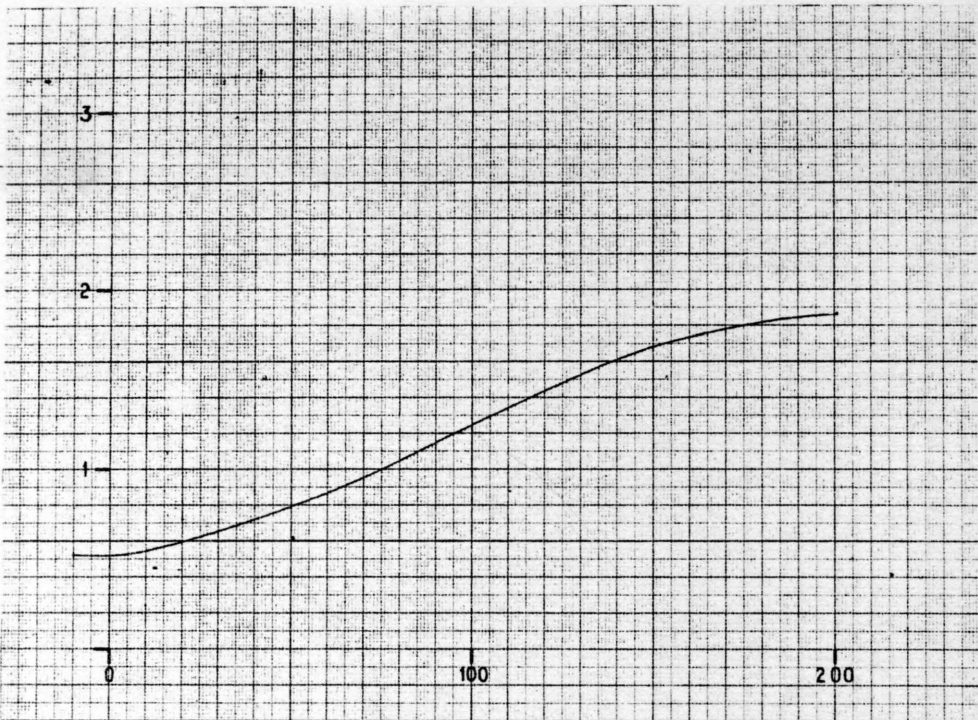
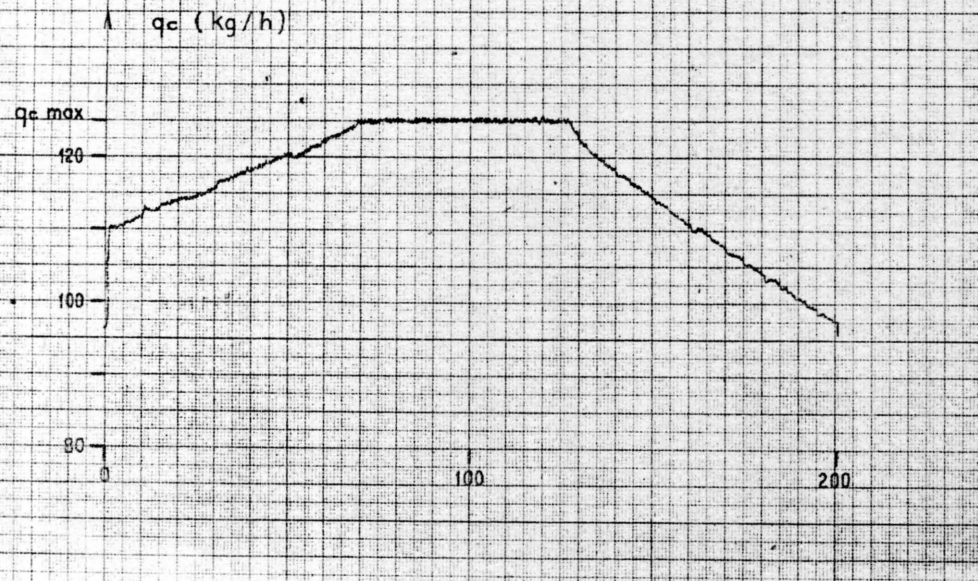


fig 14



COMPARISON OF DYNAMICS BETWEEN NATURAL CIRCULATION BOILER AND FORCED CIRCULATION BOILER

K. Itoh *
 M. Fujii **
 H. Ohno **
 K. Sagara**

Introduction:

An allowance for load fluctuation of a boiler has become more important to the regulation of a power system. A number of efforts have been made to clear the dynamics of a boiler in order to increase the allowance.

The two different types of boiler discussed in this paper have been installed to serve for the regulation of power system which have the load of electric railway in the suburbs of Tokyo. One is a natural circulation boiler (N-type) and the other is a forced one (C-type) of 75 MW nominal rating respectively. The boiler installed in the power system has been disturbed with a random load fluctuation, of which power spectrum has a large amount of 2 - 3 minute periodic components as shown in Fig.1, owing to the start-stop of trains. Moreover, the boiler has been required to shut down in midnight for the reason of no train running.

The boiler containing a large size pressure part is, generally, not able to start quickly due to the thermal shock problem. On the contrary, for the large heat capacity, it is apt to absorb a rapid periodic load fluctuation. In this sense, the boiler suited for this situation must satisfy such an incompatible requirement as to cope with the rapid load fluctuation as well as to be able to start quickly.

C-type boiler shortens start up time by half as much as N-type. This is because of decrease in size of pressure part, such as drum, downcomer etc. and it can take a large heat flux in furnace in the warming up process by securing the stable circulation with a pump. The stable circulation being secured the nominal circulation ratio of C-type is reduced to one half or less than that of N-type. This causes to decrease water holding and metal weight in the circulating loop by about 60-70%. However, this may be an undesirable tendency for the load fluctuation. Therefore, the experiment has been carried out to clarify the allowance for periodic load fluctuation of these two types of boiler.

* Tokyo Power Supply Control Division, Japanese National Railways,

Tokyo, Japan.

** Technical Headquarters, Mitsubishi Heavy Industries, Ltd., Tokyo, Japan.

The goal of this investigation is to compare the dynamics of both types of boiler to clarify the essential factor of the difference in the allowances.

Boilers discussed are different from each other in design philosophy due to the different erection time and in main fuel such as pulverized coal for N-type and heavy oil for C-type.

Comparison of Allowances between Two Types of Boiler:

The experiments have been carried out by means of changing the load demand including controllers.

The disturbances used in the experiments are sinusoidal for N-type and M-sequence of 20 sec. a bit, 127 bits per period for C-type.¹ The allowance for such variable of each boiler as drum level, pressure and temperature shown in Fig.3, is calculated from experimental data and the design limits.

Usually, as a large dead time exists in coal pulverizer, the pulverized coal-fired boiler is inferior to the oil-fired one on the load follow-up performance. Therefore, in order to improve the follow-up performance, N-type which is coal-fired as mentioned above has been operated with oil for the fluctuating load.

The allowances for two boilers are different from each other in the range of 1-5 minute period.

Theoretical Analyses and Experimental Results of Dynamics:

In connection with analysis of dynamics, the circulating system is particularly discussed, since it is considered that both types of boiler are similar to each other except for the circulating loop. The circulating loop is simplified as shown in Fig.2. As for the downcomer-riser loop, two models are considered, one with head loss and the other without head loss. The following assumption are given:

(1) saturated part in steady state always keeps its condition, (2) in riser, heat flux is uniform lengthwise, (3) feed water is mixed with circulating water at the downcomer inlet, (4) in tubes, heat transfers only in radial direction, (5) the physical constants of water in downcomer are uniform, (6) metal temperature is equal to the integrated mean value of temperature distributed in radial direction, (7) in evaporating segment, water and vapor are mixed uniformly and no slip exists between them, (8) to be uniform mixing in steam drum, (9) energy given by the circulating pump to water turns into pressure head. Therefrom, the following fundamental equations are derived.

Downcomer - riser loop

$$\text{Continuity: } a \frac{\partial \gamma}{\partial t} + \frac{\partial M}{\partial x} = 0 \quad (1)$$

$$\text{Momentum: } \frac{\partial}{\partial t} M + 2 \frac{M}{a\gamma} \frac{\partial M}{\partial x} - a \frac{M^2}{a^2 \gamma^2} \frac{\partial \gamma}{\partial x} + g a \frac{\partial}{\partial x} (p + \gamma H) = -\frac{1}{2} \lambda_0 \frac{M^2}{a\gamma} \quad (2)$$

$$\begin{aligned} \text{Energy: } \frac{\partial}{\partial t} i + \frac{M}{a\gamma} \frac{\partial i}{\partial x} - A \frac{1}{\gamma} \left(\frac{\partial}{\partial t} p + \frac{M}{a\gamma} \frac{\partial p}{\partial x} \right) + A \frac{H}{a\gamma} \frac{\partial}{\partial x} M \\ - A \frac{H}{\gamma} \frac{M}{a\gamma} \frac{\partial \gamma}{\partial x} = \frac{R_1}{a\gamma} + \frac{A}{\gamma} \frac{\lambda_0}{2} \left(\frac{M}{a\gamma} \right)^3 \end{aligned} \quad (3)$$

$$\text{State: } \gamma = \gamma(i, p) \quad (4)$$

$$\text{Energy in metal: } c_m W_m \frac{\partial}{\partial t} T_m = R - R_1, \quad R_1 = F \alpha (T_m - T) \quad (5)$$

Mixing point

$$\text{Continuity: } M_d + M_f = M_1, \quad M_d = a_d \gamma_1 u_1 \quad (6)$$

$$\text{Energy: } M_d i' + M_f i_f = M_1 i_1 \quad (7)$$

$$\text{Bernoulli: } \frac{H}{\gamma} \frac{a_d \gamma_1}{a_w \gamma'} \frac{d}{dt} u_1 + \frac{1}{2g} u_1^2 - \frac{p_{10}}{\gamma'} + \frac{p_1}{\gamma_1} - H = 0 \quad (8)$$

Steam drum

$$\text{Continuity: } \frac{d}{dt} \left(V_s \frac{1}{v''} + V_w \frac{1}{v'} \right) = M_{10} - M_s - M_d \quad (9)$$

$$\text{Energy: } c_m W_m \frac{d}{dt} T + \frac{d}{dt} \left(V_s \frac{e''}{v''} + V_w \frac{e'}{v'} \right) = M_{10} i_{10} - M_s i'' - M_d i' \quad (10)$$

$$\text{Circulating pump: } p_{pe} - p_{pc} = \gamma \cdot (H_{p0} - K Q^2), \quad Q = \frac{M}{\gamma} \quad (11)$$

where, H_{p0} is pump head for $Q = 0$

As regards the downcomer - riser loop, the following differential vector equation is obtained from Eq.(1) - (5) by normalizing each variable with its steady state value, by linearizing it considering small perturbation from the steady state and by Laplace transformation in regard to time.

$$\begin{aligned}
 \frac{d}{dx} \begin{bmatrix} m \\ \xi \\ h \end{bmatrix} &= \begin{bmatrix} 0 & -\frac{S}{\beta k u_0} & \frac{S}{\beta u_0} \\ -\beta' k u \psi^2 \frac{S}{u_0} - \frac{1}{C_2} & (n+1) \psi^2 \frac{S}{u_0} - \frac{1}{C_3} & k u \psi^2 \frac{S}{u_0} - \frac{1}{\beta' C_3} \\ + k u \psi^2 \frac{1}{i_0} \frac{d}{dx} i_0 (1-nG) & + k u \psi^2 \epsilon_m G & + k u \psi^2 \left(\frac{1}{i_0} \frac{d}{dx} i_0 + \delta_m G \right) \\ -\beta' (n-1) \psi^2 \frac{S}{u_0} & \frac{n-1}{k} \frac{S}{u_0} - \frac{n-1}{k n} \frac{1}{C_3} & -\frac{S}{u_0} - 2 \frac{n-1}{\beta' k n} \frac{1}{C_3} \\ -\frac{1}{i_0} \frac{d}{dx} i_0 (1-nG) & -\epsilon_m G & -\frac{1}{i_0} \frac{d}{dx} i_0 - \delta_m G \end{bmatrix} \begin{bmatrix} m \\ \xi \\ h \end{bmatrix} \\
 &+ \begin{bmatrix} 0 \\ -k u \psi^2 \left(\frac{1}{i_0} \frac{d}{dx} i_0 \right) \frac{G}{\tau_m S} \\ \left(\frac{1}{i_0} \frac{d}{dx} i_0 \right) \cdot \frac{G}{\tau_m S} \end{bmatrix} \cdot r \quad (12)
 \end{aligned}$$

Eq. (12) yields

$$\begin{aligned}
 \begin{bmatrix} m_{i-1} \\ \xi_{i-1} \\ h_{i-1} \end{bmatrix} &= \begin{bmatrix} 1 & \frac{\tau_i S}{\beta_i' k_i} & -\frac{\tau_i S}{\beta_i'} \\ \beta_i' k_i u_i \psi_i^2 \tau_i S + \epsilon_{xi} & -(n_i+1) \psi_i^2 \tau_i S + 1 + \epsilon_{xi}' & -k_i u_i \psi_i^2 \tau_i S + \frac{1}{\beta_i} \epsilon_{xi} \\ -k_i u_i \psi_i^2 (1-\eta_i)(1-n_i G_i) & -k_i u_i \psi_i^2 \epsilon_{mi} G_i & -k_i u_i \psi_i^2 (1-\eta_i + \delta_{mi} G_i) \\ \beta_i (n_i-1) \psi_i^2 \tau_i S & -\frac{1}{k_i} (n_i-1) \tau_i S + \frac{n_i-1}{k_i n_i} \epsilon_{xi}' & \tau_i S + 1 + 2 \frac{n_i-1}{\beta_i' k_i n_i} \epsilon_{xi} \\ + (1-\eta_i)(1-n_i G_i) & + \epsilon_{mi} G_i & + (1-\eta_i + \delta_{mi} G_i) \end{bmatrix} \begin{bmatrix} m_i \\ \xi_i \\ h_i \end{bmatrix} \\
 &+ \begin{bmatrix} 0 \\ k_i u_i \psi_i^2 (1-\eta_i) \frac{G_i}{\tau_{mi}} \\ -(1-\eta_i) \frac{G_i}{\tau_{mi}} \end{bmatrix} \cdot r \quad (13)
 \end{aligned}$$

Similarly, the following equation is obtained for the circulating pump:

$$\begin{bmatrix} m_{i-1} \\ \xi_{i-1} \\ h_{i-1} \end{bmatrix} = \begin{bmatrix} 1 & 0 & 0 \\ \frac{1}{C_{sp}} & \frac{1}{C_{sp}} & \frac{1}{C_{sp}} \\ 0 & 0 & 1 \end{bmatrix} \begin{bmatrix} m_i \\ \xi_i \\ h_i \end{bmatrix} \quad (14)$$

Then, equations (13) and (14) are expressed by

$$X_{i-1} = A_i \cdot X_i + B_i \cdot r \quad (15)$$

where $B_i = 0$ for Eq.(14).

Since the whole downcomer-riser loop is divided into 9 segments as shown in Fig.2, the equation of the loop is given as follow:

$$X_1 = (A_2 A_3 \cdots A_{10}) X_{10} + (A_2 A_3 \cdots A_6)(A_7 A_8 B_9 + A_7 B_8 + B_7) \cdot r \quad (16)$$

So, the relation between inputs and outputs of the downcomer-riser loop is described as follow:

$$\begin{bmatrix} m_{10} \\ \xi_1 \\ h_{10} \end{bmatrix} = \begin{bmatrix} T_{11}(s) & T_{12}(s) & T_{13}(s) & T_{14}(s) \\ T_{21}(s) & T_{22}(s) & T_{23}(s) & T_{24}(s) \\ T_{31}(s) & T_{32}(s) & T_{33}(s) & T_{34}(s) \end{bmatrix} \begin{bmatrix} m_1 \\ \xi_{10} \\ h_1 \\ r \end{bmatrix} \quad (17)$$

$T_{ij}(s)$'s in Eq.(17) are obtained by matrix inversion of Eq.(16).

Furthermore, equations of other portions of the circulating system, are derived similarly as follows:

$$\text{Mixing point: } m_1 - X_0 m_F - (1 - X_0) m_d = 0 \quad (18)$$

$$h_1 - \left\{ 1 - (1 - X_0) \frac{V_0'}{V_1'} \right\} h_f - (1 - X_0) \frac{P_{10}^0}{V_1'} \frac{\partial i'}{\partial P} \xi_{10} - (1 - X_0) \left(1 - \frac{V_0'}{V_1'} \right) (m_f - m_d) = 0 \quad (19)$$

$$m_d = \frac{c(1+c')}{T_w S + 1} \xi_{10} - \left\{ c' + \frac{V_0'}{V_1'} \frac{c(1+c')}{T_w S + 1} \right\} \xi_1 + c \frac{L_0 V_0'}{P_{10}^0} \frac{1}{T_w S + 1} \lambda \quad (20)$$

$$\text{Steam drum: } T_A S \lambda - T_P S \xi_{10} - m_{10} + (1 - X_0) m_d = -X_0 m_s \quad (21)$$

$$(T_D S + C_D) \xi_{10} - (a' + X_0) m_{10} + a'(1 - X_0) m_d - (b + X_0) h_{10} = -(1 + a') X_0 m_s \quad (22)$$

From equations (17) - (22) the matrix equation of circulating system is obtained and the relationship among variables is shown in Fig.4.

Though the head loss through the downcomer-riser loop is included in the above study, another mathematical model neglecting head loss is also discussed in the following. In this case, the loop is divided into four

parts, i.e. downcomer, preheater, evaporator, and unheated riser. Then, assuming that pressure is uniform at each divided part of the loop, transfer functions $T_{ij}(s)$'s in Eq.(17) are derived in the same way as done by Terano and Varcop.^{2,3}

Thus, in each case, frequency response of the circulating system is calculated.

The calculated results are shown in Fig.6 - Fig.7, and they are compared with the experimental results evaluated from step-responses by Fourier integral. Both analytical results in these figures agree closely with the plotted experimental results.

Matrix equations of the other subsystems shown in Fig.5 are derived in the similar manner and transfer matrices of them are respectively calculated in frequency domain. Then the matrix equation of the whole system is made up by combining those of subsystems and its transfer matrix is calculated.^{4,5}

On the other hand, experimental data are transformed from time domain to frequency domain by Fourier integral.

These corresponding results are shown in Fig.8 - Fig.9 for respective types of boiler.

Differences of Dynamics Due to Circulation Type:

A comparison of the experimental results with two theoretical results for drum level responses are given in Fig.6 and Fig.7 for respective boilers. The corresponding results have a close agreement among them.

Here, a comparison is made of the results for the drum level of N-type with those of C-type. Responses to the saturated steam flow are nearly equal to each other in the range of 1.0 - 10.0 rad/min of ω and the responses in the range of ω represent the initial swelling in time domain.

From this comparison, it may be said that the initial swelling is not affected by water holding.

In connection with responses to the feed water flow, it may be seen from Fig.7 that the dead time and the time constant of N-type are 1.5 times as large as C-type. This difference is caused by that of water holding.

From the above study, it may be mentioned regarding the dynamics of drum level that there might be a few effects of head loss through the loop and more influences of water holding and metal weight.

The pressure and drum level responses obtained from the whole boiler system, as shown in Fig.8 and Fig.9, would agree more closely in their shape. This may appear to justify the foregoing discussion.

Conclusion:

The experiments have been made to evaluate the load fluctuation allowance for and to verify the dynamic model of two types of boiler.

And the dynamics of both types have been compared to make clear the essential factors in the allowance.

A set of mathematical models has been developed and the calculated results have been compared in frequency domain with the experimental results.

Foregoing discussion suggests that whether the circulating pump is provided or not would give no essential difference between both types in the dynamics of the circulating system, so far as drum level and pressure.

And it further suggests that the differences of the dynamics and of the allowance are caused by water holding and metal weight.

Acknowledgement:

The authors wish to acknowledge to the members of Kawasaki P/S J.N.R. for their co-operations in the experiments. Also wish to express their appreciation to Miss K. Oroshibaru and Mr. T. Kishikawa for assistance in programming and in preparing data.

References:

1. K. Izawa et al.: Trans. of SICE, Vol.2, No.2, p.101-112, 1966.
2. T. Terano: Bulletin of JSME, 1960, Vol.3, No.12, p.540-546.
3. L. Varcop: Regelungstechnik Heft 9, Nr.15, 1967.
4. M. Fujii et al.: Journal of SICE Vol.2, No.7, 1963.
5. F.T. Thompson: IEEE Trans. on Power Apparatus and System, Vol. PAS-86, No.5, 1967.

Nomenclature:

a : cross sectional area, m^2	α : heat transfer coefficient, $kcal/m^2 \cdot min \cdot ^\circ C$
A : $1/427.0$ ($kcal/kg \cdot m$)	λ : normalized drum level
C : specific heat, $kcal/kg^\circ C$	λ_o : friction factor
e : internal energy, $kcal/kg$	ξ : normalized pressure
F : circumference of tube, m	Time Constant
g : acceleration of gravity, m/min^2	$\tau, \tau_m, \tau_o, \tau_A, \tau_p,$
H : head or height, m	Subscript
h : normalized enthalpy	1 : downcomer inlet
i : enthalpy, $kcal/kg$	10 : riser outlet
L : drum level, m	d : water from drum
M : flow, kg/min	f : feed water
m : normalized flow	s : steam
P : pressure, kg/m^2	O : steady state
Q : volumetric flow, m^3/min	m : metal
R : heat transfer, $kcal/min \cdot m$	w : water
r : normalized heat transfer	Superscript
s : Laplace operator	o : steady
t : time, min.	prime: saturated water
T : temperature, $^\circ C$	double prime: saturated steam
U : velocity, m/min	
v : specific volume, $m^3/kg = \frac{1}{\gamma}$	
V : volume, m^3	
W : weight, kg	
x : co-ordinate	
X : quality of wet steam	

Following nomenclatures are given through derivation of equations.

$$C, C', C_2, C_3, C_3', C_4, C_{1p}, C_{2p}, C_{3p}, C_o, \epsilon_2, \epsilon_3, \epsilon_3', \beta, \kappa, \psi^2, \epsilon_m, \delta_m, \eta, n, \kappa,$$

$$G = \tau_m s / (\tau_m s + 1).$$

$T_{ij}(s)$'s indicates the matrix element of Eq.(7).

θ_s and θ_R shown in Fig.3 indicate steam temperatures of superheater and reheater respectively.

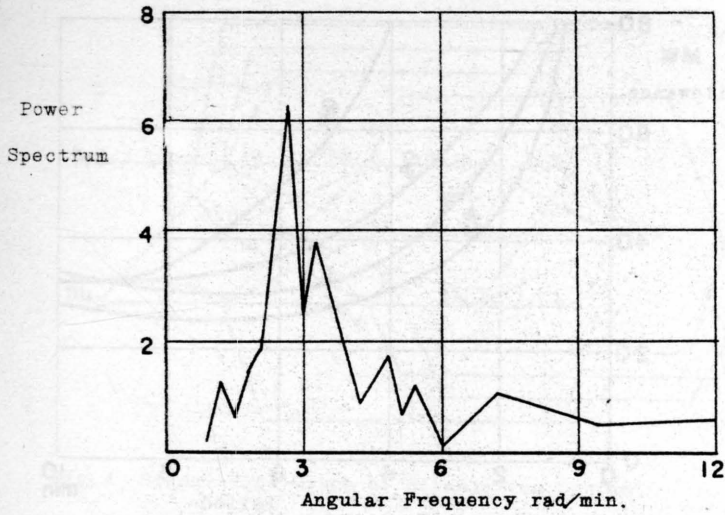


Fig.1 Power Spectrum of an Electric Railway Load

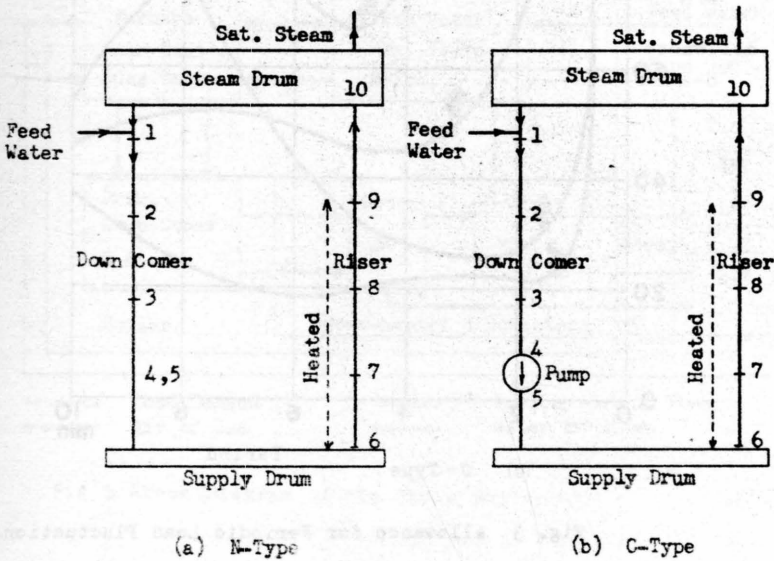
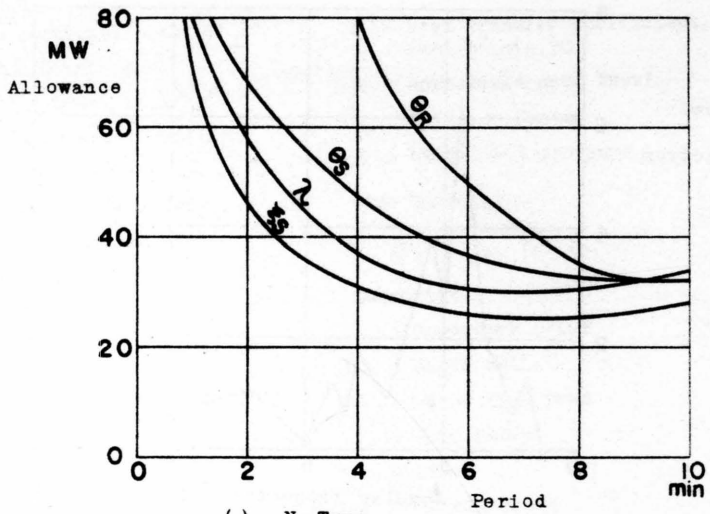
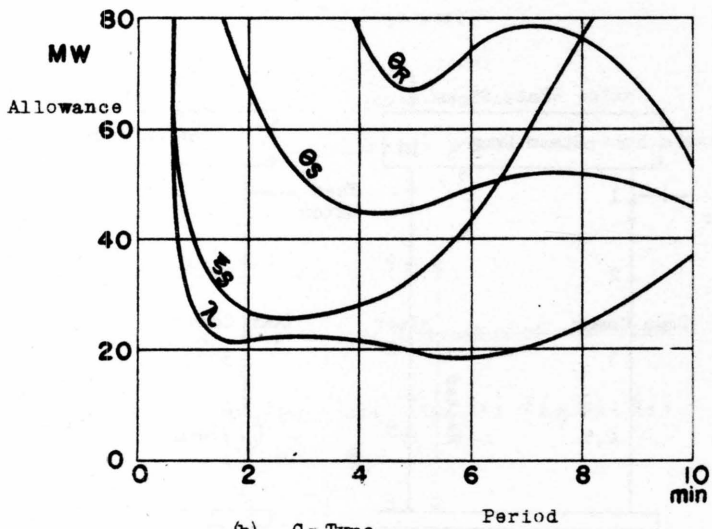


Fig.2 Models of the Circulating System



(a) N-Type



(b) C-Type

Fig. 3 Allowance for Periodic Load Fluctuation

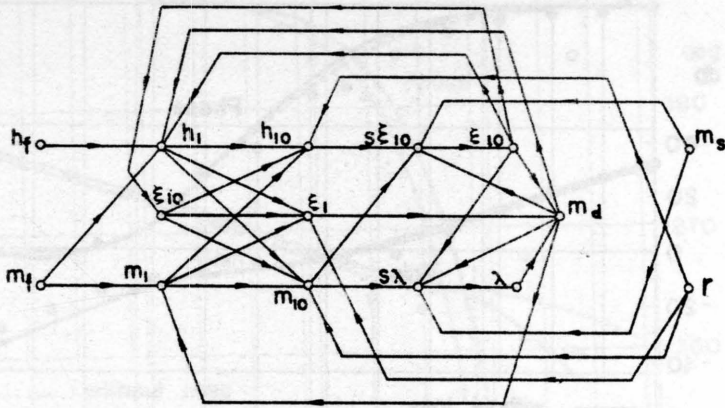


Fig. 4 Signal Flow Graph of Circulating System

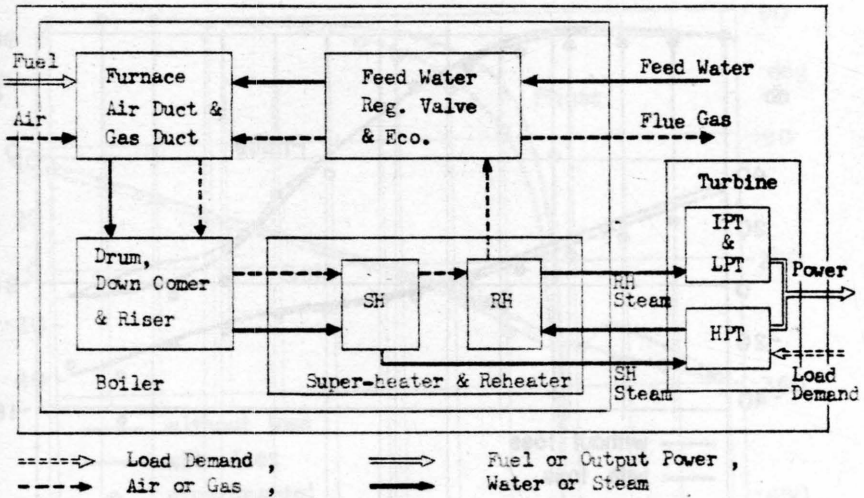
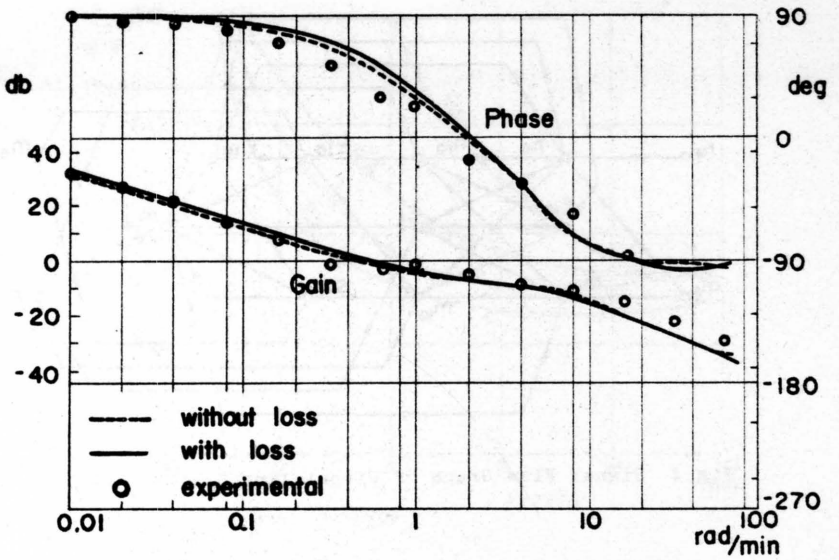
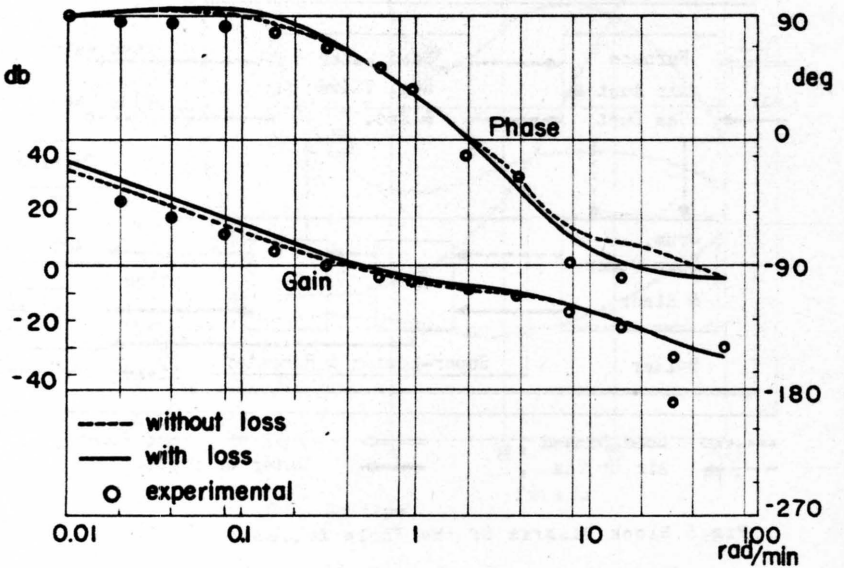


Fig. 5 Block Diagram of the Whole Boiler

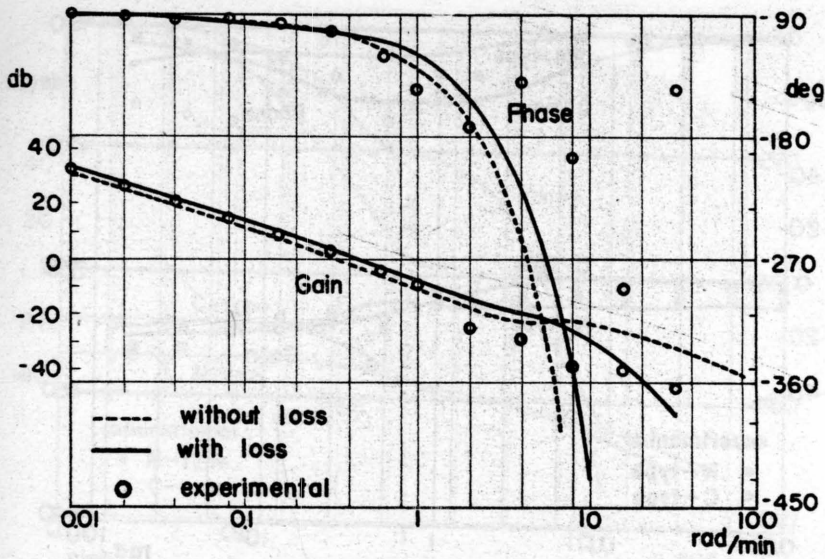


(a) N-Type

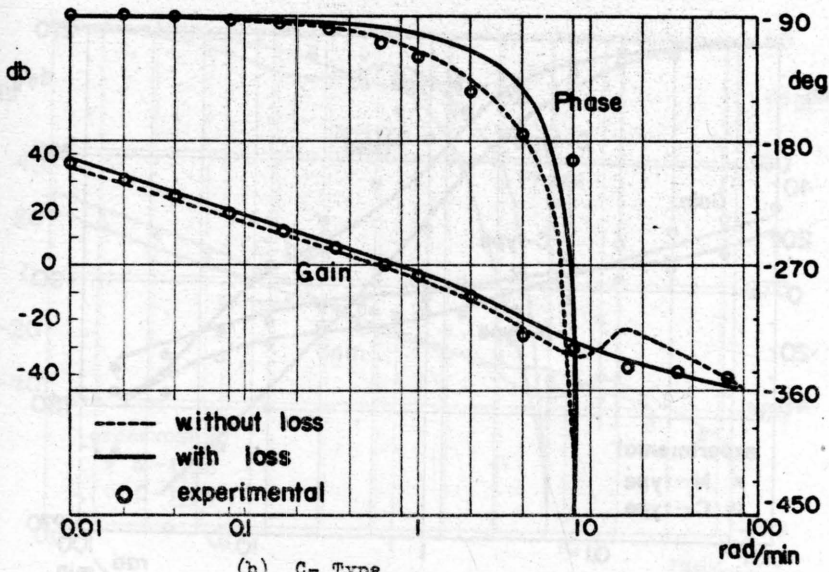


(b) C-Type

Fig.6 Frequency Response of Drum Level vs. Steam Flow

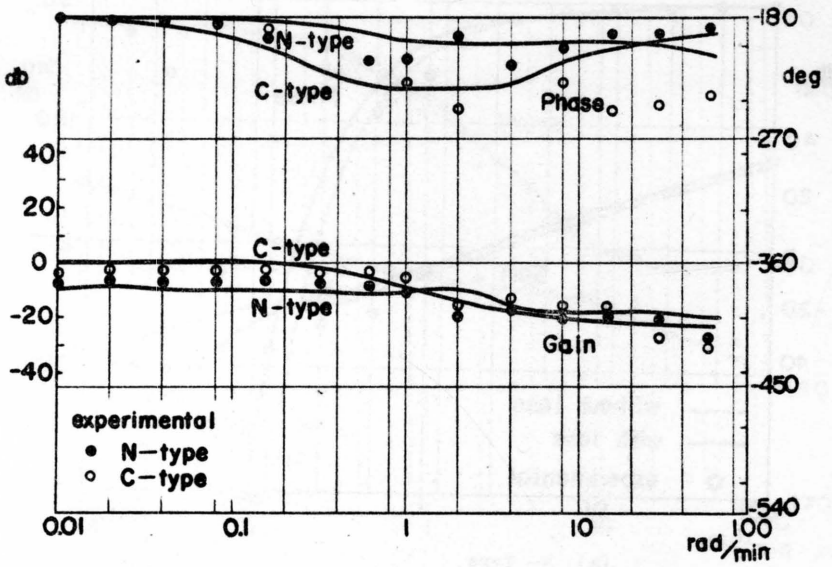


(a) N- Type

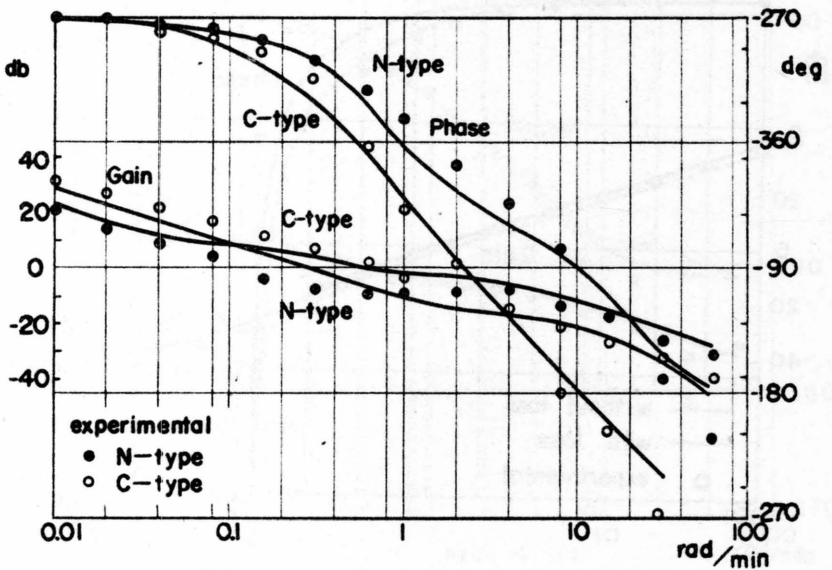


(b) C- Type

Fig.7 Frequency Response of Drum Level vs.Feed Water Flow

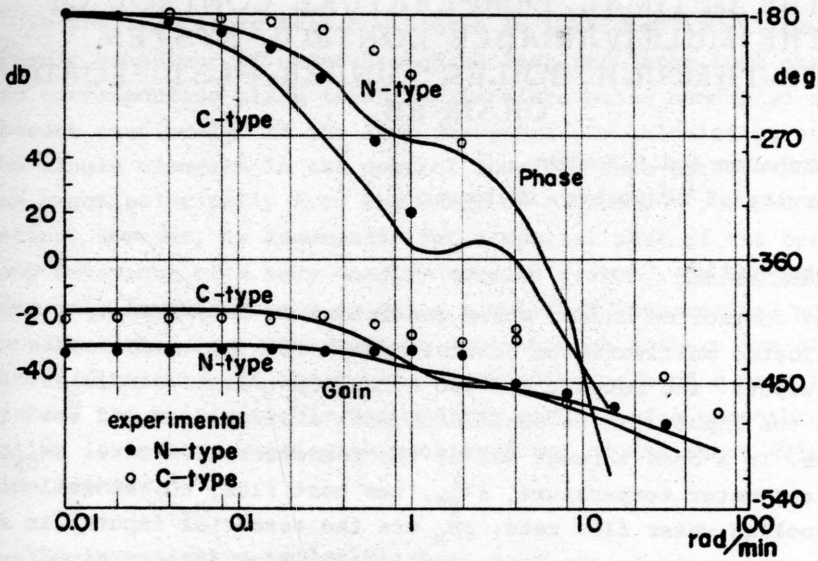


(a) Main Steam Pressure

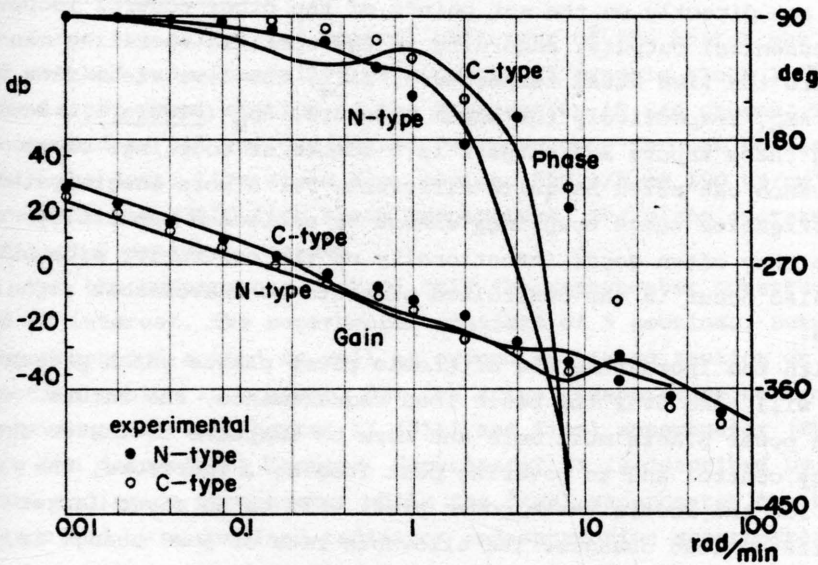


(b) Drum Level

Fig. 8 Frequency Response to Turbine Regulating Valve Position
(Controller Removed)



(a) Main Steam Pressure



(b) Drum Level

Fig.9 Frequency Response to Feed Water Valve Position
(Controller Removed)

ON THE OPTIMAL TEMPERATURE CONTROL OF THE MULTIVARIABLE CONTROL SYSTEM "ONCE-THROUGH BOILER" UNDER FAST LOAD CHANGES

H. Unbehauen and P. Necker

University of Stuttgart, Germany

1. Introduction

The control of modern steam generators is described by a very complicated multivariable control system with numerous inputs and outputs. The outputs are the actual controlled variables while the inputs can be considered both disturbances and set points. In a once-through boiler the feedwater flow rate, $\dot{\Delta M}_{SW}$, the feed water temperature, Δv_{SW}^0 , the heat flux, $\Delta \dot{Q}$, as well as the cooling water flow rate, $\dot{\Delta M}_E$ are the essential inputs, in so far as one neglects the load signal, ΔL , which effects simultaneously $\dot{\Delta M}_{SW}$, $\Delta \dot{Q}$, $\dot{\Delta M}_E$ and other system parameters but which can also act directly on the set points of the other control loops. The essential outputs, according to the specific operating manner are the live steam temperature, Δv_{Da}^0 , the live steam flow rate $\dot{\Delta M}_D$, respectively the steam pressure, Δp_D (Figure 1). Between these inputs and outputs is a number of couplings whose influence can often be quite different. For a more exact system investigation these couplings cannot be neglected especially since they often occur intentionally on the controller side but can also occur in the controlled elements as unavoidable signal paths.

With the increasing use of atomic power plants which presumably will take over the basic load requirements, the future steam power plants must more and more be adaptive to faster frequency control and to covering peak loading¹. Therefore, the task for the modern steam power plant will be to cover larger and faster load changes. The allowable rate of load change is, however, in most cases limited by the live steam temperature control system. Strong demands are required therefore on the construction and settings of the live steam temperature control. In this paper special attention will be given to the temperature control system, whereas in a later paper the power load behaviour will be further handled.

In the literature till now little is mentioned about the dynamic behaviour of once-through boilers for large load changes and corresponding plant investigations are being conducted at present cautiously. In the last few years the calculation of the single elements in the control loop for once-through boilers has begun principally from the works of P. Profos^{2,3}, whose application, however, is known only for a special case of the open loop behaviour of a very complex coupled system⁴. On the other side only investigations on quite simplified mathematical models for the closed loop behaviour of once-through boilers are at hand⁵. Similar as in the previously studied case of a drum boiler system⁶ the multivariable temperature control of a once-through boiler is to be studied with consideration of the exact calculation methods.

2. The investigated boiler plant

2.1. Technical data

Since the calculated control behaviour of the boiler was to be checked experimentally, as a practical example block 2 in the Ingolstadt power station of the Bayernwerke AG was chosen. This concerned an oil and gas heated two pass once-through boiler with the data: live steam flow maximum 530 t/h at 190 kp/cm² pressure and 535°C live steam temperature. The plant operates in "floating pressure" manner.

For the temperature control only the superheater construction is of interest. The superheater consists of 3 sections. Between the first and second as well as second and third section an injection cooler is present. For the actual temperature control behaviour the superheater II (ÜII) and final superheater (EÜ) are the determining factors. Superheater II is described by a pure radiation superheater while the final superheater can be described by a combined radiation and convection superheater.

2.2. The block diagram of the temperature control

As Figure 2 shows, the temperature control results from two cascade circuits. This type of cascade control is preferred today for Benson boilers⁷. Thereby each cascade has a principal

controller and a follower controller. The follower controller in the cascade regulates the temperature immediately behind the cooler according to the set point given by the principal controller in actuating on the cooling water flow. In this way temperature variations in \dot{v}_{Da} are quickly eliminated, assuming the injection water valve is sufficiently constructed.

A peculiarity in the block plan is the coupling of the set point signal of the follower controller $R_{2,1}$ with the controlled variable of the principal controller $R_{1,2}$. By that means the injection water valve V_2 should always work in the best position. By load changes ΔL the set points of both controllers in the first cascade are changed to counteract the inertness of the controlled system on the one hand while considering the sharp decrease in the superheater characteristic on the other hand (see Figure 3).

Figure 4 shows the heavily coupled block diagram for the temperature control system. The controllers in the plant are Siemens-Teleperm relay controllers, which with the valve motor are represented as PI-controllers. This description is possible only under certain assumptions, which will be handled nearer in chapter 3.

In the derivation of the dynamic behaviour the distinction between heated and unheated boiler portions must be made. A change in the steam flow rate $\Delta \dot{M}_D$, for example by the action of the injection cooler E_1 , or a change in the heat flux $\Delta \dot{Q}$ act as temperature disturbances in the superheater sections, which is described by the transfer functions F_{Q1} and F_{M1} respectively F_{Q2} and F_{M2} .

The live steam temperature $\Delta \dot{v}_{Da}$ is influenced, as Figure 4 shows, principally by the 5 input variables, the steam inlet temperature $\Delta \dot{v}_{De}$, the heat flux $\Delta \dot{Q}$, the cooling water flow $\Delta \dot{M}_E$, the steam flow $\Delta \dot{M}_D$ and the load ΔL . As previously mentioned, the entire control of a once-through boiler is described by a multivariable system. If a load change occurs, then all 5 input variables of the temperature control are changed. This is dependent both on the controlled system as well as the controller couplings of the multivariable system. Therefore, for further consideration of the temperature control the reaction of the above mentioned 4 input variables $\Delta \dot{v}_{De}$, $\Delta \dot{Q}$, $\Delta \dot{M}_E$ and $\Delta \dot{M}_D$ to a

step input in load ΔL is of special interest. These variables could be determined from the total behaviour by consideration of the effective connections of the multivariable system. The derivation of the mathematical model necessary for this from the physical and geometrical data would require a very large computation expense. Therefore another way was chosen.

The temperature control is computed only between the sections S_1 and S_2 in Figure 5. That is, the mathematical model is derived only for block II. The 4 unknown input variables of block II for the calculation and simulation of the mathematical model are taken directly from measurements made in the plant. In this way very precise input variables for the investigation of the temperature control are obtained, in which the internal couplings are already considered. Block I thus contains all the remaining interconnections in the multivariable system outside of the temperature control system in which ΔL influences all the outputs. The output variables of block I are again intercoupled.

Not at first considered in this model was, that variations in the steam flow change the steam pressure. Since the plant works in "floating pressure" operation, the pressure changes proportional to the flow rate. In the dynamic transient behaviour pressure overshoots of about 7% occur which can influence the behaviour of the single transfer elements of the temperature control.

3. The identification of the single transfer elements of the block diagram

The deciding factors of the temperature control system are the transfer functions $F_{\phi i}$, F_{Mi} and F_{Qi} ($i = 1, 2$). The analytic calculation of the transfer functions from geometric and physical data^{8,9} leads to well known transcendental transfer functions which, however, are not suitable for dynamic studies and especially for simulation on the analog computer. For this is the rational transfer function of the form

$$F(p) = \frac{\sum_{i=0}^m c_i p^i}{\sum_{j=0}^n d_j p^j} \quad n \geq m \quad (1)$$

more suitable.

In order to obtain such a system description several methods can be made to agree. For example it is possible to calculate the step response from the exact frequency plot $F(i\omega)$ ¹⁰ and to make an approximation of the step response in the time domain. In many cases the technique from G.Schwarze¹¹ yields good results. Sometimes also the technique described by F.Läubli¹² can be used, which results in a rational fraction for $F(i\omega)$ direct from construction data of the superheater sections. Another possibility is to approximate the frequency plot $F(i\omega)$ of the exact process, which comes from the transcendental form of the transfer function, by a frequency plot of a rational fraction¹³.

From the above mentioned methods the latter is universally and best applicable for the simulation of heat transfer systems. This can be established both in view of the calculated order of the transfer function as well as in view of the exactness of the approximation. The order of the transfer function is the deciding factor in simulation on an analog computer. As shown earlier¹⁴, this method supplies the most exact results and at the same time the smallest circuitry. A very exact system description is insured as shown by a check in the frequency and time domains. In these investigations the previously mentioned frequency functions of interest were approximated by rational functions of 3rd order. Table I shows a section of the identification of temperature control system.

Next to the identification of the controlled system the dynamic behaviour of the controller is also of interest for the simulation on the analog computer. The plant investigated is equipped with Siemens-Teleperm controllers. This is a 3-point controller with two delayed feedback networks, the "short time" and the "long time" feedback network. This controller in connection with its valve setting motor is approximated as having a PI-behaviour. As a special investigation¹⁵ has shown, this controller can not be simulated on an analog computer without great expense. In order to investigate the control system this controller and the valve setting motor were simulated as an ideal PI-controller with the transfer function

$$F_R = K_R \left(1 + \frac{1}{T_{IP}} \right) \quad (2)$$

This approximation naturally has to a certain extent an error, especially as the non-linear dependence of the controller parameters K_R and T_I on the magnitude of the set point deviation, which always occurs with such a relay controller, cannot be considered in Eq. (2). However in order to compare the parameter settings for both controllers, numerous diagrams were made from measurements of the transient function of the Teleperm controller. This permits one to establish the corresponding values of K_R and T_I of the ideal linear controller for every arbitrary combination of the 5 parameter set-possibilities of the non-linear controller by different set point deviations. Only by means of this dependence it is possible to design an ideal PI-controller for the simulation of the actual temperature control system.

4. The control behaviour of the two cascade circuits

In the temperature control system described the best parameters for the settings of the 4 PI-controllers are to be found which must be stable and also show good performance. For determination of the optimal controller setting in the sense of a performance index yet to be determined, a variation problem with 8 free parameters $K_{Ri,j}$ and $T_{Ii,j}$ ($i, j = 1, 2$) must be solved. Theoretically the solution is possible but would not justify the enormous computer expense. Therefore the two cascade circuits were studied separately.

Although the cascade circuit describes an often used control system, previously only estimations were made in view of optimization of the free parameters. Therefore, special attention is given first to this question for the present cascade circuits. First the performance index must be established. In our multi-variable control system the actuating variable of the follower controller $R_{1,1}$ becomes simultaneously the disturbance for both the principal control loop as well as the second cascade by means of the steam flow change $\Delta \dot{M}_D$. Therefore, for optimization of the first cascade circuit, the controlled variable x as steam temperature $\Delta \vartheta_D$ after the superheater section II as well as the actuating variable $y = y_{1,1}$ of controller $R_{1,1}$ are considered the variables (see Figure 6). The "expense criterion"¹⁸

$$I_a = \int_0^{\infty} (x^2 + y^2) dt \rightarrow \text{Min.} \quad (3)$$

is for this preferable. Thereby large unwanted overshoots are emphasized and avoided by the x^2 -factor. On the other hand the actuating variable movement of the cooling water valve is kept small by the y^2 -factor which is desirable in such a complex steam boiler control. As disturbance we further assume a step change in the inlet temperature ΔT_{De} . Thus the integral

$$I_a = f(K_{R1,1}, T_{I1,1}, K_{R1,2}, T_{I1,2}) \quad (4)$$

describes a function of the 4 controller adjustment values and forms a hyperplane in a 5-dimensional Euclidian space, whose minimum must be found. The analytic calculation of I_a is possible, however, from the constraint equation for an extremum

$$\frac{\partial I_a}{\partial K_{R1,j}} = 0 \quad \text{and} \quad \frac{\partial I_a}{\partial T_{I1,j}} = 0 \quad (5)$$

with $j = 1, 2$ the optimal parameters of the controller can not be explicitly expressed. Although from Eq.(4) the optimum could be found with the help of a test-step technique on a digital computer, the task was given to the analog computer for the clearness and better control possibilities.

In the optimization first the momentary optimum was found for fixed follower controller settings by systematic variation of the principal controller. This process was repeated for numerous different, although constant, follower controller parameters $K_{R1,1}$ and $T_{I1,1}$. In this way the absolute minimum in the sense of Eq.(3) could be determined by comparison with the integral value for every case. Also interesting is the shape of the optimal controller settings for the various combinations in a stability plot. For this purpose the according stability limits were calculated numerically on a digital computer.

Table II shows a section of the essential part of this investigation.

As Table II shows, different stability domains can occur according to the settings of the 4 controller parameters. In this investigation the integrals and stability limits were calculated

only for values $K_{R1,2} \leq 400$ because larger values are of no more interest for a practical controller. There are cases in which only a stable domain occurs to the left of the asymptote of $K_{R1,2}$ but on the other hand also cases, in which additionally a stable domain occurs which becomes broader and broader and finally takes in the entire right hand plane without further restriction. Also other cases can occur where the unstable domain of the controller parameters is a "peninsula" projecting into the otherwise stable domain. The shape of the relative minimum behaves correspondingly. For the first case described above one single optimum occurs. For the second case a minimum is found in the left hand stable domain which satisfies the conditions

$$\frac{\partial I_a}{\partial K_{R1,2}} = 0 \quad \text{and} \quad \frac{\partial I_a}{\partial T_{I1,2}} = 0, \quad (6)$$

but whose integral is still larger than that evaluated at the right hand boundary for $K_{R1,2} = 400$. In the third case both an absolute minimum corresponding to Eq.(6) and a "boundary" minimum can occur inside of the stable domain. Here one must test which of the two minima supplies the smaller integral. In many cases the boundary minimum contains the smaller integral value. The path of the line $I_a = \text{const}$ is for this consideration quite informative as a constant integral topograph (see Figure 7).

In the investigation of the first cascade circuit the controller settings for full load gives the minimum integral I_a for the values

$$K_{R1,1} = 10; T_{I1,1} = 100 \text{ s}; K_{R1,2} = 2,8; T_{I1,2} = 100 \text{ s}.$$

In this case all the 4 conditions set on Eq.(5) are fulfilled. This absolute minimum is shown in the stability plot of Fig.7.

For the calculation of this stability plot the transfer function of the whole cascade circuit was calculated

$$F(p) = \frac{\mathcal{L}\{\Delta v_D\}}{\mathcal{L}\{\Delta v_{De}\}} = \frac{\frac{F_{\phi 1} + F_{M1} F_{T1,1} F_{R1,1}}{1 + F_{St} F_{T1,1} F_{R1,1}}}{1 + F_{R1,2} \frac{F_{T1,2} F_{R1,1} (F_{St} F_{\phi 1} - F_{M1})}{1 + F_{St} F_{T1,1} F_{R1,1}}} \quad (7)$$

The structure of Eq.(7) corresponds, however, to the transfer function of a single-loop system for a disturbance behaviour

$$F(p) = \frac{F_z}{1 + F_R F_S} \quad (8)$$

where $F_R = F_{R1,2} = K_{R1,2} (1 + \frac{1}{T_{I1,2} p})$ and both the disturbance transfer function F_z of the controlled system and the actuating variable transfer function F_S contain the above transfer elements of the cascade circuit. Thereby is $F_{E1} \cdot F_{SW1} = 1$ and $F_{E1} \cdot F_{SW1} = F_{St}$. Using the Nyquist Criterion the stability limit is found by setting the numerator expression of Eq. (7) to zero. From

$$F_{R1,2} = \frac{-(1 + F_{St} F_{T1,1} F_{R1,1})}{F_{T1,2} F_{R1,1} (F_{St} F_{\beta 1} - F_{M1})} \quad (9a)$$

and with $p = i\omega$

$$F_{R1,2} = R(\omega) + iI(\omega) = K_{R1,2} (1 + \frac{1}{i\omega T_{I1,2}}) \quad (9b)$$

results the stability limit in parameter form

$$K_{R1,2} = R(\omega) \quad \text{and} \quad T_{I1,2} = \frac{-R(\omega)}{\omega I(\omega)} \quad (10)$$

for various ω -points assuming the transfer system does not have a special all-pass factor. With Eq. (10) all the stability limit curves were calculated for the first cascade circuit and likewise for the second cascade circuit with the necessary changes.

The results for the second cascade circuit are shown in Table III. Quite interesting here is the occurrence of unstable islands in the stability plot. For this case the quadratic integral criterion

$$I_q = \int_0^{\infty} x^2 dt \rightarrow \text{Min} \quad (11)$$

is used for the optimization with $x = \Delta \vartheta_{Da}$. In this control system no large overshoots namely of the life steam temperature should occur. As optimal controller settings the parameter combination

$$K_{R2,1} = 1; T_{I2,1} = 100 \text{ s}; K_{R2,2} = 400; T_{I2,2} = 20 \text{ s}$$

results in the smallest integral value of Eq. (11). This controller setting corresponds, however, to a boundary minimum.

5. The behaviour of the total simulated temperature control and comparison with the plant measurements

The connection of both cascade circuits first is executed for a combination of 8 controller settings which correspond to the set parameters of the 4 Teleperm controllers in the power plant. For this purpose the measured signals of $\Delta \dot{M}_D$, $\Delta \dot{M}_E$, $\Delta \dot{\vartheta}_{De}$ and $\Delta \dot{Q}$ are simulated with the help of function generators on an analog computer for a step increase in load $\Delta L = 10$ MW at an operating point of 135 MW (see Figure 8). The blocks I and II of the total system described in Fig. 5 can now be connected at the section point S_1 . For the simulation on an analog computer 29 integrators, 55 summing and sign changing amplifiers, 4 function generators, 2 multipliers and 95 attenuators are necessary.

Fig. 8 shows as the essential results of this simulation the temperature signals $\Delta \dot{\vartheta}_D$ and $\Delta \dot{\vartheta}_{Da}$. The agreement between measurement (solid line) and calculation (broken line) can thereby be considered good especially when one considers the numerical preparation (e.g. the identification problem) and difficulties for such an all encompassing simulation which must be overcome. Thereby, one must remember that it is always difficult to hold constant the plant operation over a long period of time for the purpose of measurements.

After the practicability and effectiveness of the mathematical model have been proven by comparison with plant measurements, the optimization of the temperature control can be conducted. Here special attention must be paid to the behaviour of $\Delta \dot{\vartheta}_D$ since in the plant measurements this signal had been proven as quite critical. From the behaviour of $\Delta \dot{\vartheta}_D$ the magnitude and the permissible rate of load change is limited.

The optimal settings of the 4 controllers, which were calculated from the models of the two separated cascade circuits, are now used for the total temperature control system. Further it must be noticed that by the separate optimization of the two cascade circuits the actual disturbances could not be used. These settings, however, supply an essential improvement of the behaviour of the complex temperature control system even under the action of the actual disturbances, as Figure 9 shows. There the temperature curves $\Delta \dot{\vartheta}_{Da}$ and $\Delta \dot{\vartheta}_D$ are plotted for the original settings of the controllers in "b", while those as a result of

the optimization are plotted in "a". For the live steam temperature Δv_{Da} a maximum overshoot of about 1°C occurs after a step increase in load $\Delta L = +10 \text{ MW}$. Also the originally disadvantageous behaviour Δv_D could be essentially improved and indicates only an overshoot of 5°C and a small temperature gradient. Thereby still larger step changes in load could be permitted with the determined optimal controller settings by the same thermal conditions of the superheater. It should be mentioned here that the calculated optimal controller settings are also technically possible.

By small changes in the analog circuit other structures can be studied besides the described structure of temperature control. Thereby other structures have established that, at least in view of temperature control, the additional load signal furnished no remarkable improvement. On the other hand the separation of the direct signal coupling of the two cascade circuits caused no large deterioration of the controller results. The overshoot of the temperature signals will increase thereby, but the settling time will be smaller.

Finally the load dependence of the stability limits should be indicated. Figure 7 contains also the stability limit for 60% load while maintaining the optimal controller settings of $K_{R1,1}$ and $T_{I1,1}$ for full load. Thereby is shown for the first cascade circuit that the optimal controller settings for full load lie already in the instable region for 60% load. In order to operate such a temperature control at a momentary optimum for different loads, the controller settings of the principal controller must be adapted to the momentary load by means of a self-adaptive control system. Thereby an adjustment of the controller gain factor alone would suffice.

6. Conclusion

Further investigations on other boiler structures have shown that no fixed rule can be derived for the optimal setting of the temperature control system on a Benson-boiler. That is because the stability regions and optimal controller settings of the cascade circuits depend considerably on the data as well of the controlled system as of the controllers. An optimization must

therefore be conducted separately for every plant. The present investigation has shown, however, that the numerical calculation of optimal controller settings for a multivariable temperature control system is possible. Hereby, the optimal settings found furnish such good results regarding temperatures, that still larger step changes in load can be permitted. It is characteristic, however, that the stability limits and the optimal controller settings change considerably with different loads, so that for a strongly changing boiler load, a self-adaptive controller for the gain factor should be considered to obtain the best operating condition.

Acknowledgement: The authors would like to thank the staff of the Bayernwerk AG for the opportunity of conducting measurements at their Ingolstadt power station. Also to be thanked is Prof. Dr.-Ing. R.Quack for the inspiration and constant interest in these investigations.

References

1. Profos, P.: Betrachtungen über künftige Regelaufgaben und Regelprobleme im Dampfkraftwerk. Mitt. VGB Heft 109 (1967) S.224/232.
2. Profos, P.: Dynamisches Verhalten von Zwangstrom-Verdampfersystemen. Sulzer-Forschungsheft 1960 S.5/12.
3. Profos, P.: Die Dynamik zwangsdurchströmter Verdampfersysteme. Regelungstechnik 10 (1962), S.529/36.
4. Voß, K.: Das Übertragungsverhalten der Strecken eines Zwangsdurchlaufkessels. Fortschr.-Ber. VDI-Z. Reihe 6, Nr.18 (1968).
5. Klefenz, G.: Regeldynamische Untersuchung eines Bensonkessels. Diss. TH Darmstadt 1965.
6. Unbehauen, H.: The load dependence of the stability and optimal controller settings of the multivariable steam temperature control system in a boiler. IFAC-Symposium on Multivariable Control Systems, Düsseldorf 1968.
7. Friedewald, W. und H.Zwetz: Regelung der Temperatur im Wasser-Dampf-Gemisch von Benson-Kesseln. Regelungstechnik 13 (1965), S.62/68.
8. Profos, P.: Die Regelung von Dampfanlagen. Berlin: Springer Verlag 1962.
9. Isermann, R.: Das regeldynamische Verhalten von Überhitzern. Fortschr.-Ber. VDI-Z. Reihe 6, Nr.4 (1965).
10. Unbehauen, H.: Fehlerbetrachtungen bei der Auswertung experimentell mit Hilfe determinierter Testsignale ermittelter Zeitcharakteristiken von Regelsystemen. messen, steuern, regeln 11 (1968) Nr.4, S.134/40.
11. Schwarze, G.: Algorithmische Bestimmung der Ordnung und Zeitkonstanten bei P-, I- und D-Gliedern mit zwei unterschiedlichen Zeitkonstanten und Verzögerung bis 6.Ordnung. messen, steuern, regeln 7 (1964) Nr.1, S.10/19.

12. Läubli, F.: Zum Problem der Nachbildung des dynamischen Verhaltens von Dampferzeugern auf Analogie-Rechenmaschinen. Techn. Rundschau Sulzer (1961) Nr.2, S.35/42.
13. Unbehauen, R.: Ermittlung rationaler Frequenzgänge aus Meßwerten. Regelungstechnik 14 (1966), S.268/273.
14. Unbehauen, H.: Nachbildung der Frischdampf-temperaturregelung eines Dampferzeugers am Analogrechner unter Berücksichtigung der Kopplung mit anderen Regelkreisen. AICA-Congress Lausanne 1967. Paper in Session C 4 (in print).
15. Ernsberger, K.: Diplomarbeit Nr.736 am Inst.f.Verfahrenstechnik u.Dampfkesselwesen der Universität Stgt. 1968.
16. Ankel, Th. u.K.Hengst: Die Verbesserung der Regelfähigkeit eines Systems mit Hilfe der Kaskadenregelung. Regelungstechnik 6 (1958), S.361/66.
17. Pressler, G. u.F.Schreiner: Untersuchungen an Kaskadenregelkreisen. Regelungstechnik 12 (1964), S.164/70.
18. Unbehauen, H.: Zur Optimierung verfahrenstechnischer Regelkreise. Diss. Universität Stuttgart 1964.

	100%		60%			100%		60%	
	c_0	c_1	c_2	c_3		c_0	c_1	c_2	c_3
$F_{d,1}$	$0,8758 \cdot 10^{-4}$	$0,1008 \cdot 10^{-3}$	$0,1624 \cdot 10^{-2}$	$0,1328 \cdot 10^{-2}$	$F_{d,1}$	$0,5293 \cdot 10^{-4}$	$0,9510 \cdot 10^{-3}$	$0,8697 \cdot 10^{-2}$	$0,8867 \cdot 10^{-2}$
	$0,8705 \cdot 10^{-5}$	$-0,1042 \cdot 10^{-3}$	$0,2425 \cdot 10^{-2}$	$-0,5038 \cdot 10^{-2}$		$0,1389 \cdot 10^{-4}$	$0,3343 \cdot 10^{-3}$	$0,9157 \cdot 10^{-2}$	$0,2133 \cdot 10^{-1}$
	$0,5865 \cdot 10^{-4}$	$0,7218 \cdot 10^{-3}$	$0,4082 \cdot 10^{-2}$	$0,5865 \cdot 10^{-4}$		$0,6997 \cdot 10^{-4}$	$0,8531 \cdot 10^{-3}$	$0,8531 \cdot 10^{-3}$	$0,8531 \cdot 10^{-3}$
	$0,9789 \cdot 10^{-1}$	$0,4387 \cdot 10^{-1}$	$0,9789 \cdot 10^{-1}$	$0,9789 \cdot 10^{-1}$		$0,4582 \cdot 10^{-2}$	$0,1040 \cdot 10^{-2}$	$0,1040 \cdot 10^{-2}$	$0,1040 \cdot 10^{-2}$
	$1,0000$	$1,0000$	$1,0000$	$1,0000$		$0,1076$	$0,4453 \cdot 10^{-1}$	$0,4453 \cdot 10^{-1}$	$0,4453 \cdot 10^{-1}$
	$1,0000$	$1,0000$	$1,0000$	$1,0000$		$1,0000$	$1,0000$	$1,0000$	$1,0000$

Table I. Portion of the identification of the transfer function coefficients corresponding to Eq.(1) for 100% and 60% load

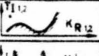
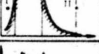
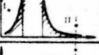


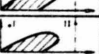
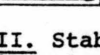
$K_{R1,1}$	$T_{11,1}$ (s)	Stab.-Rand Stability Limit	Opt. Einstellwerte Opt. Controller Settings $K_{R1,2}$ $T_{11,2}$ (s)	Opt. Integratwert Opt. Integral value $I_{a,opt}$
0,5	1		2,8 200	2,677
	10		I 1,0 100	5,966
			II 400 100	0,938
	100		I 3,0 200	5,12
5,0	100		II 400 20	1,003
			400 400	0,863
10	1		400 400	0,881
	100		I 2,8 100	0,753
			II 400 400	0,883
	200		400 400	0,868

Table II. Stability limits and optimal controller settings of the cascade circuit of superheater UII for variations in $K_{R1,1}$ and $T_{11,1}$

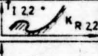



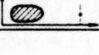
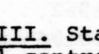
$K_{R2,1}$	$T_{12,1}$ (s)	Stab.-Rand Stability Limit	Opt. Einstellwerte Opt. Controller Settings $K_{R2,2}$ $T_{12,2}$ (s)	$I_{a,opt}$
0,5	1,0		35 50	0,344
	10		400 50	0,366
1,0	1		400 20	0,302
	10		400 20	0,287
	100		400 20	0,279
10	100		400 20	0,329

Table III. Stability limits and optimal controller settings of the cascade circuit of the final superheater EU for variations in $K_{R2,1}$ and $T_{12,1}$

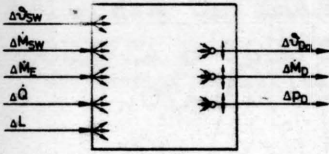


Fig. 1. Once-through boiler as a multivariable control system

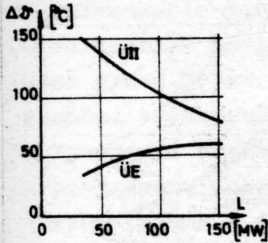


Fig. 3. Load-dependent characteristic of superheater ÜII and final super-heater EÜ

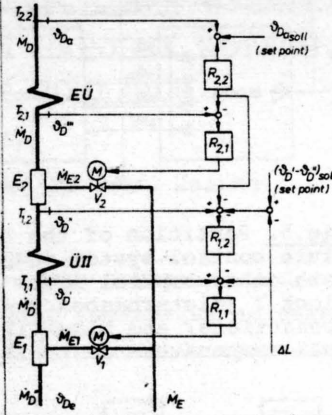


Fig. 2. Schematic for the temperature control of the investigated once-through boiler

$R_{1,j}$ = controller ($i, j=1, 2$)
 $T_{1,j}$ = temperature measurement

E_1 = injection cooler
 V_1 = control valve

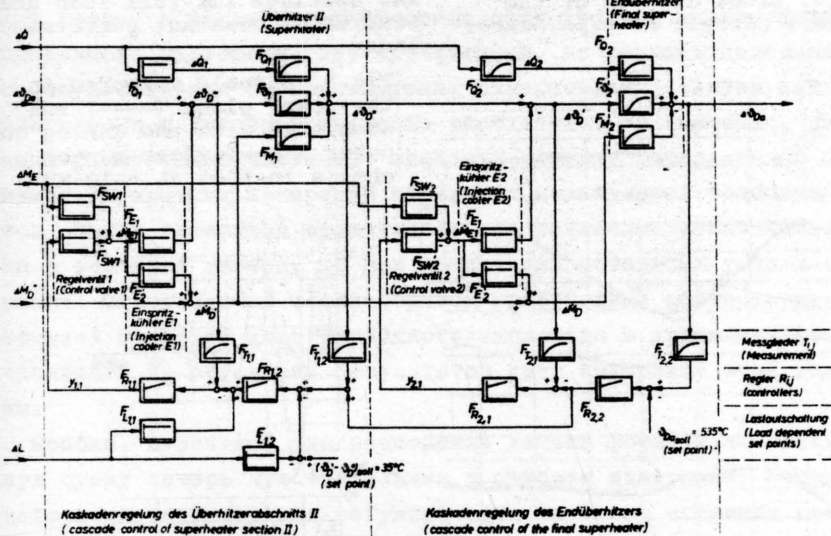


Fig. 4. Block diagram of the multivariable temperature control system of the investigated once-through boiler

ΔQ heat flux [kcal/h] ΔL load [KW] or [%]
 $\Delta \theta_{De}$ steam inlet temperature [°C] $\Delta \theta_{Da}$ live steam temperature [°C]
 ΔM_E feed-water flow [t/h] ΔM_D outlet steam flow [t/h]
 ΔM_D inlet steam flow [t/h]

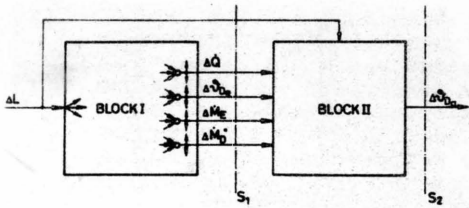


Fig. 5. Partition of the temperature control system coupled with other control loops in block I (disturbances and interconnections) and block II (actual temperature control)

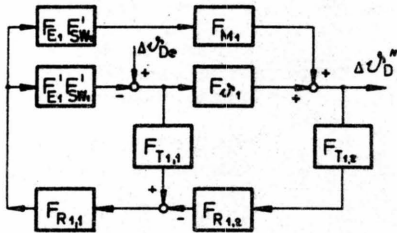


Fig. 6. Block diagram of the cascade circuit of superheater UII

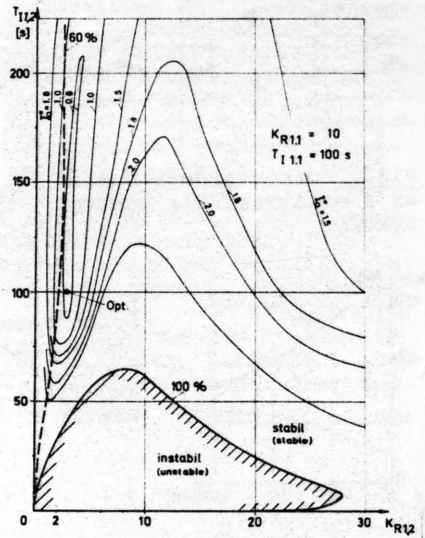
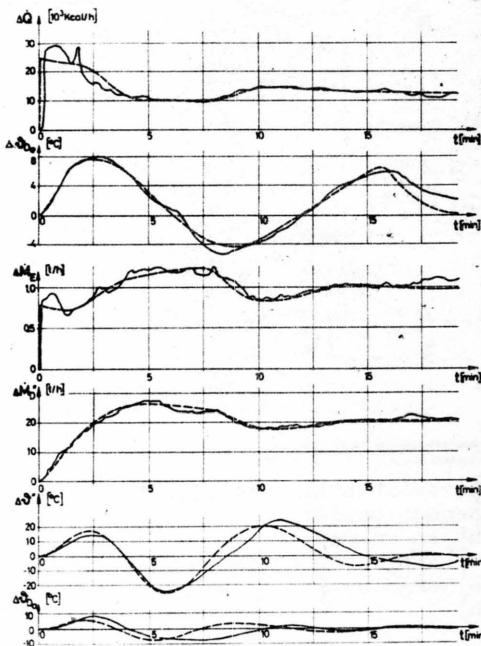


Fig. 7. Stability diagram for UII for full load (100%) and 60% load with optimal controller settings for full load and curves of constant performance index

Fig. 8. Signals measured in the power plant (—) and simulated with the analog computer (----) after a step change in load $\Delta L = 10$ MW

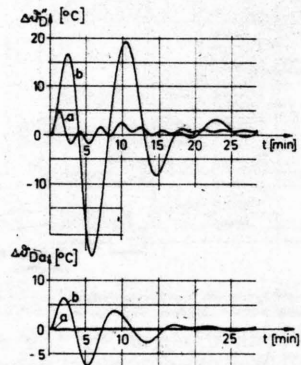


Fig. 9. Step responses of the controlled temperatures Δv_D and Δv_{Da}

- a) with optimal controller settings
- b) with original controller settings

АЛГОРИТМ ОПТИМАЛЬНОГО РЕГУЛИРОВАНИЯ ИЗБИТКА ВОЗДУХА В ТОПОЧНЫХ КАМЕРАХ ПАРОВЫХ КОТЛОВ, ОТАПЛИВАЕМЫХ ТВЕРДЫМ ТОПЛИВОМ

Казимеж ТАРАМИНА

Институт Автоматики Энергосистем, Вроцлав, Польша

1. Вступление

Оптимальное регулирование избытка воздуха в паровых котлах, отапливаемых твердым топливом служит цели уменьшения до минимума сумми потерь с уходящими газами и от неполного сгорания в любых эксплуатационных условиях.

Уравнение определяющее оптимальный избыток воздуха получено в результате дифференцирования выражения на сумму потерь с уходящими газами и от неполного сгорания, относительно молярной доли свободного кислорода в сухих топочных газах на выходе котла и приравнивания первой производной к нулю, а также в результате проведения некоторых преобразований. В уравнении выступают молярные доли некоторых компонентов сухих или влажных топочных газов, а также их производные относительно молярной доли свободного кислорода. Эти производные, по причине невозможности осуществления соответствующих измерительных систем для непрерывного и непосредственного определения их значения, заменены разностными частными, значения которых вычислены на основании двукратных измерений отдельных компонентов топочных газов. Такие измерения проводились при различных избытках воздуха в топочной камере, но при неизменных остальных условиях сгорания. Определяемые таким образом производные соответствуют средней молярной доле свободного кислорода в уходящих газах вычисленной на основании результатов двух измерений этой величины.

Вообще, известно, что разностная запись формулы на минимальную сумму потерь чувствительная к ошибкам измерений. Отсюда до алгоритма оптимального регулирования процесса сгорания введены дополнительные зависимости для согласования результатов измерений. Согласовав результаты первых и вторых измерений, следует вычислить значение функции, обуславливающей минимум потерь, которая в большинстве случаев не равна нулю, а, следовательно, является недостаточной для определения оптимального избытка воздуха. С этой целью следует изменить избыток воздуха в камере в известном уже направлении и, после стабилизации процесса сгора-

ния, провести третье измерение. Далее, согласовав результаты вторых и третьих измерений, следует вычислить второе значение функции на минимум потерь. После этого рассчитывают оптимальную молярную долю свободного кислорода в уходящих топочных газах, по формуле полученной в результате приравнивания к нулю линейной функции, проходящей через два значения функции обуславливающей минимальные потери и два средние значения оптимизированного параметра.

Вычислив оптимальную молярную долю свободного кислорода в топочных газах, следует изменить количество воздуха, подводимого к топочной камере, так, чтобы содержание свободного кислорода в топочных газах было равным или приближалось бы к оптимальному значению.

2. Выведение формулы на минимум суммы потерь с уходящими газами и от неполного сгорания

2.1. Основные зависимости

При выведении формулы на минимум потерь, использованы следующие зависимости:

А. Общая формула на сумму этих потерь

$$q_1 = q_2 + q_3 + q_4 = \frac{[100 \cdot \bar{C}_p (T_{sp} - T_0) + CO \cdot W_{CO}] (1-x) + \frac{12 \cdot W_c}{22,715} (RQ_2 + CO) \cdot x}{\frac{12}{22,715} \cdot \frac{Q_c - 2512(9h+w)}{c + 0,375s} (RQ_2 + CO)} \quad (2.1)$$

где: \bar{C}_p - средняя теплоемкость влажных топочных газов $\left[\frac{\text{kJ} \cdot \text{deg}^{-1}}{(\text{H}_2\text{O}) m_u} \right]$;
 $[\text{H}_2\text{O}]$ - молярная степень увлажнения топочных газов, выраженная десятичной дробью;

$T_{sp} - T_0$ - разница температур топочных газов на выходе котла и температуры окружающей среды [deg];

$RQ_2 + CO$ - сумма молярных долей двуокиси углерода с учетом двуокиси серы и окиси углерода в сухих топочных газах на выходе котла [%];

W_{CO} - теплотворность окиси углерода $\left[\frac{\text{kJ}}{\text{m}_u^3} \right]$;

Q_c - теплотворность топлива $\left[\frac{\text{kJ}}{\text{kg}} \right]$;

c, h, n, o, s, w - весовые доли: углерода, водорода, азота, кислорода, горючей серы и влаги в топливе, выраженные десятичной дробью;

W_c - теплотворность горючих компонентов в твердых продуктах сгорания $\left[\frac{\text{kJ}}{\text{kg}} \right]$;

x - соотношение неполного сгорания;

22,715 - объем киломолекулы газа в нормальных условиях [m_u^3];

12 - атомный вес углерода;

0,375 - соотношение масс атомов углерода и серы;

2512 - теплота испарения 1 кг влаги содержащейся в топливе [$\frac{kJ}{kg}$].

В. Общая формула на среднюю теплоемкость влажных топочных газов, умноженная на 100

$$100 \bar{c}_p = N_2 \cdot c_{pN_2} + RO_2 \cdot c_{pCO_2} + O_2 \cdot c_{pO_2} + CO \cdot c_{pCO} + H_2O \cdot c_{pH_2O} \left[\frac{kJ}{(1+[H_2O])m_u^3 \cdot deg} \right] \quad (2.2)$$

Где: N_2, O_2 - молярные доли азота и свободного кислорода в сухих топочных газах на выходе котла [%];

H_2O - молярная степень увлажнения топочных газов [%];

$c_{pN_2}, c_{pCO_2}, c_{pO_2}, c_{pCO}$ - средние теплоемкости компонентов топочных газов [$\frac{kJ}{m_u^3 \cdot deg}$].

В. Зависимость¹ соотношения неполного сгорания от химического состава топлива и сухих топочных газов, а также молярной степени увлажнения топочных газов и воздуха

$$1-x = \frac{n'_{H_2} + n'_{H_2O} + \frac{x}{100} \left(\frac{1}{2} n'_{H_2} - n'_{O_2} - n'_{N_2} \right)}{n'_c} \cdot \frac{RO_2 + CO}{H_2O - \left(1 - \frac{CO}{200}\right) x_L} = \frac{A(RO_2 + CO)}{H_2O - \left(1 - \frac{CO}{200}\right) x_L} \quad (2.3)$$

Где: $n'_c, n'_{H_2}, n'_{H_2O}, n'_{N_2}, n'_{O_2}$ - количество киломолекул: углерода, водорода, влаги, азота и кислорода на весовую единицу топлива;

x_L - молярная степень увлажнения воздуха [%].

Г. Зависимость¹ соотношения неполного сгорания от химического состава топлива и сухих топочных газов на выходе котла

$$1-x = \frac{0,79 \left(\frac{1}{2} n'_{H_2} - n'_{O_2} \right) + 0,21 \cdot n_{N_2}}{n'_c} \cdot \frac{RO_2 + CO}{N_2 - 79 + 0,395 \cdot CO} = \frac{(L_R - 1)(RO_2 + CO)}{N_2 - 79 + 0,395 \cdot CO} = \frac{(L_R - 1)(RO_2 + CO)}{21 - RO_2 - O_2 - 0,605 \cdot CO} \quad (2.4)$$

Где: $L_R = 1 + 0,79 \cdot 0,375 \frac{8h - o + 0,3 \cdot n_c + 0,375 \cdot s}{s}$ - коэффициент, характеризующий химический состав топлива. На основании статистических данных^{5,6} получается, что значения этого коэффициента почти постоянны и равны: $L_R = 1,1034 \pm 0,0237$ - для каменного угля из Верхней Силезии и $L_R = 1,083 \pm 0,033$ - для бурого угля из Турошова.

Отсюда:
$$N_2 = 79 + \frac{L_R - 1}{1-x} (RO_2 + CO) - 0,395 \cdot CO \quad [\%] \quad (2.5)$$

Д. Баланс сухих топочных газов на выходе котла

$$N_2 + RO_2 + O_2 + CO = 100 \quad [\%] \quad (2.6)$$

Подставив (2.5) в (2.6) получаем зависимость

$$RQ_2 + CO = \frac{1-x}{L_R x} (21-Q_2 + 0,395 \cdot CO) \quad [\%] \quad (2.7)$$

необходимую для согласования результатов измерений а также для проверки правильности показаний измерительных систем RQ_2 , Q_2 и CO которую ввиду того, что их частное $\frac{1-x}{L_R x}$ в минимальной степени зависит от соотношения неполного сгорания, можно записать

$$L_R (RQ_2 + CO) = 21 - Q_2 + 0,395 \cdot CO \quad (2.8)$$

Данные выше зависимости (2.3), (2.5) и (2.7) использованы для написания общей формулы (2.2) на среднюю теплоемкость топочных газов, а именно:

а. в случае определения состава сухих топочных газов на выходе котла

$$100 \bar{C}_p = 100a - f \cdot CO + d \cdot x_L + \frac{RQ_2 + CO}{1-x} (b - e \cdot x) \left[\frac{kJ}{(1+[H_2O]) m_u^3 \cdot deg} \right] \quad (2.9)$$

б. в случае определения состава влажных топочных газов

$$100 \bar{C}_p = 100a - f' \cdot CO + \frac{RQ_2 + CO}{1-x} (p - e \cdot x) + d \cdot H_2O \left[\frac{kJ}{(1+[H_2O]) m_u^3 \cdot deg} \right] \quad (2.10)$$

где: $a = 0,79 C_{PN_2} + 0,21 C_{PO_2} = 13075 \pm 0,0033 \left[\frac{kJ}{m_u^3 \cdot deg} \right]$ ($T_p = 463 \pm 30^\circ K$, $T_o = 288 \pm 15^\circ K$);

$b = C_{PCO_2} - C_{PO_2} - L_R (C_{PO_2} - C_{PN_2}) + A C_{PH_2O} = 1278 \pm 0,277$ - для котлов отопляемых каменным углем и $3,217 \pm 0,322$ - для котлов отопляемых бурным углем

$$d = C_{PH_2O} = 1,522 \pm 0,0075 \left[\frac{kJ}{m_u^3 \cdot deg} \right]; \quad e = C_{PCO_2} - C_{PO_2} = 0,456 \pm 0,031 \left[\frac{kJ}{m_u^3 \cdot deg} \right];$$

$$f = C_{PCO_2} - C_{PO_2} - 0,395 (C_{PO_2} - C_{PN_2}) + \frac{x_L}{200} C_{PH_2O} = 0,470 \pm 0,033 \left[\frac{kJ}{m_u^3 \cdot deg} \right]; \quad f' = C_{PCO_2} - C_{PO_2} - 0,395 (C_{PO_2} +$$

$$- C_{PN_2}) = 0,456 \pm 0,032 \left[\frac{kJ}{m_u^3 \cdot deg} \right]; \quad p = C_{PCO_2} - C_{PN_2} - L_R (C_{PO_2} - C_{PN_2}) = 0,452 \pm 0,031 \left[\frac{kJ}{m_u^3 \cdot deg} \right].$$

Тогда общая формула (2.1) на сумму потерь принимает вид:

а. при определении состава сухих топочных газов

$$q_r = q_2 + q_3 + q_4 = \frac{\left\{ [100a + d \cdot x_L - f \cdot CO + \frac{RQ_2 + CO}{1-x} (b - e \cdot x)] (T_p - T_o) + CO \cdot W_{CO} \right\} (1-x) + \frac{12 \cdot W_C}{22,715} (RQ_2 + CO) \cdot x}{\frac{12}{22,715} \cdot \frac{Q_C - 2512(9 \cdot h + w)}{c + 0,375 \cdot s} (RQ_2 + CO)} \quad (2.11)$$

б. при определении состава влажных газов

$$q_r = q_2 + q_3 + q_4 = \frac{\left[(100a + p \cdot RQ_2 + d \cdot H_2O) (T_p - T_o) + CO \cdot W_{CO} \right] (1-x) + \frac{12 \cdot W_C}{22,715} (RQ_2 + CO) \cdot x}{\frac{12}{22,715} \cdot \frac{Q_C - 2512(9 \cdot h + w)}{c + 0,375 \cdot s} (RQ_2 + CO)} \quad (2.12)$$

2.2. Общий вид формулы обуславливающей минимум потерь с уходящими газами и от неполного сгорания

Запись формулы обуславливающей минимум потерь получена в результате дифференцирования (2.11) или (2.12) относительно молярной доли свободного кислорода в сухих топочных газах на выходе котла и приравнивания первой производной к нулю. В место $\frac{1}{1-x} \frac{dx}{d\alpha_2}$ подставляют равнозначные выражения полученные в результате дифференцирования зависимостей (2.7) и (2.3) относительно O_2 и деления производных $\frac{dx}{d\alpha_2}$ на их первоначальное выражения (2.7) и (2.3) а именно:

$$\frac{R\alpha_2 + CO}{1-x} \frac{dx}{d\alpha_2} = 1 - 0,395 \frac{dCO}{d\alpha_2} - \frac{21 - O_2 + 0,395 CO}{21 - O_2 - R\alpha_2 - 0,605 CO} \left(\frac{dR\alpha_2}{d\alpha_2} + 0,605 \frac{dCO}{d\alpha_2} + 1 \right) \quad (2.13)$$

$$\frac{R\alpha_2 + CO}{1-x} \frac{dx}{d\alpha_2} = \frac{R\alpha_2 + CO}{H_2O - (1 - \frac{CO}{200})X_L} \left[\frac{d(H_2O - X_L)}{d\alpha_2} + \frac{X_L}{200} \frac{dCO}{d\alpha_2} \right] - \left(\frac{dR\alpha_2}{d\alpha_2} + \frac{dCO}{d\alpha_2} \right) \quad (2.14)$$

Тогда запись в общем виде формулы обуславливающей минимум потерь принимает следующий вид:

а. при определении состава сухих топочных газов

$$\begin{aligned} \frac{dq}{d\alpha_2} = & \left[\frac{12 \cdot W_c}{22,715} - e(T_{sp} - T_0) \right] + \left[W_{CO} - \frac{0,395 \cdot 12 \cdot W_c}{22,715} - (f - 0,395e)(T_{sp} - T_0) \right] \frac{dCO}{d\alpha_2} + \left[100a + d \cdot X_L - fCO + \frac{R\alpha_2 + CO}{1-x} (b - ex) \right] \cdot \\ & \cdot \frac{d(T_{sp} - T_0)}{d\alpha_2} \left\{ (21 - O_2 - R\alpha_2 - 0,605CO) - \left[\frac{12 \cdot W_c}{22,715} - e(T_{sp} - T_0) \right] (21 - O_2) - \left[W_{CO} - \frac{0,395 \cdot 12 \cdot W_c}{22,715} - (f - 0,395e)(T_{sp} - T_0) \right] CO + \right. \\ & \left. - (100a + d \cdot X_L)(T_{sp} - T_0) \right\} \left(\frac{dR\alpha_2}{d\alpha_2} + 0,605 \frac{dCO}{d\alpha_2} + 1 \right) = F(O_2) = 0 \end{aligned} \quad (2.15)$$

б. при определении состава влажных топочных газов

$$\begin{aligned} \frac{dq}{d\alpha_2} = & \left[\frac{12 \cdot W_c}{22,715} - e(T_{sp} - T_0) \right] R\alpha_2 + \left[\frac{12 \cdot W_c}{22,715} - W_{CO} + (f - e)(T_{sp} - T_0) \right] CO - (100a + d \cdot X_L)(T_{sp} - T_0) \left\{ \frac{d(H_2O - X_L)}{d\alpha_2} + \frac{X_L}{200} \frac{dCO}{d\alpha_2} \right\} + \\ & - \left[\frac{12 \cdot W_c}{22,715} - e(T_{sp} - T_0) \right] \frac{dR\alpha_2}{d\alpha_2} + \left[\frac{12 \cdot W_c}{22,715} - W_{CO} + (f - e)(T_{sp} - T_0) \right] \frac{dCO}{d\alpha_2} - (100a + pR\alpha_2 + d \cdot H_2O) \frac{d(T_{sp} - T_0)}{d\alpha_2} \left\{ H_2O - \left(1 + \right. \right. \\ & \left. \left. - \frac{CO}{200} \right) X_L \right\} = F(O_2) = 0 \end{aligned} \quad (2.16)$$

2.3. Упрощенные записи формул обуславливающих минимум суммы потерь с уходящими топочными газами и от неполного сгорания

Из анализа зависимости (2.15) и (2.16) видим, что некоторые компоненты в ничтожной степени зависят от выступающих изменений температуры топочных газов ($T_{sp} = 463 \pm 30$ °К), температуры окружающей среды ($T_0 = 288 \pm 15$ °К) и разницы температур ($T_{sp} - T_0 = 180 \pm 40$ [deg]), а следовательно:

а. при сгорании каменного угля.

$$\frac{12 \cdot W_c}{22,715} - e(T_{sp} - T_0) = 17832 \pm 24 \left[\frac{kJ}{m_u^3} \right]; W_{co} - \frac{0,395 \cdot 12 \cdot W_c}{22,715} - (f - 0,395e)(T_{sp} - T_0) = 5517 \pm 15 \left[\frac{kJ}{m_u^3} \right];$$

$$\frac{12 \cdot W_c}{22,715} - W_{co} + (f' - e)(T_{sp} - T_0) = 5274 \pm 1 \left[\frac{kJ}{m_u^3} \right]$$

б. при сгорании бурого угля

$$\frac{12 \cdot W_c}{22,715} - e(T_{sp} - T_0) = 17235 \pm 24 \left[\frac{kJ}{m_u^3} \right]; W_{co} - \frac{0,395 \cdot 12 \cdot W_c}{22,715} - (f - 0,395e)(T_{sp} - T_0) = 5753 \pm 15 \left[\frac{kJ}{m_u^3} \right];$$

$$\frac{12 \cdot W_c}{22,715} - W_{co} + (f' - e)(T_{sp} - T_0) = 4677 \pm 1 \left[\frac{kJ}{m_u^3} \right]$$

Ввиду того что значения компонентов $[100a + d \cdot X_L - f \cdot CO + \frac{RO_2 + CO}{1-x}(b - ex)] \cdot \frac{d(T_{sp} - T_0)}{dO_2}$ и $[100a + p \cdot RO_2 + d \cdot H_2O] \frac{d(T_{sp} - T_0)}{dO_2}$ значительно меньше от остальных компонентов, выступающих в выражениях (2.15) и (2.16), и кроме того, измерения доказали что значения производной $\frac{d(T_{sp} - T_0)}{dO_2}$ близки к единице, эти компоненты можно с достаточной точностью вычислить по упрощенным формулам:

а. для котлов, отопляемых каменным углем:

- при определении состава сухих топочных газов

$$[100a + d \cdot X_L - f \cdot CO + \frac{RO_2 + CO}{1-x}(b - ex)] \frac{d(T_{sp} - T_0)}{dO_2} \approx (133,8 + 1,3 \cdot RO_2) \frac{d(T_{sp} - T_0)}{dO_2} \quad (2.17)$$

- при определении состава влажных топочных газов

$$[100a + p \cdot RO_2 + d \cdot H_2O] \frac{d(T_{sp} - T_0)}{dO_2} \approx (130,75 + 0,452 \cdot RO_2 + 1,52 \cdot H_2O) \frac{d(T_{sp} - T_0)}{dO_2} \quad (2.18)$$

б. для котлов, отопляемых бурным углем:

- при определении состава сухих топочных газов

$$[100a + d \cdot X_L - f \cdot CO + \frac{RO_2 + CO}{1-x}(b - ex)] \frac{d(T_{sp} - T_0)}{dO_2} \approx (133,8 + 3,36 \cdot RO_2) \frac{d(T_{sp} - T_0)}{dO_2} \quad (2.19)$$

- при определении состава влажных топочных газов

$$[100a + p \cdot RO_2 + d \cdot H_2O] \frac{d(T_{sp} - T_0)}{dO_2} \approx (130,75 + 0,453 \cdot RO_2 + 1,52 \cdot H_2O) \frac{d(T_{sp} - T_0)}{dO_2} \quad (2.20)$$

В соответствии с выше изложенными упрощающими предположениями, формулы 2.15 и 2.16 принимают следующий вид:

а. для котлов, отопляемых каменным углем:

- при определении состава сухих топочных газов

$$\frac{dq}{dO_2} = [17832 + 5517 \frac{dCO}{dO_2} + (133,8 + 1,3 \cdot RO_2) \frac{d(T_{sp} - T_0)}{dO_2}] (21 - O_2 - RO_2 - 0,605 \cdot CO) - [17832(21 - O_2) + 5517 \cdot CO - 133,8(T_{sp} - T_0)] (\frac{dRO_2}{dO_2} + 0,605 \frac{dCO}{dO_2} + 1) = F(O_2) = 0 \quad (2.21)$$

- при определении состава влажных топочных газов

$$\frac{dq}{dO_2} = [17832 \cdot RO_2 + 5274 \cdot CO - (130,75 + 1,52 \cdot X_L)(T_{sp} - T_0)] \left[\frac{d(H_2O - X_L)}{dO_2} + \frac{X_L}{200} \frac{dCO}{dO_2} \right] - [17832 \frac{dRO_2}{dO_2} + 5274 \frac{dCO}{dO_2} - (130,75 + 0,452 \cdot RO_2 + 1,52 \cdot H_2O) \frac{d(T_{sp} - T_0)}{dO_2}] [H_2O - (1 - \frac{CO}{200}) X_L] = F(O_2) = 0 \quad (2.22)$$

б. для котлов, отапливаемых бурным углем:

- при определении состава сухих топочных газов

$$\frac{dq}{dq_2} = [17235 + 5735 \frac{dCO}{dq_2} + (133,8 + 3,36R_{O_2}) \frac{d(T_{sp}-T_0)}{dq_2}] (21 - q_2 - R_{O_2} - 0,605CO) - [17235(21 - q_2) + 5753CO - 133,8(T_{sp}-T_0)] (\frac{dR_{O_2}}{dq_2} + 0,605 \frac{dCO}{dq_2} + 1) = F(q_2) = 0 \quad (2.23)$$

- при определении состава влажных топочных газов

$$\frac{dq}{dq_2} = [17235R_{O_2} + 4677CO - (130,75 + 1,52X_L)(T_{sp}-T_0)] [\frac{d(H_2O-X_L)}{dq_2} + \frac{X_L}{200} \frac{dCO}{dq_2}] - [17235 \frac{dR_{O_2}}{dq_2} + 4677 \frac{dCO}{dq_2} - (130,75 + 0,453R_{O_2} + 1,52H_2O) \frac{d(T_{sp}-T_0)}{dq_2}] [H_2O - (1 - \frac{CO}{200})X_L] = F(q_2) = 0 \quad (2.24)$$

Из записанных выше выражений видно, что они весьма чувствительны на ошибки измерений, а, следовательно, не могут быть непосредственно использованы для оптимизации процесса сгорания без согласования результатов измерений.

2.4. Разностные записи формул обуславливающих минимум сумм потерь с уходящими газами и от неполного сгорания

Ввиду невозможности реализации соответственных измерительных систем для непрерывного и непосредственного определения производных $\frac{dR_{O_2}}{dq_2}$, $\frac{dCO}{dq_2}$, $\frac{d(H_2O-X_L)}{dq_2}$ и $\frac{d(T_{sp}-T_0)}{dq_2}$, значение этих производных определяются разностными частными:

$$\frac{dR_{O_2}}{dq_2} \approx \frac{R_{O_2}' - R_{O_2}''}{q_2' - q_2''}; \quad \frac{dCO}{dq_2} \approx \frac{CO' - CO''}{q_2' - q_2''}; \quad \frac{d(H_2O-X_L)}{dq_2} \approx \frac{(H_2O' - X_L') - (H_2O'' - X_L'')}{q_2' - q_2''}; \quad \frac{d(T_{sp}-T_0)}{dq_2} = \frac{(T_{sp}' - T_0') - (T_{sp}'' - T_0'')}{q_2' - q_2''} \quad (2.25)$$

Где: $R_{O_2}', O_2', CO', H_2O', X_L', (T_{sp}' - T_0')$ - измерения проведенные перед изменением избытка воздуха в топочной камере и после стабилизации процесса сгорания,

$R_{O_2}'', O_2'', CO'', H_2O'', X_L'', (T_{sp}'' - T_0'')$ - измерения проведенные после изменения избытка воздуха в топочной камере и после стабилизации процесса сгорания.

Для упрощения задачи принимают что эти производные соответствуют среднему значению O_2 , вычисленному на основании зависимости

$$O_2 = \frac{1}{2}(O_2' + O_2'') [\%] \quad (2.26)$$

Подобным способом можно вычислить средние значения остальных параметров, измеренных в двух последующих промежутках времени измерения, а именно:

$$R_{O_2} = \frac{1}{2}(R_{O_2}' + R_{O_2}''); \quad CO = \frac{1}{2}(CO' + CO''); \quad H_2O = \frac{1}{2}(H_2O' + H_2O''); \quad X_L = \frac{1}{2}(X_L' + X_L''); \quad T_{sp} - T_0 = \frac{1}{2}[(T_{sp}' - T_0') + (T_{sp}'' - T_0'')] \quad (2.27)$$

Подставив зависимости (2.25), (2.26) и (2.27) в выражения (2.21), (2.22), (2.23) и (2.24) получим окончательные записи разностных выражений, необходимых для определения минимума потерь, а именно:

а. для котлов, отапливаемых каменным углем:

- при определении состава сухих топочных газов

$$F(O_2)_{1,2} = [17832(21-O_2'') - 5517CO' - 133,8(T_{sp}'' - T_0'')] \frac{21-O_2' - RO_2' - 0,605CO'}{O_2' - O_2''} + \\ - [17832(21-O_2') - 5517CO' - 133,8(T_{sp}' - T_0')] \frac{21-O_2'' - RO_2'' - 0,605CO''}{O_2' - O_2''} \quad (2.28)$$

- при определении состава влажных топочных газов

$$F(O_2)_{1,2} = \left\{ 17832RO_2'' + 5274CO' - [130,75 + 0,76(X_L' + X_L'')](T_{sp}'' - T_0'') \right\} \frac{H_2O' - X_L' + \frac{CO'}{400}(X_L' + X_L'')}{O_2' - O_2''} + \\ - \left\{ 17832RO_2' + 5274CO' - [130,75 + 0,76(X_L' + X_L'')](T_{sp}' - T_0') \right\} \frac{H_2O'' - X_L'' + \frac{CO''}{400}(X_L' + X_L'')}{O_2' - O_2''} \quad (2.29)$$

б. для котлов, отапливаемых бурным углем:

- при определении состава сухих топочных газов

$$F(O_2)_{1,2} = [17235(21-O_2'') - 5753CO' - 133,8(T_{sp}'' - T_0'')] \frac{21-O_2' - RO_2' - 0,605CO'}{O_2' - O_2''} + \\ - [17235(21-O_2') - 5753CO' - 133,8(T_{sp}' - T_0')] \frac{21-O_2'' - RO_2'' - 0,605CO''}{O_2' - O_2''} \quad (2.30)$$

- при определении состава влажных топочных газов

$$F(O_2)_{1,2} = \left\{ 17235RO_2'' + 4677CO' - [130,75 + 0,76(X_L' + X_L'')](T_{sp}'' - T_0'') \right\} \frac{H_2O' - X_L' + \frac{CO'}{400}(X_L' + X_L'')}{O_2' - O_2''} + \\ - \left\{ 17235RO_2' + 4677CO' - [130,75 + 0,76(X_L' + X_L'')](T_{sp}' - T_0') \right\} \frac{H_2O'' - X_L'' + \frac{CO''}{400}(X_L' + X_L'')}{O_2' - O_2''} \quad (2.31)$$

Вычисленное таким образом значение $F(O_2)_{1,2}$ после согласования результатов первых и вторых измерений указывает только недостаток или избыток воздуха в топочной камере и, следовательно, является недостаточным для определения оптимального значения O_2 . С этой целью следует изменить избыток воздуха в топочной камере и после стабилизации процесса сгорания провести третьи измерения и далее, согласовать результаты первых, вторых и третьих измерений. Далее, следует вычислить $F(O_2)_{2,3}$ по одной из зависимостей (2.28), (2.29), (2.30) или (2.31) заменяя индексы 1 на 2 и 2 на 3.

После вычисления $F(O_2)_{1,2}$ и $F(O_2)_{2,3}$ нетрудно вычислить оптимальную долю кислорода в уходящих топочных газах из зависимости

$$(O_2)_{opt.} = \frac{(O_2' + O_2'') \cdot F(O_2)_{1,2} - (O_2' + O_2'') \cdot F(O_2)_{2,3}}{2[F(O_2)_{1,2} - F(O_2)_{2,3}]} \quad (2.32)$$

которая получена путем приравнивания к нулю линейной функции, проходящей через координаты двух пунктов $\{F(\alpha_{1,2}; \frac{1}{2}(\alpha_2' + \alpha_2''))\}$ и $\{F(\alpha_{2,3}; \frac{1}{2}(\alpha_2'' + \alpha_2'''))\}$.

Зависимость (2.32) на $(\alpha_2)_{opt}$ может быть использована непосредственно только в следующих случаях:

а. когда $F(\alpha_{1,2}) > 0$ и $\alpha_2' > \alpha_2''$

б. когда $F(\alpha_{1,2}) < 0$ и $\alpha_2' < \alpha_2''$

В остальных случаях следует изменить порядок вторых измерений на первые и наоборот, а именно:

$$(\alpha_2)_{opt} = \frac{(\alpha_2' + \alpha_2'') \cdot F(\alpha_{1,2}) - (\alpha_2' + \alpha_2''') \cdot F(\alpha_{1,3})}{2[F(\alpha_{1,2}) - F(\alpha_{1,3})]} \quad (2.33)$$

3. Согласование результатов измерений, проведенных в двух и трех последовательных отрезках времени

Согласование результатов измерений имеет целью уменьшение степени чувствительности зависимости (2.32) на ошибки измерений.

В случае определения состава сухих топочных газов на выходе котла, количество исходных уравнений для согласования результатов измерений равно трем и получаются они из зависимости (2.8) а именно:

$$f_1 = L_R \cdot R \alpha_2' + (L_R - 0.395) \cdot CO' + \alpha_2' - 21 = -w_1 \quad (3.1)$$

$$f_2 = L_R \cdot R \alpha_2'' + (L_R - 0.395) \cdot CO'' + \alpha_2'' - 21 = -w_2 \quad (3.2)$$

$$f_3 = L_R \cdot R \alpha_2''' + (L_R - 0.395) \cdot CO''' + \alpha_2''' - 21 = -w_3 \quad (3.3)$$

где: L_R - среднее наиболее вероятное значение этого коэффициента, соответствующее данному топливу,

w_1, w_2, w_3 - несовпадения основного уравнения (2.8) в трех последующих отрезках времени измерения.

В случае определения состава влажных топочных газов, результаты трех последовательных измерений $R\alpha_2, \alpha_2, CO, H_2O$ и X_L могут быть согласованы по двум исходным уравнениям, получающимся из зависимости

$$(21 - \alpha_2 - R\alpha_2 - 0.605CO) \left[\frac{d(H_2O - X_L)}{d\alpha_2} + \frac{X_L}{200} \frac{dCO}{d\alpha_2} \right] + \left[H_2O - \left(1 - \frac{CO}{200}\right) X_L \right] \left(\frac{dR\alpha_2}{d\alpha_2} + 0.605 \frac{dCO}{d\alpha_2} + 1 \right) = 0 \quad (3.4)$$

которая получена после сравнения выражений (2.13) и (2.14), а именно:

$$f_1 = (21 - \alpha_2' - R\alpha_2' - 0.605CO') \left[H_2O' - X_L' + \frac{CO'}{400} (X_L' + X_L'') \right] - (21 - \alpha_2'' - R\alpha_2'' - 0.605CO'') \left[H_2O'' - X_L'' + \frac{CO''}{400} (X_L' + X_L'') \right] = -w_1 \quad (3.5)$$

$$f_2 = (21 - \alpha_2'' - R\alpha_2'' - 0.605CO'') \left[H_2O'' - X_L'' + \frac{CO''}{400} (X_L'' + X_L''') \right] - (21 - \alpha_2''' - R\alpha_2''' - 0.605CO''') \left[H_2O''' - X_L''' + \frac{CO'''}{400} (X_L'' + X_L''') \right] = -w_2 \quad (3.6)$$

Два последующих исходных уравнения для согласования результатов трех последующих измерений состава влажных топочных газов (RO_2, O_2, CO, H_2O и X_L) получены в результате подстановки в формулы (3.5) и (3.6) равноценных выражений, возникающих из равенств (3.1), (3.2) и (3.3) вместо $21-d_2'-RO_2'-0,605CO'$, $21-d_2'-RO_2'-0,605CO'$ и $21-d_2'-RO_2'-0,605CO''$ а именно:

$$21-d_2'-RO_2'-0,605CO' = (L_R-1)(RO_2'+CO') \quad \text{и т.д.} \quad (3.7)$$

Тогда два последующих исходных уравнения для согласования результатов трех последовательных измерений состава влажных топочных газов примут следующий вид:

$$f_3 = (RO_2'+CO') \left[H_2O'-X_L' + \frac{CO'}{400}(X_L'+X_L'') \right] - (RO_2'+CO') \left[H_2O''-X_L'' + \frac{CO''}{400}(X_L'+X_L'') \right] = -w_3 \quad (3.8)$$

$$f_4 = (RO_2''+CO'') \left[H_2O''-X_L'' + \frac{CO''}{400}(X_L'+X_L'') \right] - (RO_2'+CO') \left[H_2O''-X_L'' + \frac{CO''}{400}(X_L'+X_L'') \right] = -w_4 \quad (3.9)$$

Согласование результатов измерений ведут следующим способом:
а. линеаризуют основные зависимости служащие согласованию результатов измерений относительно каждого измерения данного параметра

$$\sum_i a_{ki} \cdot V_i = w_k \quad (3.10)$$

где: a_{ki} — частные производные исходного уравнения k относительно измерения i данного параметра,
 V_i — поправка значения измерения i данного параметра,
 w_k — несовпадение исходного уравнения.

б. используют условие наименьших квадратов

$$m_i^2 V_i = \sum_k a_{ki} \cdot k_k \quad (3.11)$$

где: m_i — абсолютная ошибка измерений, определенная посредством класса точности данного измерительного прибора и его верхнего предела измерений,
 k_k — неопределенный коэффициент Лагранжа для исходного уравнения.

Решив уравнения (3.1), (3.2), (3.3), (3.10) и (3.11) или (3.5), (3.6), (3.8) (3.9), (3.10) и (3.11) получим величины поправок V_i а тем самым согласованные величины отдельных параметров, измеренных в трех отдельных промежутках времени.

4. Выводы

А. После согласования результатов измерений ошибки этих измерений будут меньше, чем до согласования. Результаты основанных на примерах вычислений собраны в таблицах Т.4.1. и Т.4.2.

Т.4.1. Сравнение ошибок измерений с ошибками полученными после согласования результатов трех измерений отдельных компонентов сухих топочных газов

измеряемые параметры	RO ₂ [%]			O ₂ [%]			CO [%]			L _R
	1	2	3	1	2	3	1	2	3	
последовательность измерений										
состав топочных газов	14,30	13,98	13,65	5,0	5,4	5,8	0,374	0,307	0,274	1,1
класс точности измерителя	2,5	2,5	2,5	2,5	2,5	2,5	2,5	2,5	2,5	
m _i -ошибка измерителя	0,5	0,5	0,5	0,25	0,25	0,25	0,0125	0,0125	0,0125	0,026
\bar{m}_i -ошибка после согласования	0,238	0,235	0,224	0,186	0,185	0,184	0,010	0,010	0,010	0,0155

Т.4.2. Сравнение ошибок измерений с ошибками полученными после согласования результатов трех измерений отдельных компонентов влажных топочных газов

измеряемые параметры	RO ₂ [%]			O ₂ [%]			CO	H ₂ O [%]		X _L
	1	2	3	1	2	3	1	1	2	1
последовательность измерений										
состав топочных газов	14,30	13,98	13,65	5,0	5,4	5,8	0,374	10,00	9,78	2
класс точности измерителя	2,5	2,5	2,5	2,5	2,5	2,5	2,5	2,5	2,5	2,5
ошибка измерителя	0,5	0,5	0,5	0,25	0,25	0,25	0,0125	0,25	0,25	0,125
ошибка после согласования	0,238	0,236	0,222	0,151	0,150	0,146	0,009	0,193	0,135	0,085

В. Задача оптимизации процесса сгорания не может быть решена без согласования результатов измерений. Вывод этот сделан в результате вычислений максимальных ошибок $m_{(O_2)opt}$ перед и после согласования результатов трех измерений состава влажных топочных газов. Результаты вычислений этих максимальных ошибок собраны в таблице Т.4.3.

Т.4.3. Сравнение ошибок $m_{(O_2)opt}$ перед и после согласования результатов трех измерений состава влажных топочных газов

Диапазон изменения O_2 в уходящих топочных газах относительно $(O_2)_{opt} = 5,7\%$			Ошибка $m_{(O_2)opt}$ - метода оптимализации процесса сгорания			
O_2'	O_2''	O_2'''	класс точности из мерителей - 2,5		класс точности из мерителей - 1,5	
			без согласования	после согласования	без согласования	после согласования
52	54	56	43,50	5,07	26,10	3,11
50	54	58	10,17	1,55	6,10	0,96
48	54	60	4,42	0,84	2,65	0,55
46	54	62	2,53	0,61	1,52	0,38

В. В результате подсчетов, приведенных в таблице Т.4.3. получается, что задача оптимализации процесса сгорания может быть достаточно точно решена при помощи измерительных систем класса точности 1,5 а также при изменении количества O_2 в уходящих газах не менее чем на 0,8 % между двумя последующими измерениями

Г. По поводу отсутствия в данное время конкретных измерений, оценку ошибок перед и после согласования результатов измерений произведено на основании следующих предположений:

а. известны характеристики $CO=f(O_2)$ и $x=\varphi(O_2)$ определяющие процесс сгорания в данных эксплуатационных условиях

$$CO=f(O_2)=2 \frac{6-O_2}{3+2O_2}+0,22 [\%], \quad x=\varphi(O_2)=0,002(6-O_2)^2+0,005.$$

б. содержания остальных компонентов топочных газов, соответствующие данному содержанию свободного кислорода в уходящих топочных газах перечислено из зависимостей:

$$RO_2=(21-O_2+0,395 \cdot CO) \frac{1-x}{L_R-x} - CO [\%], \quad H_2O=\frac{RO_2+CO}{1-x} \cdot A + (1-\frac{CO}{200}) \cdot X_L [\%].$$

причем принято, что: $A=0,542$; $L_R=1,1$; $X_L=2$ [%].

в. несовпадения основных уравнений для согласования результатов измерений перечислено по формуле

$$w_k = \sqrt{\sum_i a_{ki}^2 \cdot m_i^2}$$

где: m_i - максимальное отклонение измерительного прибора определенное по класс точности и верхний диапазон.

Из того взгляда результаты подсчетов следует принимать как ориентировочные.

Literatura

1. St. Ochęduszek, J. Szargut - Metody wyznaczania stosunku niecałkowitego spalania. Gospodarka Ciepła - Energetyka Przemysłowa. Zeszyt 6. 1953 r.
2. J. Szargut, Z. Kolenda - Uzgadnianie bilansów substancji i energii w procesach chemicznych. Pomiary Automatyka Kontrola. 1967 r.
3. J. Szargut - Gospodarka ciepła w hutnictwie wydanie książkowe - w druku .
4. J. Szargut, Z. Kolenda - Theory of coordination material and energy balances in chemical processes. Archiwum Hutnictwa (w druku) .
5. K. Taramina - Teoretyczne podstawy ciągłego pomiaru straty wylotowej wyrażonej w kotłach parowych (rozprawa doktorska). Wrocław. 1962 r.
6. K. Taramina - Nowe postacie wzorów na stratę wylotową wyróżną w kotłach parowych opalanych węglem brunatnym. Prace Instytutu Automatyki Systemów Energetycznych. Zeszyt 4, Wrocław. 1965 r.
7. K. Taramina - Teoretyczne podstawy optymalizacji procesu spalania w kotłach parowych opalanych węglem kamiennym i brunatnym. Prace Instytutu Automatyki Systemów Energetycznych. Zeszyt 7, Wrocław. 1967 r.

INVESTIGATION OF THE DIRECT DIGITAL CONTROL OF AN ONE-THROUGH-BOILER

B. Hanuš

Technical College VŠST
Liberec, Czechoslovakia

The application of a digital computer in the power engineering has a progressive tendency. The computer is used for checking and for evaluation of the technological process and for control of the energetic system, as well as of the power plant and of the energetic block itself. Here, the computer is used not only for control under normal operating conditions but also for automatic starting up and loading. In order to obtain much more experience with a digital computer, control processes are investigated under application of different control algorithms. Algorithms for a general error compensation according to a quadratic criterion appeared to be very suitable. These algorithms are varied and enable therefore good adaptation for the given real conditions. The calculations of the algorithms are carried out by means of a digital computer on the basis of dynamic characteristics of the control system. The characteristics are given in the time sequence-form of dynamic responses. Normal procedure using Z-transformation was not applied at all.

1. Calculation of a control algorithm

The calculation of a control algorithm is carried out in two steps :

In the first step from the beginning of the control process until the ℓ -th interval the state values x_m of the system are measured. The minimum number of these state values / of vector elements / is $n + r$, where n is the order of the controlled system and r is the number of the controlled variables. The different physical values and their derivatives or the same physical values but in different sampling intervals can be used as the state values. At the same time-interval also changes of the manipulated variables y_m and entering disturbances z_m are measured / presuming that it is actually possible /. On the basis of all these measured values there are evaluated the so called substitute disturbances z_n / $n + r$ elements/

which are presumed to enter the system before beginning of the control process. The vector of the substitute disturbances is given by the relation

$$x_m = G_m z_n + H_m z_m + F_m y_m \quad / 1 /$$

where G_m , H_m , F_m are the matrices of discrete values of system responses.

When determined disturbances z_d , not measured at all, are expected to enter the system during the measuring of the state values x_m , it is possible to generalize the formula / 1 / by introducing the relation

$$z = \begin{vmatrix} z_n \\ z_d \end{vmatrix} \quad / 2 /$$

in the form

$$x_m = G_m z + H_m z_m + F_m y_m \quad / 3 /$$

In the case / 3 / of course the number of the elements of the vector x_m is to be augmented to the number of the elements of the vector z .

From / 1 / and / 3 / it follows for the vector of substitute disturbances

$$z_n = G_m^{-1} [x_m - H_m z_m - F_m y_m] \quad / 4 /$$

or

$$z = G_m^{-1} [x_m - H_m z_m - F_m y_m] \quad / 5 /$$

In the second step the criterion values $x_k(j)$ of the system are calculated for each control interval from the relation

$$x_k(j) = F(j)y + F_k(j)y_m + G_k(j)z_n + H_k(j)z_m \quad / 5 /$$

where y is the vector of the manipulated variable changes from the control interval ℓ till $u-1$ and $F(j)$ to $H_k(j)$ are matrices of discrete values of the system responses.

For the criterion values x_k and for the manipulated variable changes y in the time interval of the control process taken into account $j = \ell + k$ to u a condition of minimum functional is valid

$$J = \sum_{j=\ell+k}^u x_k^T(j) K_{kj} x_k(j) + y^T K_{2j} y \rightarrow \min \quad / 6 /$$

where K_{kj} and K_{2j} are the diagonal matrices of weight coefficients.

The number of the criterion values x_k in the control interval is only unilaterally limited / the minimum number is r /. Inserting / 4 / and / 5 / into / 6 / it holds for the vector of optimal manipulated variable changes, after the derivatives $\frac{\partial J}{\partial y} = 0$ are carried out,

$$y = - \left\{ \sum_{j=\ell+k}^u F^T(j) K_{kj} F(j) + K_{2j} \right\}^{-1} \cdot \left(\sum_{j=\ell+k}^u F^T(j) K_{kj} \{ G_k(j) G_m^{-1} x_m + [H_k(j) - G_k(j) G_m^{-1} H_m] z_m + [F_k(j) - G_k(j) G_m^{-1} F_m] y_m \} \right) \quad / 7 /$$

The control algorithm for the r -dimensional control system is given by the first r rows of the system / 7 /, which include all manipulated variables for a control interval just carried out.

2. The control algorithm for a program control and for loading

In the case of a program control a vector of

command values is prescribed for the criterion values. Instead of / 6 / it is possible to write a condition

$$J = \sum_{j=l+k}^u (x_k(j) - w(j))^T K_{kj} (x_k(j) - w(j)) + y^T K_{2j} y \quad / 8 /$$

For a control algorithm a generalized relation holds instead of / 7 /

$$y = - \left\{ \sum_{j=l+k}^u F(j)^T K_{kj} F(j) + K_{2j} \right\}^{-1} \cdot \left(\sum_{j=l+k}^u F(j)^T K_{kj} \{ -w(j) + G_k(j) G_m^{-1} x_m + [H_k(j) - G_k(j) G_m^{-1} H_m] z_m + [F_k(j) - G_k(j) G_m^{-1} F_m] y_m \} \right) \quad / 9 //$$

If a time program is given in a polynomial form

$$w_k(t) = \sum_{i=0}^Y a_i t^i \quad / 10 /$$

then for a conformity between the command values and the real criterion values inside the control interval it is required that the control loop should contain as many integrators as corresponds to the degree of the polynomial / 10 /. Usually one integrator will suffice. It is possible to realise its transfer-function by means of a digital computer directly.

In the case of program-loading the time behaviour of the disturbance z_p is given. For the criterion values in that case it holds

$$x_k(j) = F(j) y + F_k(j) y_m + G_k(j) z_n + H_k(j) z_m + P_k(j) z_p \stackrel{!}{=} w(j) \quad / 11 /$$

and for the control algorithm it follows

$$y = - \left\{ \sum_{j=l+k}^u F(j)^T K_{kj} F(j) + K_{2j} \right\}^{-1}$$

$$\begin{aligned} & \cdot \left(\sum_{j=l+k}^N F^T(j) K_{kj} \{-w(j) + G_k(j) G_m^{-1} x_m + \right. \\ & \quad + [H_k(j) - G_k(j) G_m^{-1} H_m] z_m + P_k(j) z_p + \\ & \quad \left. + [F_k(j) - G_k(j) G_m^{-1} F_m] y_m \} \right) \end{aligned}$$

/ 12 /

3. Quadratic criterion with additional conditions

Additional conditions for the criterion values during the control process can be attached to the functional / 6 / or / 8 /. These conditions can be expressed by means of a criterion values vector $x_v(k)$ joined to a sampling interval k

$$e = x_v(k) - w_v(k) = 0$$

/ 13 /

where

$$x_v(k) = F_v(k) y + F_{mv}(k) y_m + G_v(k) z_n + H_v(k) z_m + P_v(k) z_p / 14 /$$

By means of the additional conditions / 13 / it is possible e.g. to obtain a control process in a finite control interval number. In this way the additional conditions enable to derive one general formula for calculating control algorithms for a finite control process and according to the quadratic criterion.

Connecting conditions / 8 / and / 13 / and using a vector of Lagrange factorials we obtain

$$F = J + \lambda^T e \quad \rightarrow \quad \min$$

/ 15 /

After carrying out the derivatives according to the manipulated variables y it holds

$$\begin{aligned} 0 &= \frac{\partial J}{\partial y(j)} + \frac{\partial}{\partial y(j)} (\lambda^T e) = \\ &= \sum_{j=l+k}^N F^T(j) K_{kj} \{-w(j) + G_k(j) G_m^{-1} x_m + \\ & \quad + [H_k(j) - G_k(j) G_m^{-1} H_m] z_m + P_k(j) z_p + \\ & \quad + [F_k(j) - G_k(j) G_m^{-1} F_m] y_m + \\ & \quad + F(j) y\} + K_{2j} y + F_v^T(k) \lambda \end{aligned}$$

/ 16 /

and after derivatives according to the Lagrange factorials λ it holds

$$\begin{aligned} 0 &= \frac{\partial J}{\partial \lambda_s} + \frac{\partial}{\partial \lambda_s} (\lambda^T e) = \frac{\partial}{\partial \lambda_s} (\lambda^T e) = e = \\ &= -w_v(k) + G_v(k)G_m^{-1}x_m + \\ &\quad + [H_v(k) - G_v(k)G_m^{-1}H_m]z_m + P_v(k)z_p + \\ &\quad + [F_{mv}(k) - G_v(k)G_m^{-1}F_m]y_m + F_r(k)y \end{aligned} \quad / 17 /$$

After joining both systems and after introducing simplified symbols we obtain

$$\mathcal{F} \begin{vmatrix} y \\ \lambda \end{vmatrix} = Ww - X_m x_m - Z_m z_m - Z_p z_p - Y_m y_m \quad / 18 /$$

Then it holds for a vector of optimal manipulated values

$$\begin{vmatrix} y \\ \lambda \end{vmatrix} = \mathcal{F}^{-1} \{ Ww - X_m x_m - Z_m z_m - Z_p z_p - Y_m y_m \} \quad / 19 /$$

The argument k of the vector $w_v(k)$ is calculated from the beginning of the whole control process and is being reduced by 1 for every following control interval. Therefore it is not possible to take for a control algorithm the first r rows of the system / 19 / as was done in the previous cases. The procedure for the evaluation of the control algorithm is then as follows:

The time behaviour of all criterion or state values are calculated on the basis of the optimal manipulated values vector y . This time behaviour is taken as given and corresponding coefficients of the control algorithm are calculated in the way described in the next chapter.

4. The control algorithm for a given control process

Let y_q ($q = 1$ to r) be the time behaviour of the q -th manipulated variable and let x_k ($k = 1$ to m) be the time behaviour of the corresponding state values for a given control process caused by the i -th ($i = 1$ to r) determined disturbance. Further let us suppose that the control algorithm

is given by the relation

$$\Delta_{iq} y(j) = \sum_{k=1}^m \sum_{g=0}^h q^{a_{kg}} \cdot x_{ik}(j-g) + \sum_{f=1}^r \sum_{g=1}^h q^{b_{fg}} \cdot \Delta_{fq} y(j-g) \quad / 20 /$$

$j = 0 \text{ to } u-1$
 $q = 1 \text{ to } r$

After inserting the time behaviour of manipulated variable changes $\Delta_{fq} y(j)$ and of state values $x_{ik}(j)$ into equation / 20 /, it is possible to calculate the values of all the coefficients of the control algorithm $q^{a_{kg}}, q^{b_{fg}}$. When however the number of the equations / 20 / is greater than the number of unknown coefficients of the control algorithm, the values of the coefficients are to be evaluated from the minimum square error condition

$$J = \sum_{i=1}^r \sum_{j=0}^{u-1} k_{ijq} \varepsilon_{iq}^2(j) \rightarrow \min \quad q=1 \text{ to } r \quad / 21 /$$

where k_{ijq} is the weight coefficient,
 $\varepsilon_{iq}(j)$ is the error

$$\varepsilon_{iq}(j) = \Delta_{iq} y(j) - \sum_{k=1}^m \sum_{g=0}^h q^{a_{kg}} \cdot x_{ik}(j-g) - \sum_{f=1}^r \sum_{g=1}^h q^{b_{fg}} \cdot \Delta_{fq} y(j-g) \quad / 22 /$$

After some treatment it holds for the values of the coefficients of the control algorithm for the q -th manipulated variable

$$\begin{vmatrix} a_q \\ b_q \end{vmatrix} = \left\{ |X, Y|^T K_{ijq} |X, Y| \right\}^{-1} |X, Y|^T K_{ijq} y_q \quad / 23 /$$

$q = 1 \text{ to } r$
 $i = 1 \text{ to } r$
 $j = 0 \text{ to } u-1$

where X, Y are the matrices of discrete values of state values and of manipulated variables from the given control process for all entering disturbances $i = 1 \text{ to } r$,

y_q is the vector of manipulated variable changes for all entering disturbances $i = 1 \text{ to } r$ and K_{ijq} is the diagonal matrix of weight coefficients.

Conclusion

The investigation of control algorithms was carried out by calculating algorithm coefficients and by evaluating control processes for different disturbances. The time behaviour was calculated either directly by means of the digital computer or by means of a model on the analogue computer connected with the digital computer. This connection was brought about in the laboratory of the national enterprise ZPA, Prague /analogue computer ARS, AR, MN 7 and digital computer LGP 21 / and in the laboratory of the Technical College VŠST, Liberec / analogue computer AP 3, MEDA and digital computer MINSK 22 /. For the investigation of the direct digital control a One-through-boiler is made available in the power plant Ledvice in connection with a digital computer LGP 21. The Institute EGÚ Prague is in charge of all this research work.

References

- Hanuš B., Untersuchungen von Algorithmen für digitale Mehr - fachregelung, Messen-Steuern-Regeln, No. 9, 1968.

DIGITAL CONTROL TECHNIQUES FOR POWER PLANT APPLICATIONS

Theodore Giras
Advisory Engineer
Westinghouse Electric Corp.
Hagan/Computer Systems Div.
Pittsburgh, Pa. 15238

Robert Uram
Senior Engineer
Westinghouse Electric Corp.
Hagan/Computer Systems Div.
Pittsburgh, Pa. 15238

INTRODUCTION

A trend of major significance in the design of electric power plants today is the use of once-through boilers to provide superheated steam for the turbine generator. In these modern plants it is not possible to use conventional boiler-follow or turbine-follow control concepts since the boiler and turbine can no longer be operated as separate power plant entities. The once-through boiler imposes an ever increasing challenge on the control engineer to develop a control philosophy which includes consideration of all elements of the power plant in a coordinated plan. 1

To ensure proper operation of such a complex scheme all the techniques of modern control theory must be used. These include nonlinear feed forward characterization of major plant variables such as load demand, boiler demand, feedwater demand, fuel demand and air demand; calibration of the feed forward control action by measured variables such as pressures, temperatures and flows; adaptive controllers sensitive to real plant variables and adjusted to operate over the entire range from no load to full load; minor-loop feedback control which is coordinated throughout the entire system; and finally, logical interaction of all control loops to ensure bumpless transfer from manual to automatic, and from automatic to manual, modes of operation.

The wide range of controllability required for the steam plant of today suggests the use of high-speed digital controllers to implement the sophisticated control philosophy necessary for proper operation.

This paper will describe some of the techniques used to implement control in a steam power plant.

DIGITAL CONTROL ALGORITHM REQUIREMENTS FOR POWER PLANTS

There are a number of basic requirements which a digital system must satisfy in order to control a complex process. First and foremost is the ability to alter or modify the control package easily and quickly in the field to

accommodate process dynamic characteristics which could not be anticipated early in the design. The digital system must lend itself to a building block format, with the inter-connections between blocks simple and easy to program or modify as more is learned about the process. It must be possible to remove individual blocks or groups of blocks, and to replace these with other individual blocks or groups of blocks. The programming effort to do this interchanging must be relatively simple so that plant engineers who are not expert computer programmers can make the changes with a high degree of accuracy and in a minimum of time.

In addition to this block flexibility, the digital package must be designed so that process parameters can be changed quickly and accurately. Thus plant gains, biases, set points, limits, time constants and other important system data must be arranged in the computer storage in such a fashion that inexperienced field personnel may adjust these values literally at will. This is of paramount importance, for as more is learned over a period of time in controlling a plant with a computer, refinements in the control system must be made to improve operating efficiency and reliability.

Another major requirement of a digital system is careful selection of the computing schemes used in the various controllers and functional blocks. Since all implementation within the computer must ultimately be done with numerical methods, the general formulation and selection of any algorithm structure becomes quite critical. Thus the numerical schemes for integration, differentiation, smoothing, and characterization must be carefully selected to assure proper control action, and yet be simply and easily programmed.

Superimposed on this selection are the two classical constraints one is faced with in digital computer utilization: computing time and computer storage capacity. Clearly, there is a finite time in which all computations must be done in a feedback control system for a typical plant, and there is a finite limit to the storage one must realistically face. Therefore sophisticated mathematical algorithms which require lengthy computing time and large storage capacity must give way to acceptable alternatives which do the job satisfactorily in reasonable time and with minimum storage. However, one must not allow the pendulum to swing too far in the other direction, for inaccurate mathematical algorithms will not do the proper job in a complex control system. Thus a compromise is required which is acceptable from all points of view.

DIGITAL CONTROLLER ALGORITHMS

The conventional dynamic controllers required in any process system consist of the following: reset, rate, proportional plus reset, proportional plus rate, and proportional plus reset plus rate. Since these five standards are combinations of two fundamental controllers - the reset and rate - it is only necessary to develop these basic controller algorithms. Then by providing means for interconnecting these within the computer, all possible controllers may be formulated.

The following discussion will develop these two basic algorithms; in addition the first order lag function will be presented. Although technically it is not a controller, the first order lag occurs many times in a process control system and must therefore be accounted within a digital package.

Reset Controller

Figure 1a shows a diagrammatic representation of the reset controller with time varying input $x(t)$ and output $y(t)$, while Figure 1b lists the conventional transfer function in terms of the Laplace variables and the controller reset time T . The mathematical relationship between the reset controller input and output is that of integration as given in Eq. (1) below.

$$y(t) = \frac{1}{T} \int x(t) dt \quad (1)$$

The numerical solution of this equation may be accomplished by a number of different schemes. The simplest of these is the rectangular integration method as follows:

$$y(n) = y(n-1) + \frac{\Delta T}{T} x(n) \quad (2)$$

Here ΔT is the sampling interval, at which instant the digital algorithm will compute the current value of y ; the integers n and $(n-1)$ represent discrete sampling periods.

From the point of view of computer storage and running time, the rectangular rule is ideal since each of these is minimized. However, the method is inaccurate for systems in which the reset time T is of the same order of magnitude as the sampling time ΔT . The only alternative then is to reduce the sampling interval to a much smaller value, which then requires many more computations and thus defeats the purpose of the digital controller.

A second numerical method of solving Eq. (1) is with the trapezoidal rule as follows:

$$y(n) = y(n-1) + \frac{\Delta T}{2T} [x(n) + x(n-1)] \quad (3)$$

It is clear that this method requires additional storage to save the past value of input $x(n-1)$, and also requires additional computation due to the more complex formulation. However these points are more than matched by the much higher accuracy of the algorithm due to the knowledge of the past history of the input function; thus the method may be used with a larger sampling interval and a net reduction in computation time.

The technical literature ² contains additional analytical verification of the merits of the trapezoidal integration method over the rectangular method in terms of frequency response and phase shift.

Figure 1c lists the FORTRAN programming statement required to execute the trapezoidal reset algorithm, while Figure 1d shows the output curve for a unit step input. It will be noted that the initial slope of the output differs slightly from the succeeding slope, because the initial computation had no past history value for $x(n-1)$ in Eq. (3) above. Note also that the output ramp has been limited to a maximum value of unity; this is a built-in feature of the algorithm and may be set at any value in the field. The quantity denoted YARRAY in Figure 1c has both high and low limits at which the integral action is held and not permitted to windup.

Rate Controller

Figure 2a shows a diagrammatic representation of the rate controller and Figure 2b lists the transfer function. It will be seen that the transfer function includes a smoothing or filtering term $1/(1+Ts)$, because pure differencing action is highly sensitive to noise and may yield numerical instability.

In terms of the Laplace variables, the analytical relationship between input and output for the rate controller is:

$$Y(s) = \frac{Ts}{1 + Ts} X(s) \quad (4)$$

This may be solved for the derivative of the output variable, resulting in the following:

$$\frac{dy}{dt} = \frac{dx}{dt} - \frac{1}{T} y \quad (5)$$

Using the same technique of trapezoidal integration as for the reset controller, Eq. (5) may be written in the following format:

$$y(n) = \left[\frac{2T - \Delta T}{2T + \Delta T} \right] y(n-1) + \frac{2T}{2T + \Delta T} \left[x(n) - x(n-1) \right] \quad (6)$$

Figure 2c lists the FORTRAN statement which will call for evaluation of the rate algorithm controller, and Figure 2d shows the response to a unit step input. The output has the expected initial impulse due to the leading edge of the input step, followed by an exponential decay as a result of the filtering or smoothing action of $1/(1+Ts)$.

First Order Lag

Figure 3a indicates the symbolic representation for the first order lag function, and Figure 3b shows the transfer function. The relation between input and output then may be written as given below.

$$Y(s) = \frac{1}{1 + Ts} X(s) \quad (7)$$

In differential equation form the lag output is given by:

$$\frac{dy}{dt} = \frac{1}{T} y - \frac{1}{T} x \quad (8)$$

The trapezoidal formulation of Eq. (8) yields:

$$y(n) = \left[\frac{2T - \Delta T}{2T + \Delta T} \right] y(n-1) + \frac{\Delta T}{2T + \Delta T} \left[x(n) + x(n-1) \right] \quad (9)$$

Figure 3c lists the FORTRAN statement to execute the lag algorithm while Figure 3d shows that the response to a unit step input is the exponentially increasing output approaching unity.

Digital Controller Algorithm Connections

With the above algorithms serving as building blocks, it is now possible to devise many other controllers. As an example, Figure 4 shows the various diagrams, relationships and response to a unit step for the proportional plus reset controller. The output plot indicates the initial jump to unity due to the proportional gain (assumed 1.0), followed by the ramping action of the reset portion of the controller. Again the output is limited by the internal action of the algorithm to an upper level determined by the user in the field.

The appropriate diagrams and equations for the proportional plus rate controller are given in Figure 5. As may be expected the output rises immediately to 2.0 due to the combination of the proportional gain of unity and the derivative action of the rate controller. Then exponential decay of the filter portion of the rate yields an output dropping to unity.

The most elaborate of the controllers is the proportional plus reset plus rate, which is shown in Figure 6. The output response to a unit step in Figure 6d shows the combined action of each part of this three-mode controller.

Nonlinear Digital Algorithms

In addition to the controllers described above, a modern power plant control system requires a number of other special functions to assure complete and accurate controllability. Among these are nonlinear characterization, high and low signal selection, high and low signal limiting, and deadband action.

Figure 7 shows the pertinent sketches to implement nonlinear characterization of a variable. As indicated in Part c of Figure 7 the functional relationship between input and output may be any combination of straight line segments. Currently up to six points, and therefore five straight line segments, may be used in this characterization; however this may be expanded easily to any required number for higher degrees of accuracy. Many different combinations of straight line segments having positive, negative or zero slopes and positive, negative or zero intercepts have been tested and proven to be extremely accurate fits to complex curves.

The high and low signal selector building blocks required in a system are shown in Figure 8. These algorithms select the algebraically higher, or the lower, of two time varying input quantities at each sampling instant. Proper account is taken of algebraic sign, including the case of either signal being zero.

The high and low limit functions are similar to the selector blocks except that the limiting signal is often preset at a fixed value (although this is not absolutely necessary). Figure 9 indicates the appropriate information for these limiting blocks; again account of algebraic sign is included.

In Figure 10 is shown the diagram and action required for the deadband function. In this case the output is set to zero if the input is within the deadband region; otherwise the output is set equal to the input.

General Application Examples of Digital Algorithms

A few examples using the various digital algorithms described will be given to illustrate some of the possibilities for interconnecting in control systems. Consider first the situation shown in Figure 11, where a rate and a lag algorithm have been connected in cascade. Part a of the figure includes the FORTRAN statements necessary to execute the two functions, while Part b is a plot of the output response to a unit step input. This particular system is typical of portions of power plants containing energy storage which may be used in times of transient upsets to aid in system stability. Later in this paper an example of such a situation will be used in a simulation model.

A second more elaborate example is shown in Figure 12, where the system is nonlinear because of multiplication of variables in the middle part of the diagram. In illustrating the use of the algorithms described above, it has been assumed that a unit step reference has existed at the input R in Figure 12 and that the system has been in steady state for a long time. Then a momentary disturbance has occurred at time $t=0$ which drops the controlled output C to 0.9 instantly, after which the disturbance disappears.

The problem then is to determine if the system will return to its steady state value and, if so, over what kind of transient path. For this case a series of computer runs have been made using the algorithms to determine the effect of the proportional gain K_2 on the system behavior. Plots of the controlled variable C are given in Figure 13, where the important role of K_2 is dramatically shown.

Many additional computer runs have been made on the system of Figure 12 using the digital package described in this paper. Valuable information concerning both the system, which is typical of sub-loops in power plants, and the algorithms has been obtained for overall process control.

Digital Control Applied to a Feedwater Demand Loop In a Steam Power Plant

The aim of this paper has been to show the application of digital concepts to a steam power plant. Since the entire control system for a modern once-through steam boiler-turbine-generator combination is exceedingly complex, one part of the system, the feedwater demand control, will be isolated and described with the package discussed above. Then it may be possible to visualize how the complete system can be incorporated into computer control.

Figure 14 shows the control system for developing the feedwater demand signal, while definition of the various quantities is given in Table I. In the diagram the concept of feedforward control is indicated with the heavy dark lines which represent the desired plant load demand. In the left part of the diagram the characterized plant demand generates a throttle pressure set point which is differenced with actual throttle pressure to yield a throttle pressure error. Additional feedforward characterization of plant demand develops a convection pass enclosure pressure set point which is differenced with actual convection pass enclosure pressure to yield a convection pass enclosure pressure error. Each of these error signals then drive reset controllers which trim the feedforward plant demand so that the final output of feedwater demand is properly adjusted for dynamic response.

As Figure 14 indicates, the feedwater control system requires throttle pressure, convection pass enclosure pressure and convection pass enclosure temperature as feedback signals. In the real plant these would be available from measuring apparatus and transducers, so that the system could be closed and tied together. However, in the context of this paper these feedback quantities are not available per se. Thus it is necessary to develop a method of simulating these signals in order that the entire feedwater loop may be closed and the digital package demonstrated.

Figure 15 indicates the additional functions needed to generate the required dynamic feedback quantities. The upper left part of Figure 15 shows blocks which produce the desired steady state pressures, temperature and feedwater flow as a function of load demand. Normally these curves are available from the plant designer and may be easily simulated with the digital algorithms.

The desired feedwater flow then is differenced with the feedwater set point from the control system to develop a feedwater increment, which in turn is used to drive transfer functions that produce incremental pressure and temperature signals. The analytical form of these transfer functions has been derived from experimental field data which show pressure and temperature incremental change in terms of step feedwater change. Finally, the pressure and temperature increments are added to the design quantities to yield realistic feedback pressures and temperature for the control system.

With the simulation and control system as shown in Figure 15 we are ready to use the digital package to control the plant model. Each of the blocks of Figure 15 can be described with the appropriate FORTRAN statements of the previous discussion,

and the entire system connected within a digital computer. This has been done with a program written for this purpose and designed so that changes or modifications of the system can be made conveniently.

Results of a computer run are shown in Figure 16, where the system has been allowed to come to steady state with a feedwater set point of 100 per cent. Then this set point has been suddenly changed to 90 per cent, with the results of the digital control system - plant simulation model plotted as shown in Figure 16. As may be observed, the feedwater demand adjusts itself to the new value of 90 per cent after going through a typical transient excursion.

Many computer runs have been made with this system to verify its proper operation, and continuing effort is being made to learn more about, and to improve, the plant controllability. Additional parts of the control system, such as the fuel demand and the air demand circuits, are being incorporated into the digital control package so that ultimately the entire steam plant will be controlled with a digital computer.

Conclusions

Digital control techniques have been analyzed for power plant applications and a set of linear and nonlinear algorithms have been developed.

The basic approach of simple interconnections has been verified with the example of a complex "once-through" feedwater controller. A set of FORTRAN statements is used to implement the nonlinear system.

The system is simulated and the results confirm the overall expected performance.

The flexibility of the system is enhanced with the capability of in-the-field modifications.

NOMENCLATURE

<u>Symbol</u>	<u>Quantity</u>
BLRDMD	Boiler Demand
BLRTRM	Boiler Trim
CPEDES	Convection Pass Enclosure Pressure Design Value
CPEERR	Convection Pass Enclosure Pressure Error
CPEPR	Convection Pass Enclosure Pressure
CPESP	Convection Pass Enclosure Pressure Set Point

<u>Symbol</u>	<u>Quantity</u>
CPETM	Convection Pass Enclosure Temperature
CTEDES	Convection Pass Enclosure Temperature Design Value
Δ CPEPR	Convection Pass Enclosure Pressure Increment
Δ CPETM	Convection Pass Enclosure Temperature Increment
Δ FW	Feedwater Increment
Δ THRPR	Throttle Pressure Increment
FWBIAS	Feedwater Bias
FWDES	Feedwater Design Value
FWDMD	Feedwater Demand
FWERR	Feedwater Error
FWMIN	Feedwater Minimum Flow
FWSP	Feedwater Set Point
FRQERR	Frequency Error
LOAD	Load Reference
PLDMD	Plant Demand
PLMAX	Plant Demand Maximum Value
THRDES	Throttle Pressure Design Value
THRERR	Throttle Pressure Error
THRPR	Throttle Pressure
THRSP	Throttle Pressure Set Point

REFERENCES

- (1) Strohmeier, C. and Giras, T.C., "Combined Digital-Analog Control Approach for Sibley Station Unit No. 3", ASME-IEEE Joint Power Generation Conference, Detroit, Michigan, Sept. 24-28, 1967.
- (2) Giras, T.C. and Birnbaum, M., "Digital Control for Large Steam Turbine-Generators", American Power Conference, Chicago, Illinois, April 23-25, 1968.

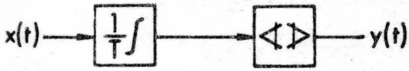


Fig. 1-(a)

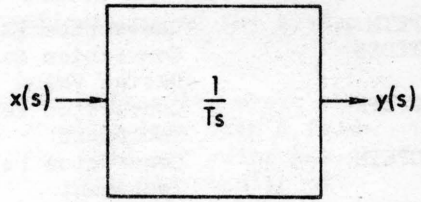


Fig. 1-(b)

$$y(n) = y(n-1) + \frac{\Delta T}{2T} [x(n) + x(n-1)]$$

CALL RESET (X,Y,YARRAY)

Fig. 1-(c)

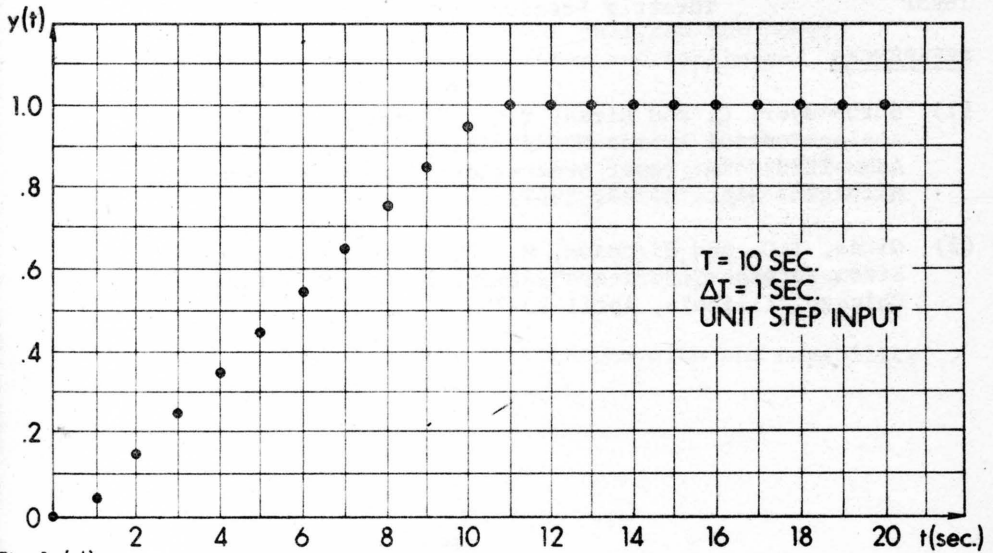


Fig. 1-(d)

FIGURE 1. RESET CONTROLLER

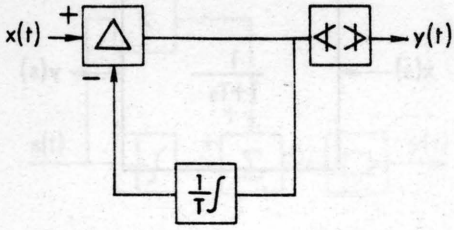


Fig. 2-(a)

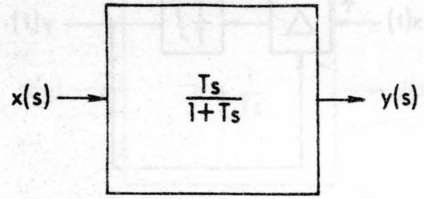


Fig. 2-(b)

$$y(n) = \frac{2T - \Delta T}{2T + \Delta T} y(n-1) + \frac{2T}{2T + \Delta T} [x(n) - x(n-1)]$$

CALL RATE (X, Y, YARRAY)

Fig. 2-(c)

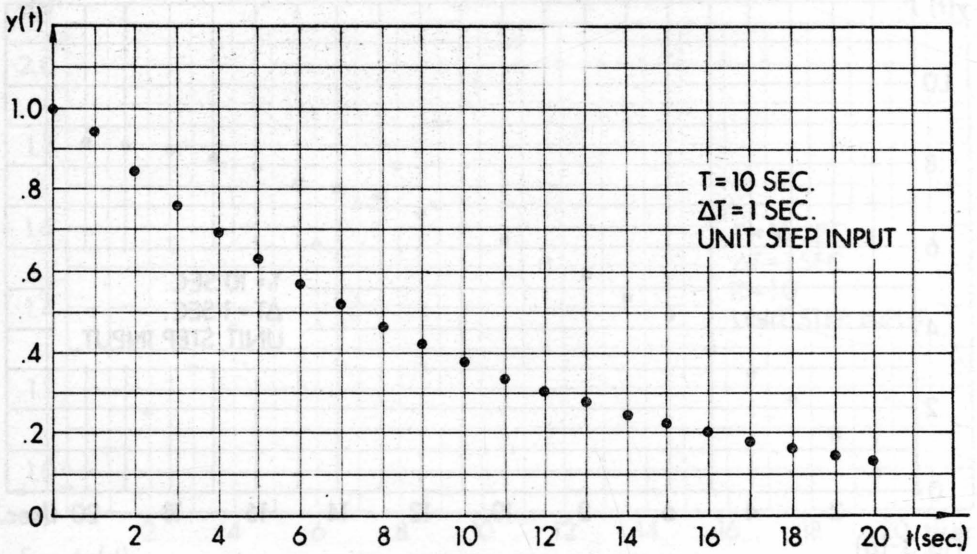


Fig. 2-(d)

FIGURE 2. RATE CONTROLLER

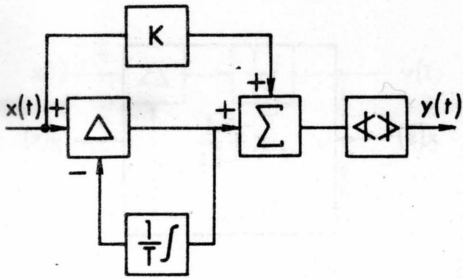


Fig. 5-(a)

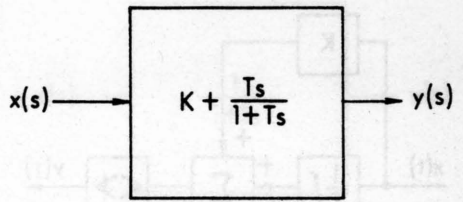


Fig. 5-(b)

$$y(n) = Kx(n) + \frac{2T-\Delta T}{2T+\Delta T} y(n-1) + \frac{2T}{2T+\Delta T} [x(n) - x(n-1)]$$

CALL PRATE (Y, Y, YARRAY)

Fig. 5-(c)

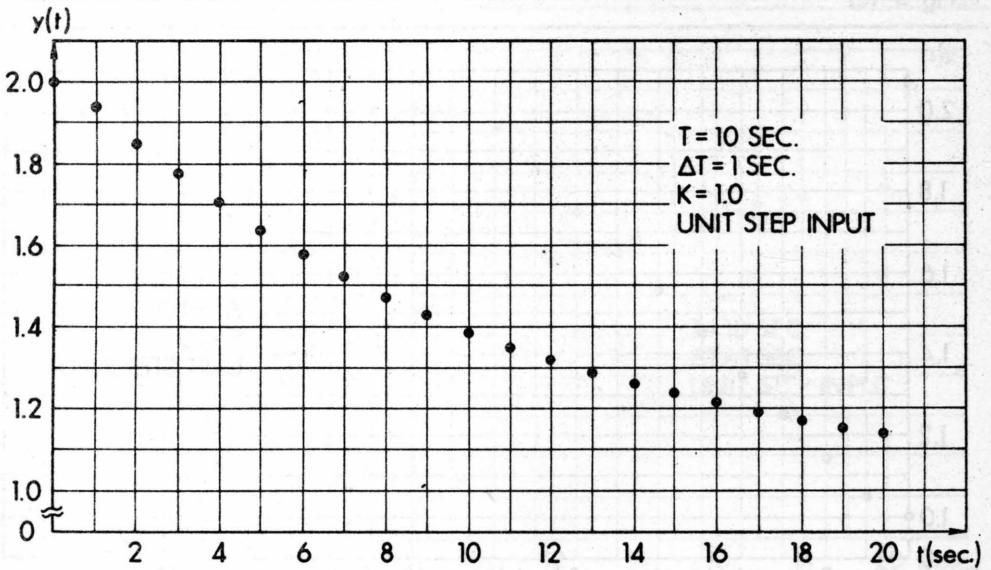


Fig. 5-(d)

FIGURE 5. PROPORTIONAL PLUS RATE CONTROLLER

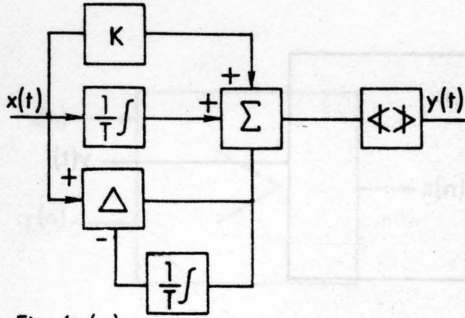


Fig. 6-(a)

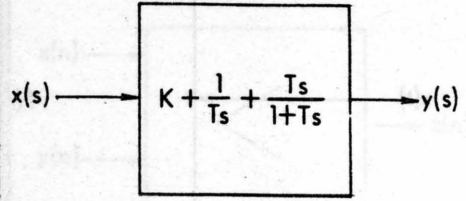


Fig. 6-(b)

$$y(n) = Ky(n) + y(n-1) + \frac{\Delta T}{2T} [x(n) + x(n-1)] + \frac{2T - \Delta T}{2T + \Delta T} y(n-1) + \frac{2T}{2T + \Delta T} [x(n) - x(n-1)]$$

CALL PID(X,Y,YARRAY)

Fig. 6-(c)

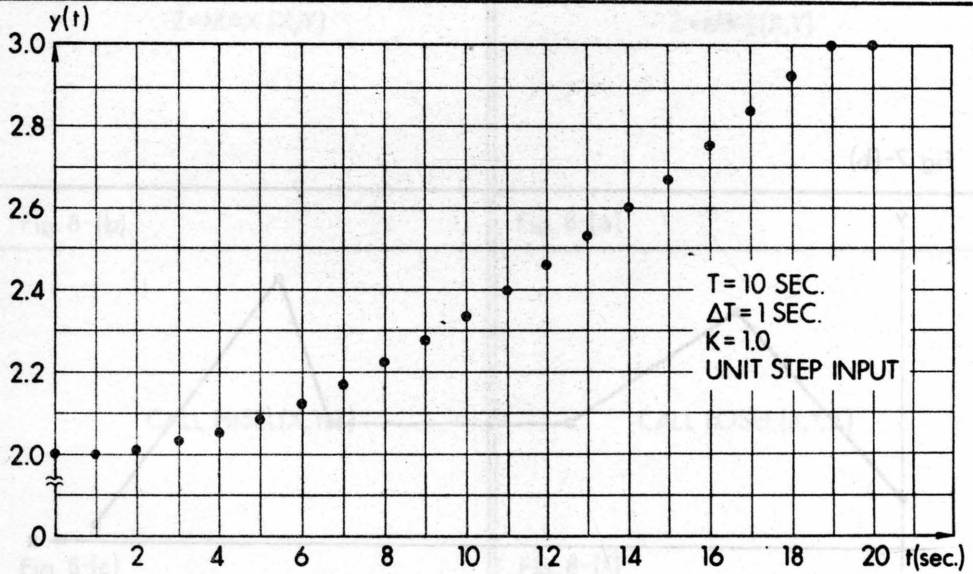


Fig. 6-(d)

FIGURE 6. PROPORTIONAL PLUS RESET PLUS RATE CONTROLLER

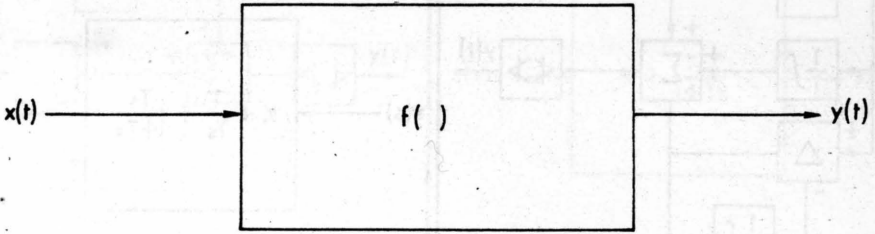


Fig. 7-(a)

CALL FUNCT(X,Y,YARRAY)

Fig. 7-(b)

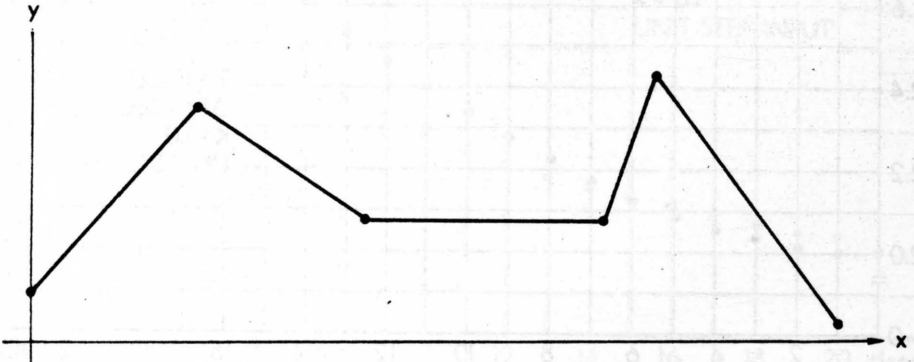


Fig. 7-(c)

FIGURE 7. NON-LINEAR CHARACTERIZATION

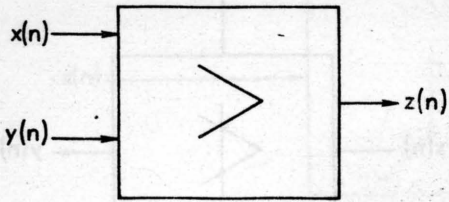


Fig. 8-(a)

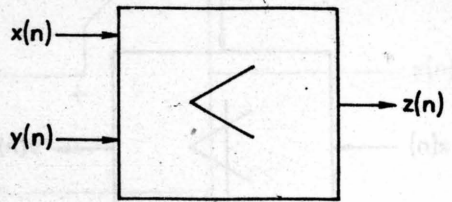


Fig. 8-(d)

$$Z = \text{MAX}(X, Y)$$

$$Z = \text{MIN}(X, Y)$$

Fig. 8-(b)

Fig. 8-(e)

CALL HISEL(X,Y,Z)

CALL LOSEL(X,Y,Z)

Fig. 8-(c)

Fig. 8-(f)

FIGURE 8. HIGH AND LOW SELECTOR FUNCTIONS

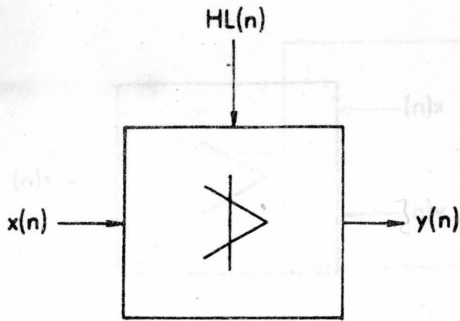


Fig. 9-(a)

$$Y = \text{MIN}(X, HL)$$

Fig. 9-(b)

CALL HILIM(X, HL, Y)

Fig. 9-(c)

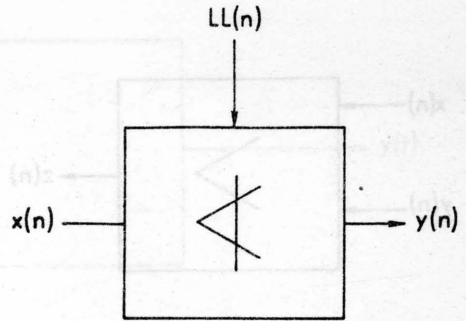


Fig. 9-(d)

$$Y = \text{MAX}(X, LL)$$

Fig. 9-(e)

CALL LOLIM(X, LL, Y)

Fig. 9-(f)

FIGURE 9. HIGH AND LOW LIMIT FUNCTIONS

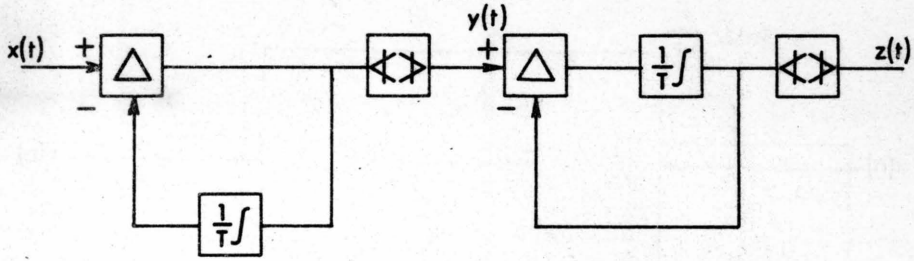


Fig. 11-(a)

CALL RATE (X, Y, YARRAY)
CALL LAG (Y, Z, ZARRAY)

Fig. 11(b)

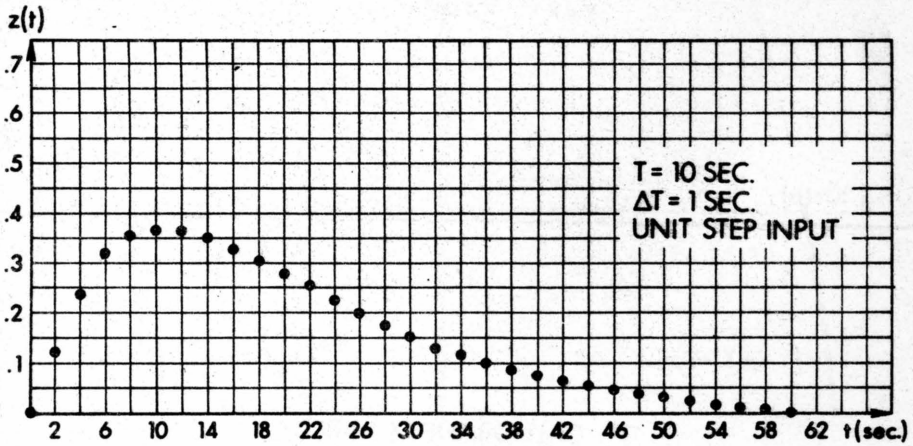


Fig. 11(c)

FIGURE 11. EXAMPLE OF RATE AND LAG ALGORITHMS IN CASCADE

$T = 10 \text{ SEC.}$
 $\Delta T = 1 \text{ SEC.}$
 $K_2 = 1.0$
 $0 \leq K_1 \leq 1.0$

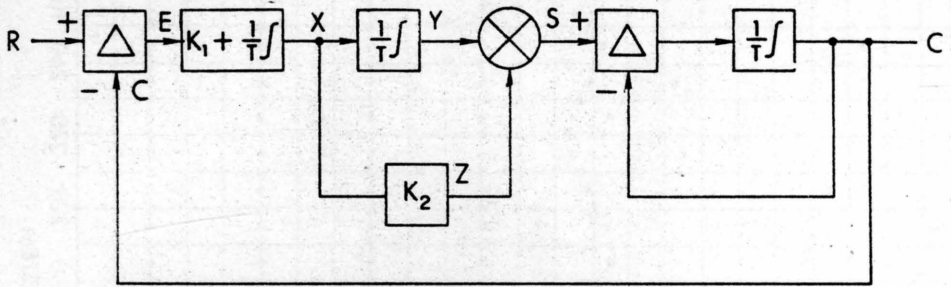


Fig. 12(a)

```

DO 100 I=1,500
CALL SUB(R,C,E)
CALL PRESET(E,X,XARRAY)
CALL RESET(X,Y,YARRAY)
CALL MULT(X,K2,Z)
CALL MULT(Y,Z,S)
CALL LAG(S,C,CARRAY)
100 PRINT

```

Fig. 12(b)

FIGURE 12 NON-LINEAR FEEDBACK SYSTEM

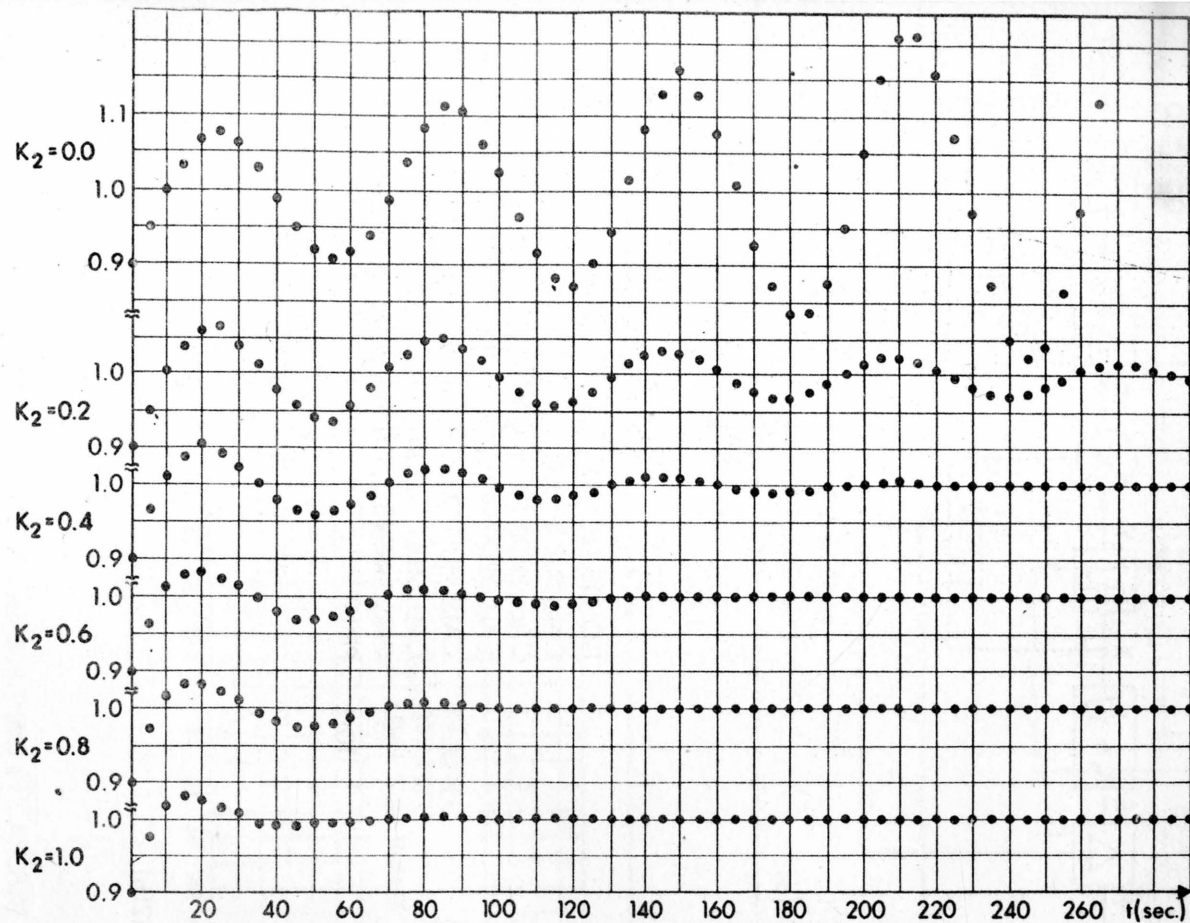


FIGURE 13. RESULTS OF NON-LINEAR FEEDBACK SYSTEM

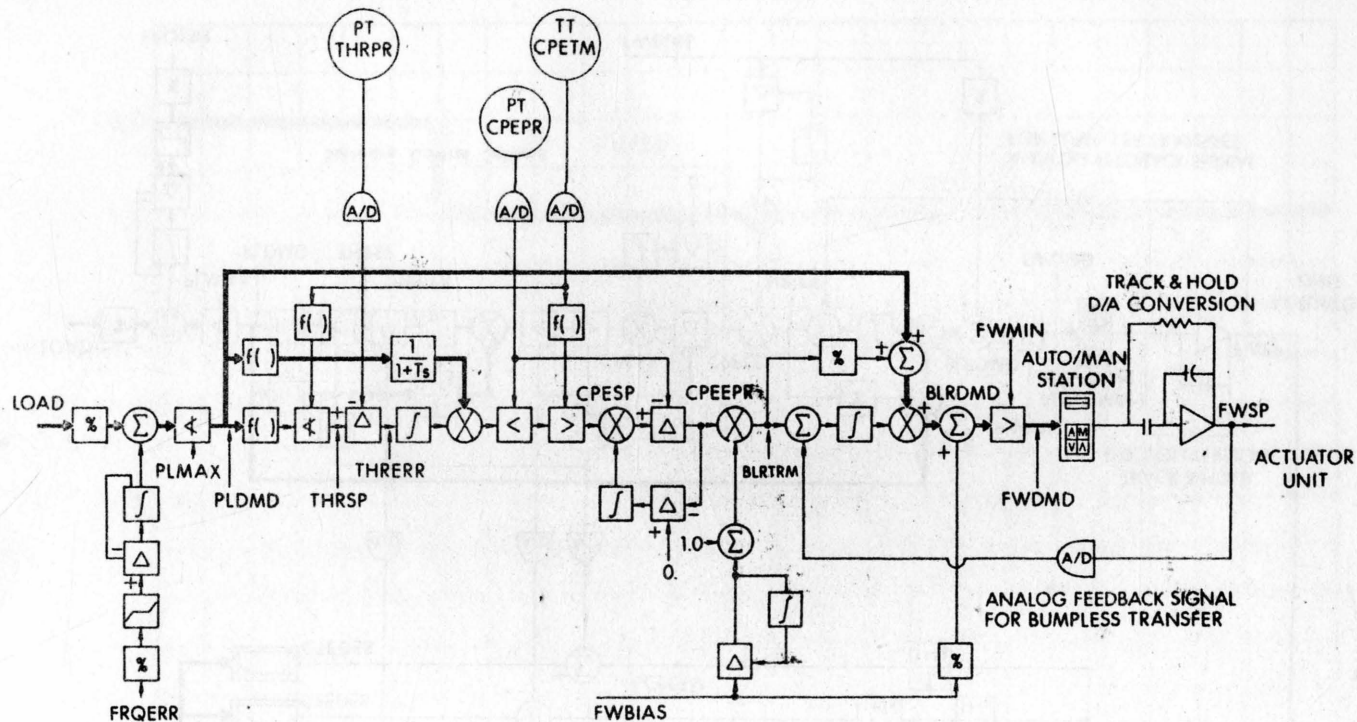


FIGURE 14. STEAM POWER PLANT FEEDWATER DEMAND CONTROL SYSTEM

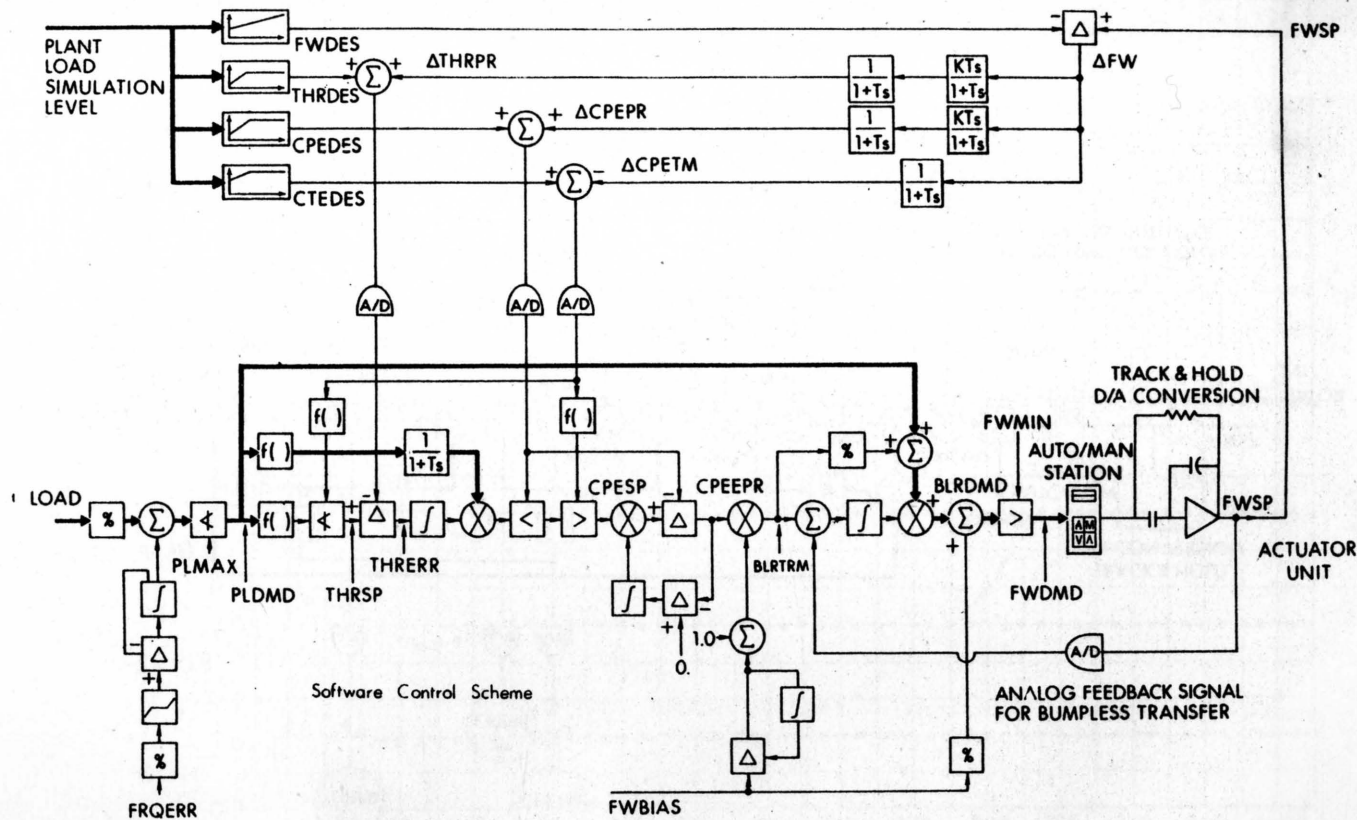


FIGURE 15. FEEDWATER DEMAND CONTROL SYSTEM WITH PLANT SIMULATION

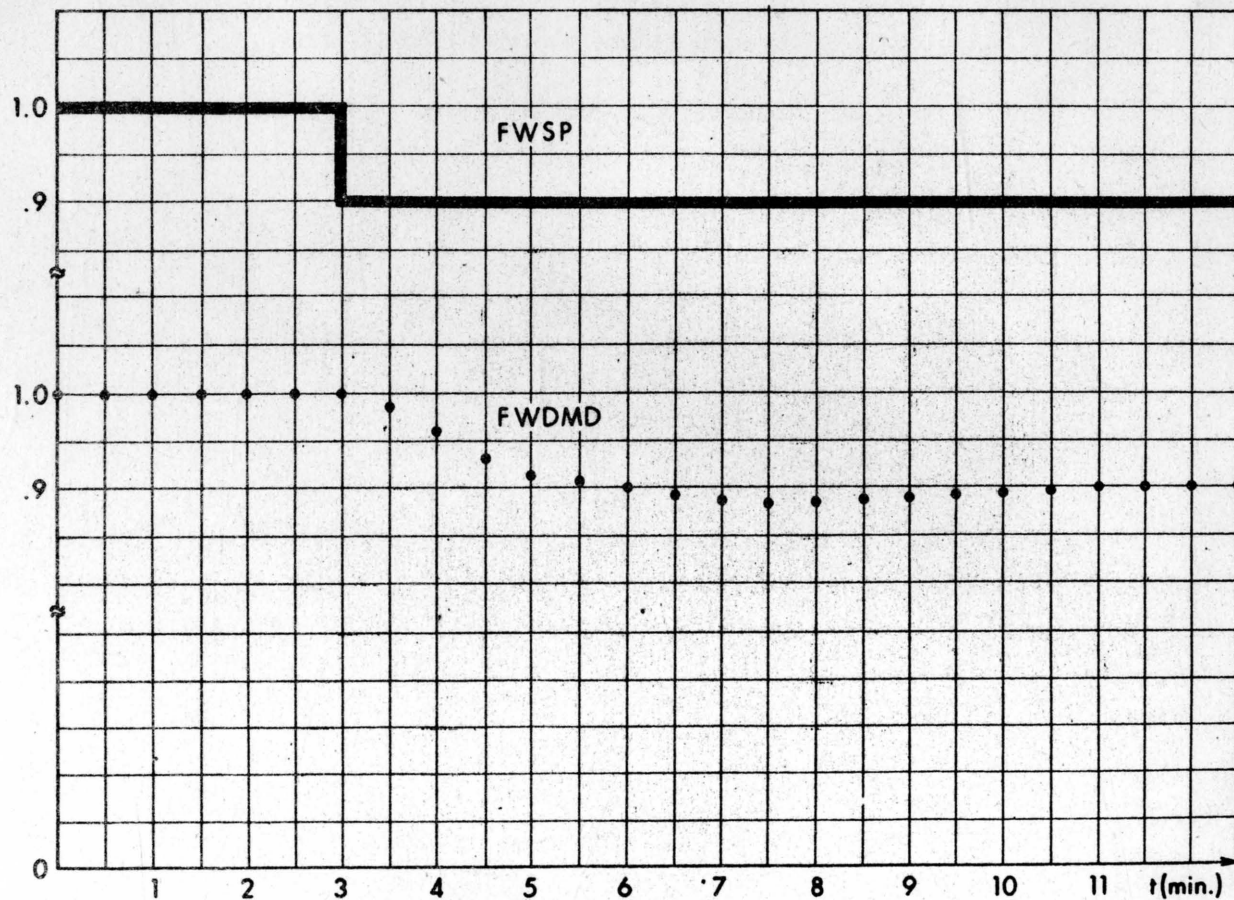


FIGURE 16. FEEDWATER DEMAND RESPONSE TO 10% DECREASE IN FEEDWATER SET POINT